6-27-2019

Iron-sulfur Cluster Biosynthesis in Methanogens

Cuiping Zhao
Louisiana State University and Agricultural and Mechanical College, mylifeinmyway123@gmail.com

IRON-SULFUR CLUSTER BIOSYNTHESIS IN METHANOGENS

A Dissertation

Submitted to the Graduate Faculty of the
Louisiana State University and
Agricultural and Mechanical College
in partial fulfillment of the
requirements for the degree of
Doctor of Philosophy

in

The Department of Biological Sciences

by
Cuiping Zhao
B.S., Anhui University, 2013
August 2019

ACKNOWLEDGEMENTS

I am so happy to be receiving my Ph.D. I first thank my family, especially my parents. They have done a great job educating their children. They have never stopped asking us to study hard and to chase our dreams. They have never stopped working hard to give us financial and mental support. They have never stopped educating us to be a good people. I love my dad! I'm sure he is very proud of me. I love my mom! She is a strong woman. She makes our family great.

I must thank my advisor, Dr. Yuchen Liu, for choosing me as her student, giving me a chance to study in the USA, and teaching me to be a great scientist. Also, I thank my advisor, Dr. David J. Vinyard, for helping me out in those struggling days and helping me in research.

I also thank members of my committee, Dr. Yong-Hwan Lee, Dr. Anne Grove, and Dr. Noemie Elgrishi, for all of their help. They have provided helpful suggestions and comments throughout my graduate study.

I would like to thank Dr. Huangen Ding, Dr. Bing-Hao Luo and Dr. Rui Lu from LSU to give me suggestions for my research. I thank Dr. Lyu Zhe, Dr. Feng Long and Dr. William B. Whiteman from University of Georgia for helping me learn how to culture methanogens. I finally thank my laboratory colleagues, Mirela Cavuzic and Evan Dunkle, and undergraduate students, Nicole Bryer, Haotian Chen, Molly M. Caluda, and Erandi M. Herath for their technical assistance.

TABLE OF CONTENTS

ABSTRACT

Methanogens live in a syntrophic consortium with bacteria, taking advantage of the metabolic abilities of their syntrophic partners to overcome energetic barriers and break down compounds that they cannot digest by themselves. Interspecies electron transfer, which is a major type of microbial communication in syntrophic processes, improves methanogenesis and anaerobic oxidization of methane (AOM) processes involved in syntrophic consortia. These processes have a significant impact on the global carbon cycle. Most of essential enzymes involved in methanogenesis are iron-sulfur proteins. Iron-sulfur clusters are one of the oldest and most versatile cofactors present in all domains of life. To date, four different Fe-S cluster assembly systems have been identified in bacteria (ISC, NIF, and SUF) and eukaryotes (ISC, CIA, and SUF). However, little is known about the Fe-S cluster assembly system in archaea. Only three proteins related to Fe-S cluster assembly are conserved in almost all sequenced archaea: SufB, SufC, and the ApbC/Nbp35 homolog. The ancestral *suf* operon likely only contains *sufBC.* Here, we provide the biochemical and spectroscopic characterizations of the *Methanococcus maripaludis* (*Mmp*) SufB, SufC and ApbC proteins. Our major findings include: (i) The SufB and SufC form a $SufB_2C_2$ complex in methanogens; (ii) The $SufB_2C_2$ is a functional scaffold, which can assemble and transfer an [4Fe-4S] cluster; (iii) The [4Fe-4S] cluster of the $SufB_2C_2$ complex is located on three highly conserved cysteine residues, Cys218, Cys237, and Cys240, on SufC; (iv) The SufC has ATPase activity, which is not required for Fe-S cluster assembly and transfer activities; (v) The archaeal Nbp35/ApbC homolog contains a [4Fe-4S] cluster which can be transferred to activate aconitase; (vi) *M. maripaludis* shows no growth defect when the archaeal *Nbp35/ApbC* gene is deleted. Together, our results suggest that the $SufB_2C_2$ complex is a functional essential scaffold for Fe-S cluster biosynthesis in archaea and that the archaeal Nbp35/ApbC homolog is a functional, but not essential scaffold/carrier protein for Fe-S cluster maturation in *M. maripaludis.*

CHAPTER 1. INTRODUCTION

1.1. Iron-sulfur cluster structure, function and properties

Iron-sulfur (Fe-S) clusters are the most versatile, inorganic cofactors and are present in all domains of life. They are found in a variety of metalloproteins involved in various fundamental cellular processes including DNA replication and repair (2), respiration (3), photosynthesis (4), and biosynthetic pathways (5). The most common function of Fe-S clusters is electron transfer involved in redox reactions based on ability of Fe to switch between two oxidation states: +3 and +2 (Figure 1) and the ability of Fe-S cluster to delocalize electron density both on Fe and S atoms (Figure 1) (6-9). The localization and delocalization patterns of Fe-S clusters give them different spin states and net oxidation states (10) (Figure 1). These properties can be studied using electron paramagnetic resonance (EPR) spectroscopy (11).

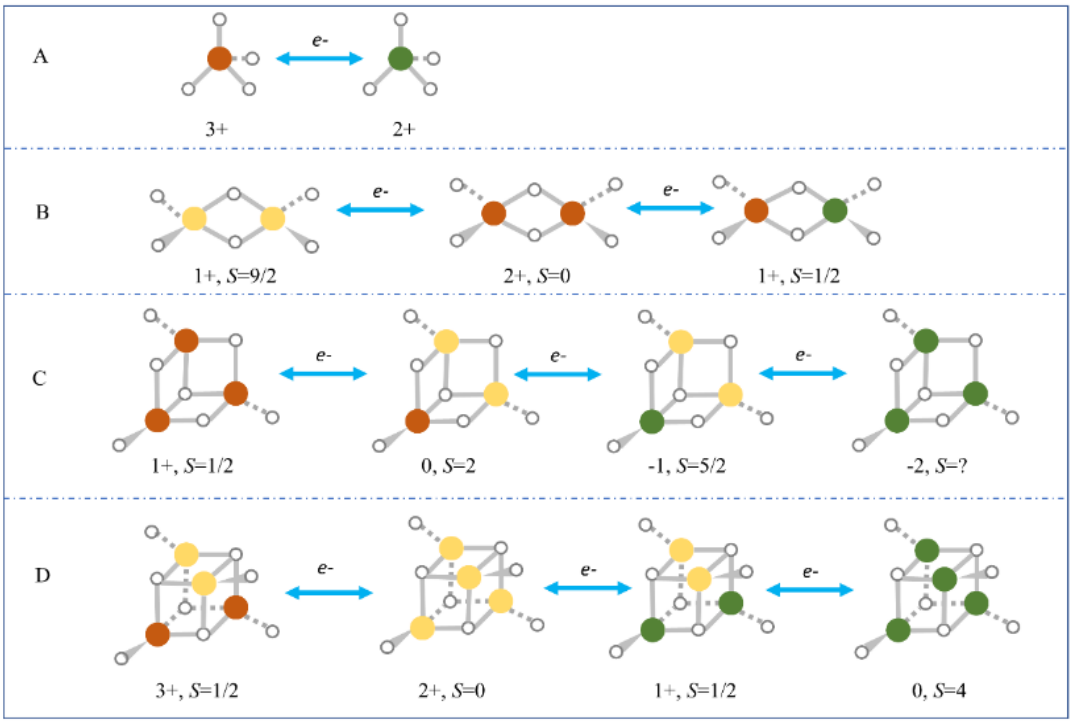

Figure 1. Localization and delocalization of Fe-S clusters.
Red: localized Fe^{3+}. Green: localized Fe^{2+}. Yellow: delocalized $Fe^{2.5+}$ $Fe^{2.5+}$ pair. The oxidation state and spin state (*S*) are labeled underneath each different Fe-S cluster.

Fe-S clusters are also involved in catalysis. They can constitute the substrate binding sites of many redox and non-redox enzymes, such as the [4Fe-4S] cluster in aconitase (12), the [Ni-4Fe-5S] in CO dehydrogenase (13), and the [4Fe-4S] in sulfite reductase (14). Fe-S clusters also play important structural and regulatory roles, like the Fe-S clusters in the DNA repair enzymes endonuclease III (15) and MutY (16). Fe-S clusters are also involved in gene regulation, for example, aconitase in *Bacillus subtilis* (17) and *Escherichia coli* (18). Fe-S clusters also function as iron/sulfur storage, for instance, [2Fe-2S] cluster in biotin synthase donates sulfur for the conversion of desthiobiotin to biotin (19), and dehydrogenase contains multiple [4Fe-4S] clusters (20). Overall, Fe-S clusters are essential throughout biochemistry.

Fe-S clusters are formed from inorganic Fe^{2+} or Fe^{3+} and S^{2-}. Because Fe-S clusters can spontaneously assemble in the presence of high amounts of iron ions and sulfide that were presumably abundant on the anoxic Earth, they are surmised to be one of most ancient cofactors in living organisms (21,22). Three classes of Fe-S clusters are most common: [2Fe-2S], [3Fe-4S], and [4Fe-4S] (Figure 2). The Fe centers are tetrahedral, and the sulfide groups are usually two- or three-coordinate. The Fe-S clusters are bound to proteins usually by sulfur atoms on cysteine residues. Other ligands are also found including nitrogen atom on arginine or histidine (23) (24), oxygen atom on aspartate or tyrosine (25), water (26), and small molecules (27).

1.2. Iron-sulfur cluster biosynthesis

Fe-S clusters can be formed directly by chemical synthesis from high concentrations of inorganic Fe ions and S ions *in vitro* (28), but it is impossible to form Fe-S cluster in this way in vivo. Accumulation of Fe ions in vivo is toxic to the cell because it can cause Fenton reactions (Figure 3) under aerobic conditions. HO· produced from the Fenton reaction can directly damage most macromolecules. Because the low Fe availability and Fe toxicity in vivo, organisms use different complex strategies to form Fe-S cluster to fulfill their needs.

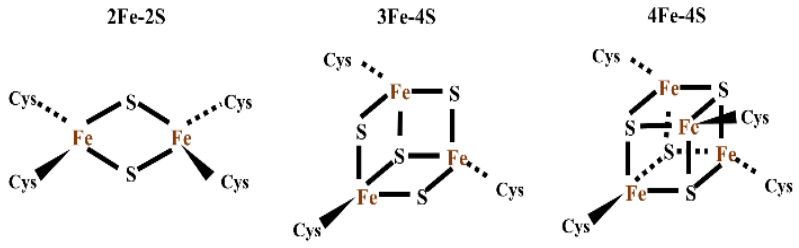

Figure 2. Three most popular different Fe-S cluster types.

In general, the biosynthesis of Fe-S clusters requires two major steps: assembly and transfer (Figure 4) (29,30). In the assembly step, a cysteine desulfurase (a pyridoxal-5'-phosphate (PLP) dependent enzyme) derives S from L-cysteine (31). Cysteine is the common sulfur source for Fe-S cluster biosynthesis. The physiological Fe donor remains uncertain (32). Electron donors facilitate Fe-S cluster assembly. A scaffold protein provides a molecular platform for Fe and S to meet and form a cluster *de novo* (33,34). In the transfer step, the pre-formed cluster is delivered to a specific target apo-form protein either directly from the scaffold—with the help of energy dependent chaperones—or indirectly through Fe-S cluster carrier proteins (32).

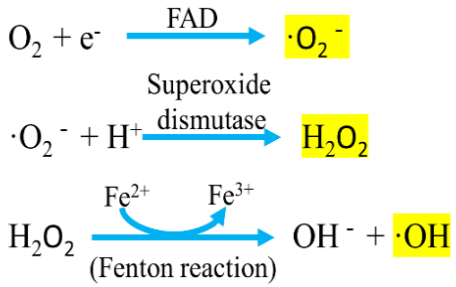

Figure 3. Reactive oxygen species (ROS) generation.
These three reactions generate ROS which are labeled with yellow color. The accumulation of Fe ions in cells can induce the Fenton reaction and thus produce hydroxyl radical.

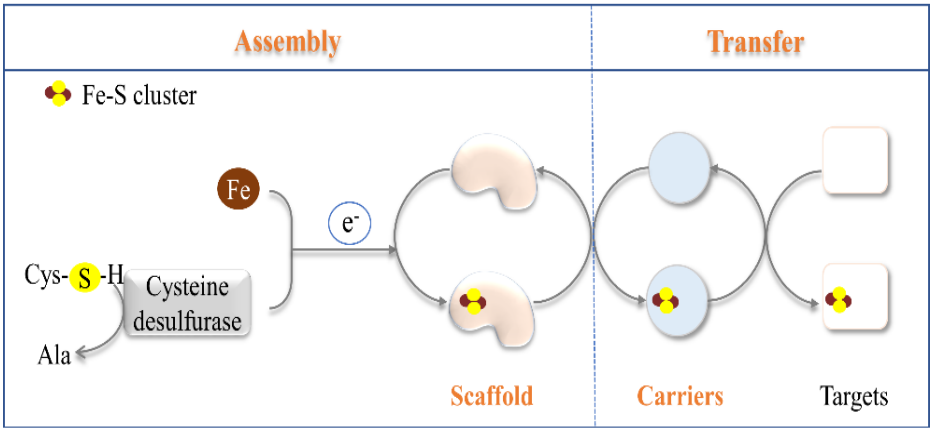

Figure 4. Fe-S cluster biosynthesis scheme in living organism.

The machineries for Fe-S cluster biosynthesis are diverse in different organisms and vary depending on growth conditions. Four different systems have been identified in the three domains of life: ISC (iron sulfur cluster), SUF (sulfur formation)), CIA (cytosolic iron-sulfur assembly), and NIF (nitrogen fixation) systems (Figure 5). Many organisms have more than one system. Bacteria have three known machineries: the NIF, ISC, and SUF systems (32,35,36). The NIF system is specific to nitrogen fixation bacteria. The ISC and SUF systems are for Fe-S cluster biosynthesis under normal and stress conditions (oxidative stress and iron limiting), respectively. Eukaryotes have the ISC system in the mitochondrion (37) and the SUF system in the plastid (38). Additionally, eukaryotes possess a CIA machinery essential for maturation of Fe-S proteins in the cytosol and nucleus (39).

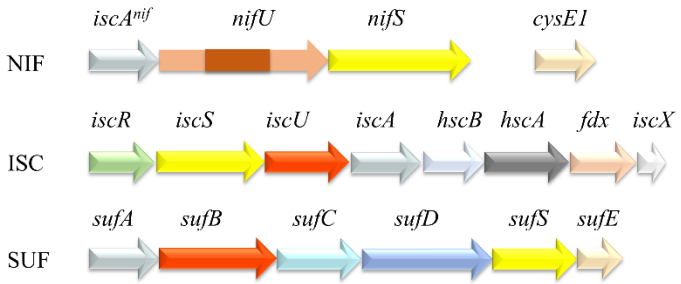

Figure 5. Examples of Fe-S cluster biosynthesis operons in NIF, ISC, and SUF operons in bacteria.

1.3. Introduction of the NIF, ISC and CIA system

The NIF system is responsible for the specific maturation of nitrogenase in diazotrophic bacteria (40,41), for instance, *Azotobacter vinelandii*, which is the first paradigm for biological Fe-S cluster assembly. Nitrogenase is responsible for nitrogen fixation, which can reduce N_2 to NH_3. Most biological nitrogen fixation is carried out by molybdenum nitrogenase (42). Molybdenum nitrogenase consists of two proteins: NifDK and NifH (43). NifDK contains one FeMo-cofactor and one [Fe_8-S_7] P-cluster (44). The FeMo-cofactor is a Mo-Fe_7-S_9-X cluster (45), which is the most complex Fe-S cluster. The NifH homodimer has one [4Fe-4S] cluster at the interface of the dimer (46). In the NIF system, NifS is a cysteine desulfurase and NifU is a scaffold protein involved in Fe-S clusters biosynthesis for nitrogenase maturation (31).

In contrast with the specificity of the NIF system, the ISC system in bacteria and eukaryotic mitochondria is a general pathway for Fe-S cluster biosynthesis. The *nifU* and *nifS* deletion strain still can produce low levels of nitrogenase and support bacterial growth under nitrogen fixation condition, which indicated that there were other housekeeping genes working redundantly with the NIF system that weakly complement the function of NifU and NifS (40). Then nine genes

from *A. vinelandii*, *cysE2*, *iscR*, *iscS*, *iscU*, *iscA*, *hscB*, *hscA*, *fdx*, and *orf3*, were found to likely have some function related to Fe-S cluster biosynthesis. IscS was found to be a cysteine desulfurase, which directly interacts with and donates sulfur to IscU for Fe-S cluster assembly (47). IscU was found to be a scaffold that has the ability to assemble both $[2Fe\text{-}2S]^{2+}$ and $[4Fe\text{-}4S]^{2+}$ clusters (48). However, inactivation of *iscS* or *iscU* is lethal in *A. vinelandii* when *A. vinelandii* grows under nitrogen-fixing conditions (49) but not in *E. coli*. This indicated there was another Fe-S cluster biosynthesis system beside ISC system in *E. coli*, which was the third found SUF system.

The fourth found Fe-S cluster system is the CIA system essential for the maturation of Fe-S clusters in the cytosol and nucleus of eukaryotes (50). The CIA system depends on the function of the mitochondrial core ISC assembly and export systems that provide the sulfur source (51). The NADPH–Tah18–Dre2 electron transfer chain is also required (51-53). Nbp35 (Nucleotide Binding Protein) and Cfd1 (Cytosolic Fe-S cluster Deficient 1) are homologous. The Nbp35-Cfd1 complex with a [4Fe-4S] cluster bridging the heterodimer is the scaffold required for the CIA system in yeast (50,54,55). Besides the Nbp35-Cfd1 scaffold, the CIA system also needs carrier Nar1 (56,57) and the CIA targeting complex consisting of Cia1, Cia2, and Mms19 (58-60) to transfer the bridging [4Fe-4S] clusters to apo-form proteins.

1.4. Introduction of the SUF system

The SUF system is widely distributed in all three domains of life (61). The *suf* operon is diverse in different species, containing two to more than six different genes that encode protein functions such as cysteine desulfurase (SufS and SufE), scaffold (SufU, SufBCD), and carrier (SufA, HscA/B) (Figure 6).

The *sufA*, *sufB*, *sufC*, *sufD*, *sufS*, *sufE* genes were first suggested to form an operon in *E. coli* (62). The SUF operon was found to have the ability to complement the function of the ISC system in the *E. coli* mutant, YT1014 (61). YT1014, in which the entire *isc* operon has been deleted, was reported to have poor growth and exhibited a significant lower activity of Fe-S proteins compared with wild-type cells. The suppression mutants showed high overexpression of *suf* operon. All six suf genes, *sufA*, *sufB*, *sufC*, *sufD*, *sufS*, and *sufE*, were essential for the viability of the suppression mutants.

In the SUF system in *E. coli*, SufS and SufE work as a cysteine desulfurase to donate sulfur to the scaffold to assemble Fe-S clusters. The SufS-SufE complex is the first example of a two-component cysteine desulfurase. SufS is the NifS/IscS homolog, eliminating sulfur from cysteine and selenium from selenocysteine (63). It has high specificity to selenocysteine and low cysteine desulfurase activity (64). The conserved cysteine residue of SufS, Cys364, was essential for its cysteine desulfurase function. The crystal structure of SufS from *E. coli* indicated that this essential cysteine was too far away from the PLP-cysteine site, which make it difficult to form a persulfide (65). Thus, the cysteine desulfurase activity of SufS is much lower than IscS or NifS.

SufE, an oxidoreductase, was shown to bind SufS tightly to form a 1:1 complex. It can drastically stimulate the cysteine desulfurase activity of SufS by 50-fold while SufE alone has no cysteine desulfurase activity (66,67). The conserved cysteine residue of SufE, Cys51, was crucial for its stimulation function (66). The mechanism of the SufSE complex starts with forming a persulfide on Cys364 of SufS (Figure 7). The sulfur is then transferred to Cys51 of SufE, forming a persulfide on SufE (67,68). The cysteine desulfurase activity of the SufSE complex is further enhanced by the SufBCD complex (68).

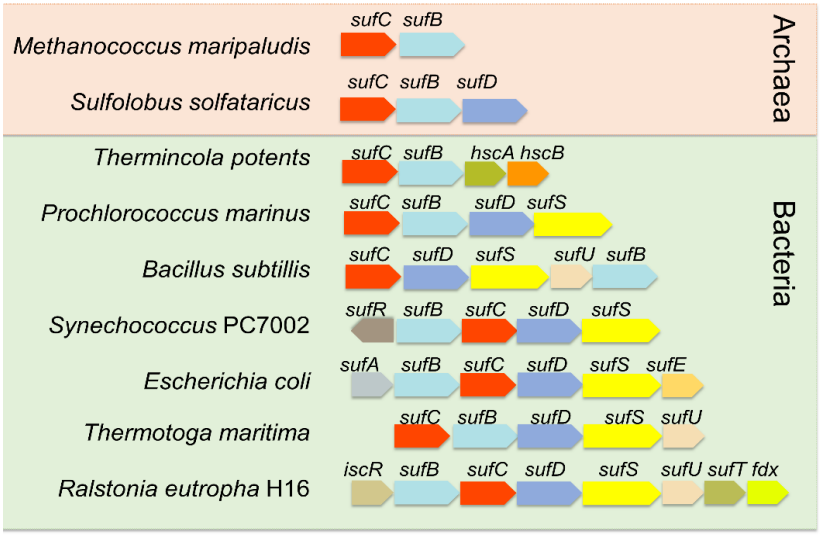

Figure 6. Diverse SUF operon examples in three life domains, archaea (pink box), and bacteria (green box). Gene homologs are labeled as same color in different organisms to reflect their homology.

SufB, SufC, and SufD in *E. coli* form a $SufBC_2D$ complex, which was suggested to be a $FADH_2$-dependent scaffold assembled a [4Fe-4S] cluster *de novo* (69,70). The crystal structure of the $SufBC_2D$ complex from *E. coli* has been solved, (PDB ID 5WAF) (71). SufB in *E. coli* was proposed to be an Fe-S scaffold protein (72) and a [4Fe-4S] cluster was observed in reconstituted SufB (73). SufE interacts with SufB to donate sulfur only when SufC is bound on SufB (73). $SufB^{C254}$ is likely involved in S transfer (74). SufD was proposed to escort iron entry into the scaffold complex (75). SufB and SufD are homologs, and both bind one SufC to form a $SufBC_2D$ complex (Figure 7) (70). $SufB^{C405}$, $SufB^{E434}$, and $SufD^{H360}$ have been proposed to be the Fe-S cluster binding sites (71,76).

Moreover, SufC is an ATPase of the ABC superfamily. Unlike typical membrane associated ABC ATPases, whose main functions are to export or import ions, pigments, or virulence factors across biological membranes, SufC was found in the cytoplasm (77). It has all three conserved motifs of typical ATP-hydrolyzing domains of ABC ATPases, Walker A and B motifs as well as an ATP binding cassette (ABC signature) (78). The crystal structure of SufC indicated that the

unique Q-loop structure on its surface is probably the binding site for SufB or SufD (78). Its ATPase activity is required for *in vivo* cluster assembly (75,77) and has been proposed to drive a conformational change of the $SufBC_2D$ complex in *E. coli* (71). The proposed model suggested: (i) SufC dimerized upon binding to ATP, which induced the conformational change of the SufBD heterodimer interface; (ii) with the exposure of Fe-S cluster binding ligands on the SufBD heterodimer, a Fe-S cluster can be assembled on $SufBC_2D$ scaffold (Figure 7) (74). The ATPase activity of SufC can be enhanced by interacting either with SufB or SufD separately or with $SufBC_2D$ complex (79,80).

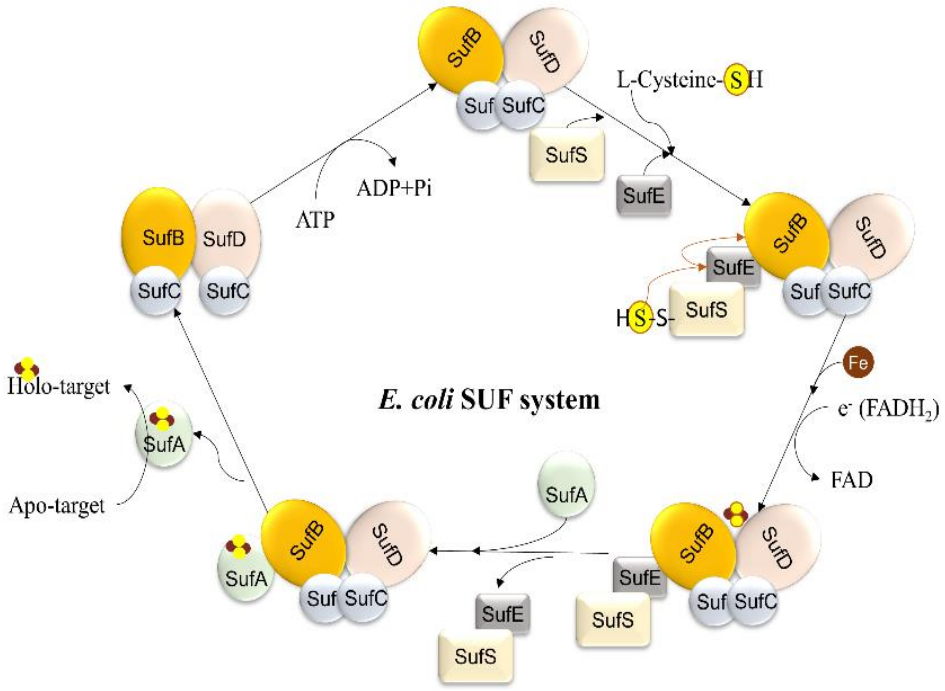

Figure 7. The mechanism of Fe-S cluster assembly by SUF system.
In the resting state, SufB and SufD form a heterodimer and both bind one SufC. Upon ATP binding, SufC forms a homodimer, which induces a conformational change in the $SufBC_2D$ scaffold. Cysteine desulfurase activity of SufSE complex generates a persulfide on Cys364 of SufS, which is then transferred to Cys51 of SufE and then to Cys254 of SufB. With the donation of Fe ions from iron donor and electrons from $FADH_2$, the Fe-S cluster can be coordinated on $SufB^{C405}$, $SufB^{E434}$, and $SufD^{H360}$. Upon SufSE dissociating from $SufBC_2D$ scaffold, carriers such as SufA, bind on SufB. The assembled cluster will be transferred to apo-form Fe-S proteins. The $SufBC_2D$ scaffold will restore to its rest form.

SufA is a homolog of IscA, which is involved in Fe-S cluster formation and repair in the ISC system. SufA either acts as a cluster carrier that delivers intact Fe-S clusters to target apo-form proteins (81) or as a Fe donor for cluster assembly (82,83). SufA was suggested to be a Fe-S

cluster carrier. The Fe-S cluster is transferred unidirectionally from scaffold to carrier as seen with the scaffold IscU and the carrier IscA (84). It was found that SufA can interact with $SufBC_2D$ to accept Fe-S clusters and then transfer the clusters to other apo-form proteins (69,81); $SufBC_2D$ can enhance Fe-S cluster formation on SufA; the Fe-S cluster can transfer from $SufBC_2D$ to SufA, but not in the reverse direction (69).

The ISC system is the housekeeping system, while only SUF system in *E. coli* is active under oxidative stress and iron-limiting conditions (Figure 8). In *E. coli*, the *isc* operon, *iscRSUAhscBAfdx*, is under control of the Fe-S cluster-containing transcription factor IscR (85). Only holo-form IscR, with a [2Fe-2S] cluster, is the active repressor of the *isc* operon (85-87). Under normal aerobic condition, the demand for Fe–S clusters is high. Apo-IscR is dominant because IscR must compete with other Fe-S proteins in acquiring Fe–S clusters from the Isc pathway, which results in low level of holo-IscR and less repression of *isc* operon. Therefore, *isc* transcription increases to meet the demand (87).

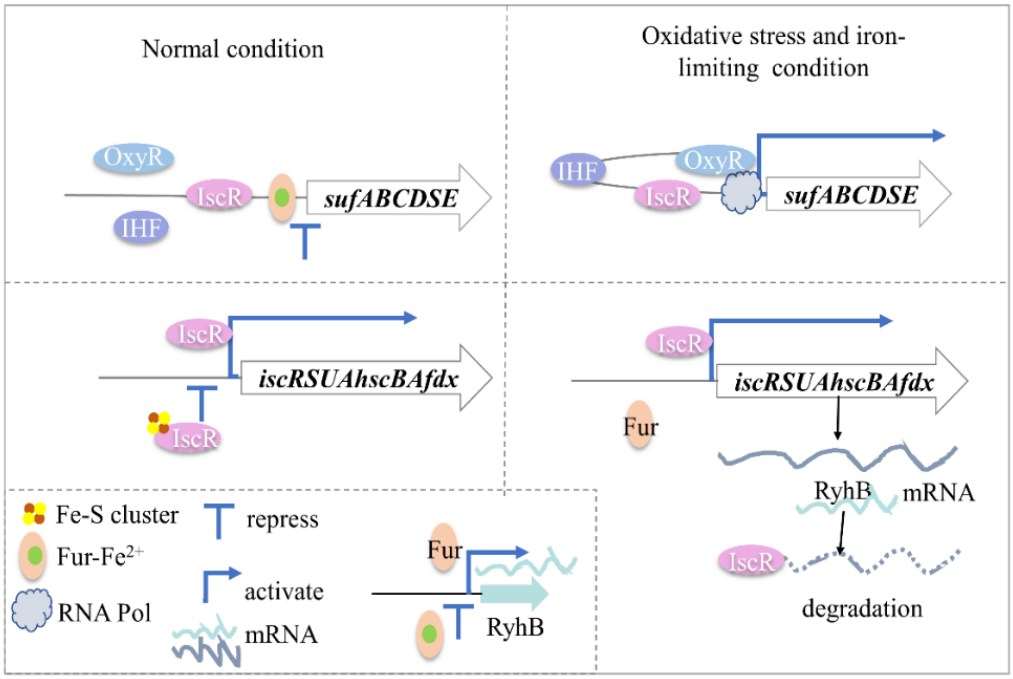

Figure 8. Genetic regulation of *isc* and *suf* operons under normal and oxidative stress or iron-limiting conditions.
Left panel: normal condition; right panel: oxidative stress and iron-limiting conditions. Upper panel: *suf* operon; lower panel: *isc* operon. RNA Pol: RNA polymerase.

Under oxidative stress and iron-limiting conditions, the *isc* operon is upregulated to fulfill the increased demand for Fe-S clusters because Fe-S clusters are sensitive to ROS. The dominant apo-IscR will relieve *isc* repression and induce its transcription with the increasing demand for

Fe-S cluster. However, the high amount of apo-form Fur (ferric uptake regulator, the iron sensing regulator) stimulates the formation of a small non-coding RNA, RyhB (88). RyhB binds on *iscS* on the *iscRSUA* polycistronic mRNA, which leads to the degradation of the *iscSUA* mRNA and apo-IscR formation. Therefore, IscS, IscU and IscA are not expressed under the oxidative stress and iron-limiting conditions (Figure 8).

The *suf* operon, *sufABCDSE*, is repressed by holo-form Fur (Figure 8). Under normal conditions, Fur is present as Fur-Fe^{2+} and binds between -32 and -3 nucleotides upstream of the SufA promoter and thus inhibits binding of RNA polymerase (89,90). Under iron-limiting or oxidative stress, Fur without Fe ions are dominant, which will release the regulator from the binding site of the SufA promoter and de-repressed *suf* operon transcription (89,91). Three other factors, OxyR, IHF (integration host factor), and IscR also regulate suf operon transcription through the binding of the oxidant-responsive elements (ORE-I, II, III) in the upstream of the SufA promoter, respectively (90,92). ORE-I, II, III are located from -236 to -197, from -156 to -127, and from -56 to -35 nucleotides from the transcriptional start site, respectively (92). OxyR was suggested to activate suf operon transcription by contacting RNA polymerase at the sufA promoter through a loop formation facilitated by IHF under oxidative strsess (90,92). Apo-IscR was found to activate suf operon transcription (90). Regulation by OxyR/IHF and IscR work independently (90).

1.5. The phylogeny and ecology of methanogens

Methanogens are obligate anaerobes and belong to the archaeal domain of life. Methanogens were found in eight orders of the *Euryarchaeota* phylum (93): *Methanococcales*, *Methanobacteriales*, *Methanosarcinales*, *Methanomicrobiales*, *Methanopyrales* (94-96), *Methanocellales* (97), *Methanonatronarchaeales* (98), *Methanomassiliicoccales* (which was named as '*Methanoplasmatales'* before) (99,100). Beside the *Euryarchaeota* phylum, new methanogens were found in the *Bathyarchaeota* (101) and *Verstraetearchaeota* (which was named as '*Candidatus Methanohydrogenales'*) phylums (102). Methanogens are likely one of the most ancient forms of life with isotopic evidence indicating biological methane production or methanogenesis about 3.46 billion years ago (103).

Methanogens are found in wide a variety of environments (104). *Methanococcales* have all been isolated from marine environments. *Methanobacteriales*, *Methanomicrobiales*, and *Methanosarcinales* were found in anaerobic habitats such as marine and freshwater sediments, soils, animal gut tracts, and anaerobic digestors. *Methanopyrus kandleri*, the only species within the order of *Methanopyrales*, was found only in hydrothermal vents. *Methanocella paludicola*, which belongs to the order of *Methanocellales*, was isolated from rice field soil in Japan (105). *Methanonatronarchaeales* were found in hypersaline lakes at moderate thermophilic conditions (98). *Methanomassiliicoccales* were found in human and animal gastro-intestinal tracts and wetlands (106). *Bathyarchaeota* were found in deep-ocean and freshwater sediments (101).

Verstraetearchaeota were found in wetlands, sediments, soils and hydrocarbon-rich environments (102).

Methanogens can be divided into two clusters. The Class I methanogens include *Methanobacteriales*, *Methanococcales* and *Methanopyrales*, while the Class II comprises *Methanocellales*, *Methanomicrobiales* and *Methanosarcinales* (107). Some methanogens actively produce methane in oxygenated soils (108-110) although most of them are sensitive to oxygen (111-113). Through analyzing functional genes relevant to ROS production, O_2/ROS elimination and self-repairing systems of six well-established methanogen orders, enrichment of antioxidant features in the Class II was found compared to the Class I (111). The Class II methanogens use cysteine as a sulfur source while Class I methanogens use sulfide. This choice is consistent with the aerobic environments inhabited by Class II methanogens because sulfide is mostly depleted under oxidative conditions (111,114). Moreover, two types of carriers, A-type carriers (for example, SufA and IscA) and ApbC, were found in the Class II methanogens compared to only one carrier (ApbC) in the Class I methanogens for Fe-S clusters assembly.

1.6. Methanogens produce methane as the primary product of catabolism through methanogenesis pathway

Methanogens produce methane as the primary product of catabolism through methanogenesis that provides energy for their growth. Three methanogenesis pathways were found and vary in the substrates used (Figure 9) (104). Although three different methanogenesis pathways use different substrates, all of them contain three common steps: the transfer of the methyl group to coenzyme M; the reduction of methyl-coenzyme M with coenzyme B; and the recycling of the heterodisulfide bond from CoM-S-S-CoB.

Aceticlastic methanogenesis uses acetate as the substrate (115). This pathway produces around two-thirds of the total biologically produced methane. Only two genera, *Methanosarcina* and *Methanosaeta*, are aceticlastic methanogens.

Hydrogenotrophic methanogenesis uses H_2 and CO_2 as substrates. This pathway produces around one-third of the total biologically produced methane. Obligate hydrogenotrophic methanogens include *Methanobacteriales*, *Methanococcales*, *Methanomicrobiales*, *Methanocellales*, *Methanopyrales*, and *Methanosarcinales* (116). Some hydrogenotrophic methanogens can also use formate as a substrate. Formate will first be oxidized to CO_2 by formate dehydrogenase before entering the pathway. Hydrogenotrophic methanogens, such as *Methanothermobacter thermoautotrophicus* and *Methanosarcina barkeri*, can also oxidize CO to CO_2 using CO dehydrogenase (CODH) and the CO_2 enters the hydrogenotrophic methanogenesis (117). As the most widespread pathway in methanogens (118), it has been suggested to represent the ancestral form of methane production (119).

Methanomassiliicoccales, *Bathyarchaeota*, *Verstraetearchaeota*, together with some *Methanobacteriales* and *Methanosarcinales*, were found to produce methane by a

methylotrophic pathway (116). They can use C1 compounds and methylated organic compounds as substrates such as methanol, monomethylamine, dimethylamine, trimethylamine, tetramethylammonium, methanethiol and dimethyl-sulfide. This pathway only produces minor methane yields compared with other two pathways. Methylotrophic methanogenesis is usually considered to be the dominant pathway in hypersaline habitats (120,121). Methylotrophic methanogenesis was first suggested to evolve independently as non-euryarchaeal methanogens only can use the methylotrophic pathway (122,123). Recently, hydrogenotrophic methanogenesis was found in archaeal phylum *Verstraetearchaeota*, which reveals the shared ancestry of all methanogens (116).

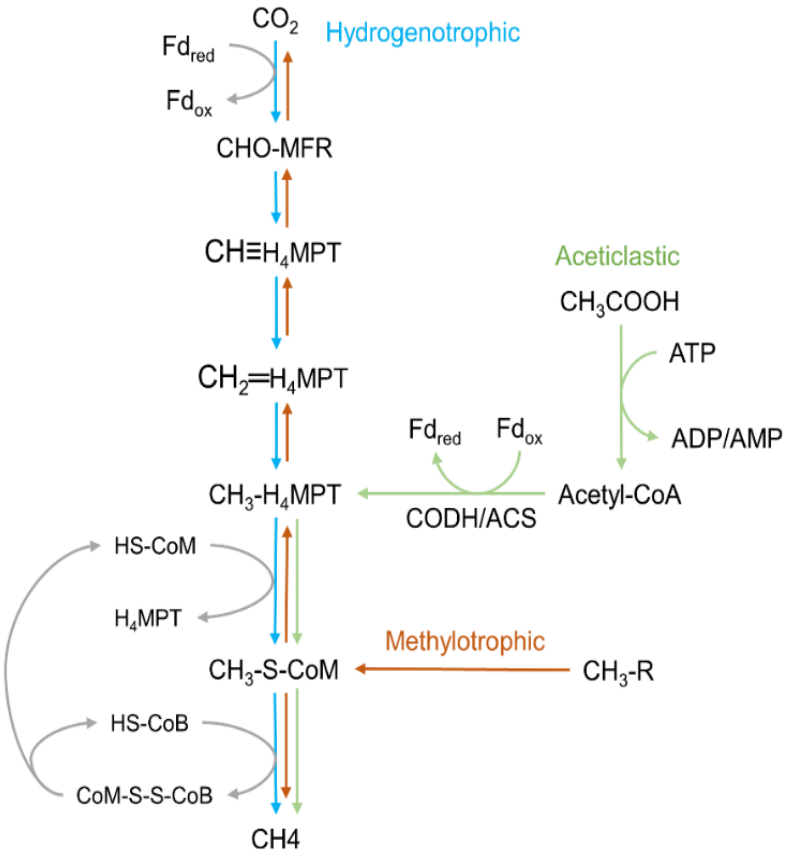

Figure 9. Three methanogenesis pathways.
Green arrows: aceticlastic methanogensis. Blue arrows: hydrogenotrophic methanogenesis. Red arrows: methylotrophic methanogenesis. Grey arrows indicate their common steps. Abbreviation: MFR, methanofuran; HS-CoM, coenzyme M; HS-CoB, coenzyme B; Fd_{red}, reduced ferredoxin; Fd_{ox}, oxidized ferredoxin; CODH/ACS, carbon monoxide dehydrogenase/acetylCoA synthase/decarbonlyase complex; CH_3-R, methylated compounds.

1.7. Methanogens obtain most of their energy through methanogenesis

In aerobic respiration, an organic energy source such as glucose is oxidized to CO_2 through glycolysis and the citrate cycle, and O_2 is reduced to H_2O. In this process, 1 mole of glucose can produce 32 moles of ATP when glucose is oxidized to CO_2 completely. However, the energy yield of methanogenesis is less than 2 ATP per methane produced (93).

Methanogens can be divided into two groups: methanogens with cytochromes and methanogens without cytochromes (118). Methanogens with cytochromes all belong to the *Methanosarcinales* order, which has a broad substrate spectrum. For example, *Methanosarcina barkeri* can use all the methanogenic substrates except formate (124). Methanogens without

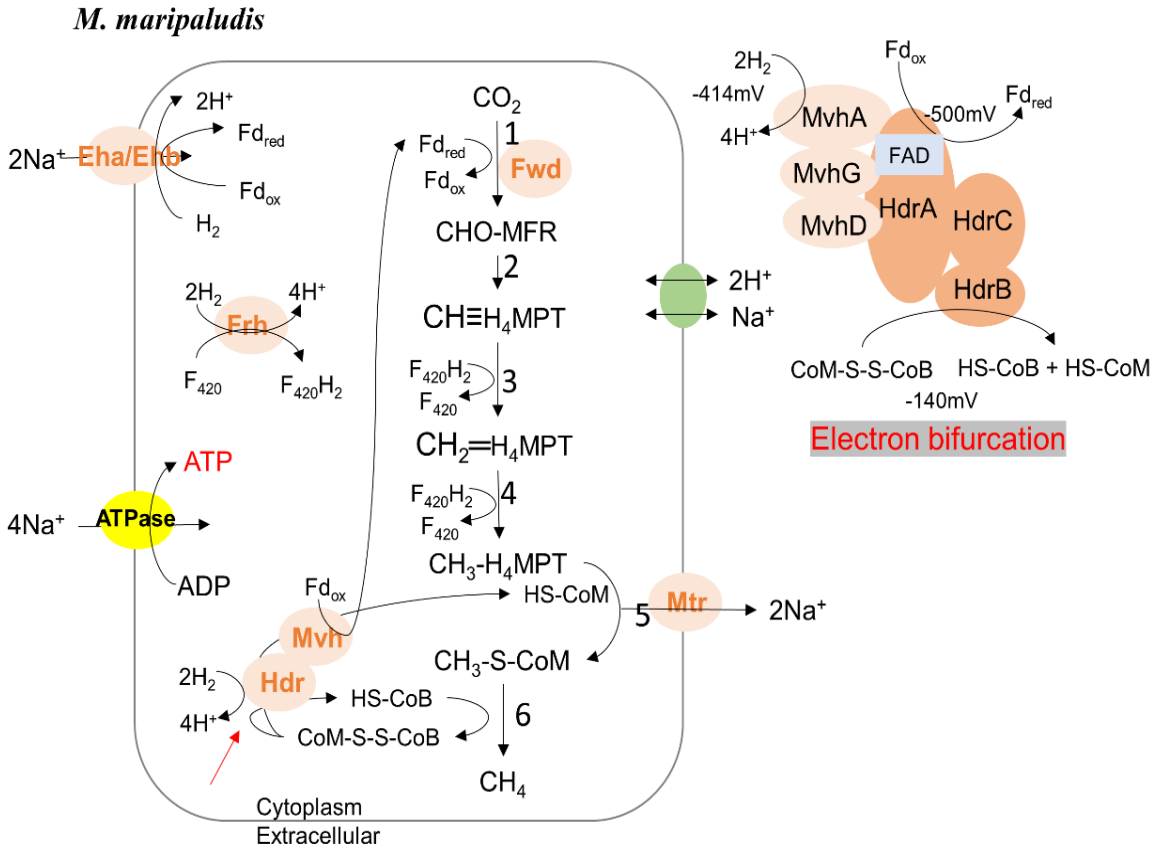

Figure 10. Methanogenesis pathway of methanogen without cytochromes (*M. maripaludis*). As shown in the electron bifurcation (red arrow), electrons from 2 mol H_2 are split between reducing ferredoxin and regenerating coenzymes B and M. Reduced ferredoxin from this reaction links it to CO_2 reduction, the first step in the pathway. Enzymes showed in light pink and orange are suggested to be Fe-S proteins. ATPase is shown in yellow color. Na^+/H^+ antiporter is shown in green color.

cytochromes include the *Methanobacteriales*, *Methanococcales*, *Methanomicrobiales*, and *Methanopyrales* orders. These four orders are all hydrogenotrophic methanogens. The methanogenesis of methanogens with and without cytochromes are described in Figure 10 and Figure 11.

ATP generation of methanogens without cytochromes, such as *M. maripaludis*, is driven by sodium motive force (Figure 10). One mole of methane is assumed to produce 0.5 moles of ATP in methanogens without cytochromes (118). All methanogens were shown to be sodium ion dependent. The sodium ion dependent step is methyl transfer from N5-methyltetrahydromethanopterin to coenzyme M, which is catalyzed by a Na+-translocating membrane-associated methyltransferase (Mtr) (125). The methyl group transfer step is driven by pumping out the sodium ions. This step is coupled with generation of a sodium motive force,

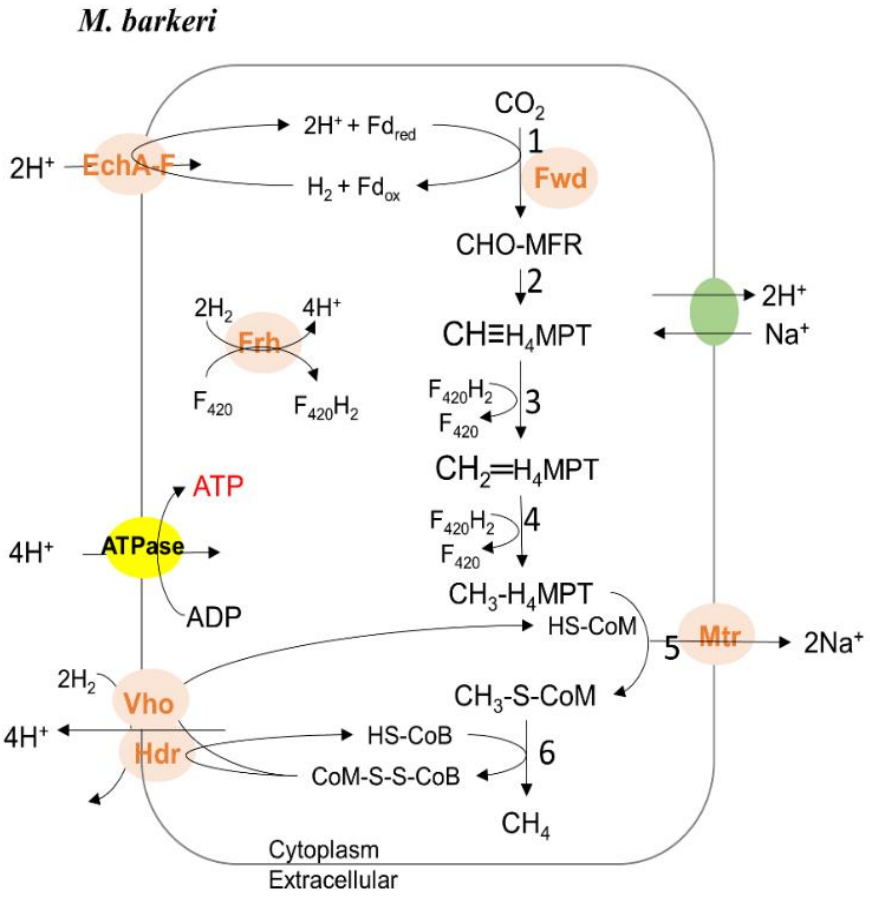

Figure 11. Methanogenesis pathway of methanogen with cytochromes (*M. barkeri*). Enzymes showed in light pink and orange are suggested to be Fe-S proteins. ATPase is shown in yellow color. Na^+/H^+ antiporter is shown in green color.

which will be recovered by oxidization of low-potential ferredoxin in the first step of hydrogenotrophic methanogenesis (Figure 10). The sodium motive force can drive ATP generation by A_1A_0-ATP synthase (118). Na^+/H^+ antiporters were suggested to be involved in maintain pH homeostasis (118).

Heterodisulfide reductase in methanogens without cytochromes is the cytoplasmic [NiFe] hydrogenase (MvhADG) and heterodisulphide reductase (HdrABC) complex, which is a flavin-based electron bifurcation system found in most hydrogenotrophic methanogens (Figure 10) (126,127). The reduction of the heterodisulfide ($E^{0\prime}$ equals –140 mV) by H_2 oxidization ($E^{0\prime}$ equals –414 mV) is coupled with the reduction of ferredoxin ($E^{0\prime}$ equals –500 mV). The reduced ferredoxin is required for CO_2 reduction in the first step of hydrogenotrophic methanogenesis. Although this step has no ATP produced, energy is saved by avoiding consuming sodium motive force for the ferredoxin reduction (93). Probably because the coupling of ferredoxin and CoM-S-S-CoB reduction with H_2 is not always tight as expected, methanogens without cytochromes yield less ATP than methanogens with cytochromes (118).

ATP generation of methanogens with cytochromes, such as *M. barkeri*, is driven by proton motive force (Figure 11). One mole of methane is assumed to produce 1.5 moles of ATP in methanogens with cytochromes (118). All methanogens can recycle heterodisulfide, CoM-S-S-CoM, back to CoM-SH and CoM-SH by heterodisulfide reductase, which is the major energy conserving step in methanogenesis (93). Heterodisulfide reductase in methanogens with cytochromes is the membrane methanophenazine-reducing [NiFe] hydrogenase (VhoACG) and methanophenazine-dependent heterodisulphide reductase (HdrDE) complex. The reduction of the heterodisulfide involves an ion-translocating electron transport chain containing cytochrome *b* subunit VhoC and the membrane-permeable electron carrier methanophenazine. The heterodisulfide reductase receives electrons from reduced methanophenazine, which is coupled to the translocation of protons across the membrane (128). Thus, the proton motive force is built up. Moreover, the sodium ion pumped outside the membrane by Mtr can also be translocated by Na^+/H^+ antiporter Nha in *M. barkeri* to build up proton motive force (118,129). The reduction of ferredoxin ($E^{0\prime}$ equals –500 mV) by H_2 ($E^{0\prime}$ equals –414 mV) requires reverse electron flow. The proton motive force can drive the reduction of ferredoxin by H_2 and ATP generation (118).

1.8. Direct interspecies electron transfer between methanogens and syntrophic bacteria helps degrade complex compounds.

Anaerobes usually obtain their energy through degradation of complex compounds, *e.g.* protein, cellulose. Around 2% of net primary production is fermented in anoxic environments (113). Biopolymers are first hydrolyzed by heterotrophic anaerobes to monomers, such as sugars, amino acids, purines, pyrimidines, fatty acids and glycerol. Fermentative bacteria convert these organic compounds to short chain alcohols, simple fatty acids (such as propionate, butyrate and acetate), and some other compounds (for example, H_2, CO_2, formate, and acetate). These

products are used as substrates by syntrophic bacteria and acetogens, which produce acetate, H_2, and CO_2. These end products of fermentative degradation are then converted to methane by methanogenesis, which is the last step of the anaerobic food chain (130). Therefore, methanogens can be used for the treatment of sewage wastes by a syntrophic relationship with bacteria (131).

During the syntrophic processes between methanogens and syntrophic bacteria, electrons move through chemical bonds and across biological membranes from one microbe to another microbe to conserve energy. This interspecies electron transfer occurs either by indirect electron transfer by electron shuttles (*e.g.* H_2, formate, acetate, or sulfur compounds) or by direct electron transfer through electron-conductive cellular materials or minerals. This direct interspecies electron transfer (DIET) is discussed in detail in Chapter 2 (131).

1.9. The importance and other applications of methanogens

The study of modern methanogens gives us a hint about early anaerobic metabolism. Their obligate anaerobic lifestyle suggests that they may have never undergone a full adaptation to aerobic environments that occurred in most other microbial lineages.

Methanogens play a vital role in the carbon cycle on Earth and are responsible for most of the methane in the atmosphere. The atmospheric concentration of methane has increased over the past 100 years from 0.9 to 1.8 parts per million (ppm) (132). Currently, from the 2 Gt (1 Gt = 10^{15} g) of methane produced per year, ~ 1 Gt is formed globally from acetate, CO_2, and formate by methanogens through methanogenesis in anoxic environments. Annually, ~ 1 Gt of methane is oxidized by anaerobic microbes through anaerobic oxidization of methane, ~ 0.6 Gt is oxidized to CO_2 by aerobic microbes, and ~ 0.4 Gt escapes into the atmosphere (118). Moreover, methane has 25 times higher global warming potential than CO_2 (133). Therefore, understanding the biological controls on methane emission may provide an opportunity to compensate for the emission of other greenhouse gases, such as CO_2.

Furthermore, methane produced by methanogens is a promising alternative fuel source. Because it produces more heat and burns cleaner than traditional fossil fuels, methane is the major component (~87%) of natural gas that used as heating fuel in household applicants (134).

1.10. *Methanococcus maripaludis* is the model organism

M. maripaludis was isolated from salt marsh sediment and belongs to the *Methanococcales* order (135). It is a hydrogenotrophic methanogen that can grow on either H_2 or formate rapidly with a doubling time of around 2 hours (135). It is a mesophile and grow best at 37°C. Its genome is relatively small and has only 1,722 protein-coding genes (136).

M. maripaludis is a premier model for systems biology to study anaerobic, archaeal, and autotrophic microbiology. It is cytochrome-lacking methanogen and continuous culturing

conditions have also been established (137,138). Genetic tools have also been established, including polyethylene glycol-mediated transformation, recombinant protein expression from shuttle vectors, insertional and markerless gene disruption, transposon insertion, and regulated gene expression. The essential genes in *M. maripaludis* have been suggested by a Tn-seq methodology (139).

1.11. Fe-S clusters are abundant in methanogens

Because Fe-S clusters are often vulnerable to oxidants including O_2 itself, methanogens possess many more Fe-S cluster proteins than aerobes (140). A genome sequence analysis predicted that *M. maripaludis* has at least 114 Fe-S cluster proteins representing 6.6% of its total proteins (133). This is more than double that of *E. coli*, which is predicted to have ~ 3% of its total proteins with Fe-S clusters (133). A direct measurement of the intracellular acid-labile S and Fe contents estimated that the amount of Fe-S clusters in *M. maripaludis* is ~20 times higher than that of aerobically grown *E. coli* (141).

Fe-S cluster proteins are directly involved in methanogenesis (Figure 10 and Figure 11). These proteins mostly have multiple clusters. For example, crystal structures showed that the formyl-methanofuran dehydrogenase (Fmd) complex involved in the first step of methanogenesis has 46 [4Fe-4S] clusters (20). The heterodisulfide reductase-[NiFe] hydrogenase (Hdr-Mvh) complex involved in the last step of methanogenesis in methanogens without cytochromes has 28 [4Fe-4S] clusters (142). The heterodisulfide reductase VhoACG-HdrDE, the energy converting [NiFe]-hydrogenases EchA–F (*E. coli* hydrogenase), and Eha/Ehb are also Fe-S proteins (143). The flavoprotein (Frh; an F_{420}-reducing [NiFe]-hydrogenase) that catalyzes the reduction of F_{420} with H_2 to $F_{420}H_2$, which is required as the electron donor for the third and the fourth steps of methanogenesis, is also a Fe-S protein (144).

1.12. Recent advance and hypothesis in the Fe-S cluster biosynthesis in methanogens

The Fe-S cluster biosynthesis system in bacteria and eukaryotes includes NIF, SUF, and ISC systems. These three systems all contain cysteine desulfurase that can donate sulfur from cysteine. However, many archaea do not contain cysteine desulfurase homologs. Instead, *M. maripaludis* was found to use sulfide, which is abundant in anaerobic habitats, rather cysteine as their sulfur source for Fe-S assembly (114). Although methanogenic archaea produce numerous Fe-S cluster proteins, the major cluster biosynthetic machineries found in bacteria and eukaryotes are generally missing in archaea (145). Only three Fe-S cluster-related proteins are conserved in almost all archaea (146): SufB, SufC, and the Nbp35/ApbC homolog.

Nbp35/ApbC proteins are P-loop nucleoside triphosphatases, which are proposed to function as scaffold or carrier for initial Fe-S cluster assembly in eukaryotes and bacteria (50,147-149). Protein sequence alignments of Nbp35/ApbC homologs show that they have three conserved

motifs: a Walker A box (ATP binding/hydrolysis motif), a CXXC motif in the C-terminal domain (Fe-S cluster binding site), and a conserved Ser residue (probably involved in enhancing ATPase activity) (148,149). Besides, Nbp35 also has a $CXXC(X)_5C$ motif in the N-terminus compared to Cfd1 (Figure 12), coordinating a [4Fe-4S] cluster, which is essential for cell growth (150).

Archaeal Nbp35/ApbC homolog was suggested to be a carrier before (148). A previous study of the archaeal Nbp35/ApbC homolog (MMP0704 from *M. maripaludis*) proved that MMP0704 can complement the tricarballylate growth defect of *S. enterica* Δ*apbC* mutant (148). Its conserved motifs, the Walker A box and the C-terminal CXXC motif, are required for the complement. Purified MMP0704 can be reconstituted with a Fe-S cluster, which has a UV-visible absorption spectrum typical of Fe-S cluster proteins (148). However, the Fe-S cluster type on MMP0704 is still unclear. These results suggested that the archaeal Nbp35/ApbC can function as a carrier in bacteria, but its physiological function in archaeal hosts is still unknown. Archaeal Nbp35/ApbC homologs have all the mentioned conserved motifs/residues as Nbp35 (Figure 12), which suggest that the archaeal Nbp35/ApbC homolog probably functions as a scaffold like eukaryotic Nbp35.

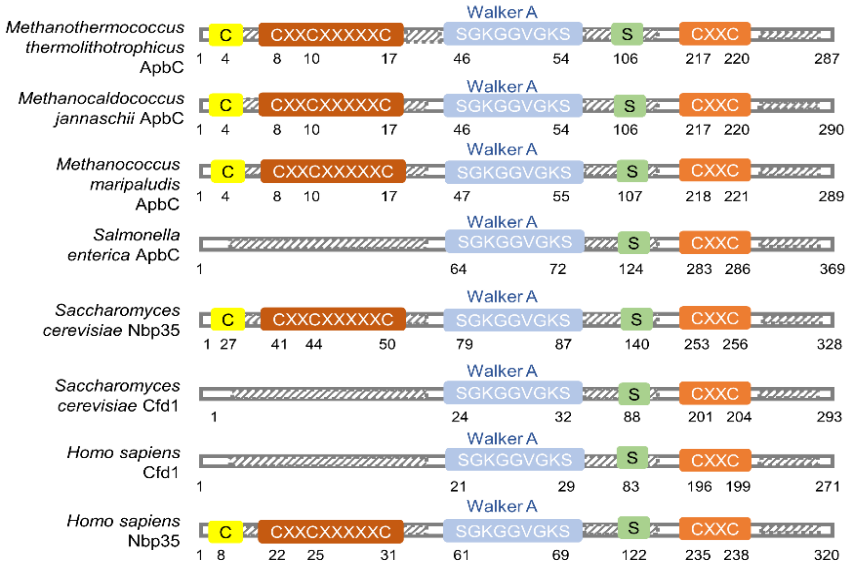

Figure 12. Comparison of conserved residues of bacterial and eukaryotic ApbC, Nbp35, Cfd1 and archaeal ApbC/Nbp35 homologs based on multiple sequence alignment.

Archaeal SufB also contain the conserved cysteine and histidine residues of *E. coli* SufB/D (Figure 13). Besides, it also has two other highly conserved cysteine residue, C145 and C175 of *Methanothermococcus thermolithotrophicus* (*Mth*) SufB, which are probably involved in Fe-S cluster assembly. Archaeal SufC have all three conserved motifs, Walker A and B motifs as well

as an ABC binding site, of *E. coli* SufC (Figure 13). The K40 residue in the Walker A motif of SufC was found to be essential for ATP hydrolysis, while K40R mutation lock SufC into an ATP binding form (75,151). The K40 residue is also conserved in archaeal SufC. Therefore, we proposed archaeal SufC is also an ATPase. Besides, SufC from most methanogens have three conserved cysteine residues in the N-terminus (Figure 13), which are probably Fe-S cluster binding sites.

Based upon a whole genome transposon mutagenesis study, *sufB* (locus tag: MMP1169) and *sufC* (locus tag: MMP1168) in *M. maripaludis* is suggested to be essential while *Nbp35/ApbC* (locus tag: MMP0704) is suggested to be non-essential (152). Accordingly, we hypothesized that SufB and SufC form a $SufB_2C_2$ complex, which plays a crucial role in Fe-S cluster biosynthesis as a scaffold in methanogens. Considering the conserved cysteine and histidine residues on archaeal SufB and SufC, we proposed that the *de novo* assembled Fe-S cluster on the $SufB_2C_2$ scaffold is either located on SufB/SufC, or on the bridging between SufB and SufC. Another possibility is both SufB and SufC bind one Fe-S cluster. Additionally, we proposed MMP0704 is a non-essential Fe-S transfer protein.

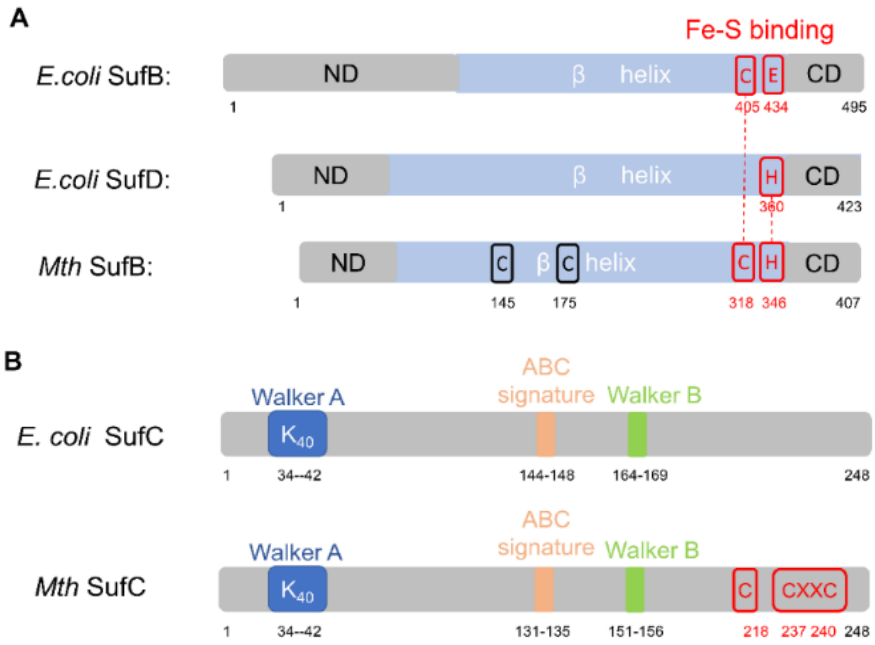

Figure 13. Sequence comparisons of *E. coli* and *Mth* Suf proteins.
(A) An alignment of *E. coli* SufB/D with *Mth* SufB/D. The residues predicted for cluster binding are labeled in red. (B) An alignment of *E. coli* SufC with *Mth* SufC. The conserved Cys residues in archaea are labeled in red. The conserved C405 and E434 residues of SufB, and the H360 residue of SufD have been proposed to be the Fe-S cluster binding sites. The K40 residue in the Walker A motif of *E. coli* SufC is essential for ATP hydrolysis.

CHAPTER 2. DIRECT INTERSPECIES ELECTRON TRANSFER BETWEEN ARCHAEA AND BACTERIA[1]

2.1. Introduction

In an anoxic environment, bioavailable energy is often achieved by anaerobic degradation of large and complex compounds, e.g. cellulose, other polysaccharides, proteins, lipids and nucleic acids. As shown in Figure 14, these large polymers are first degraded to monomers by hydrolytic reactions. Then these monomers are further degraded by primary fermenters to simple molecules,

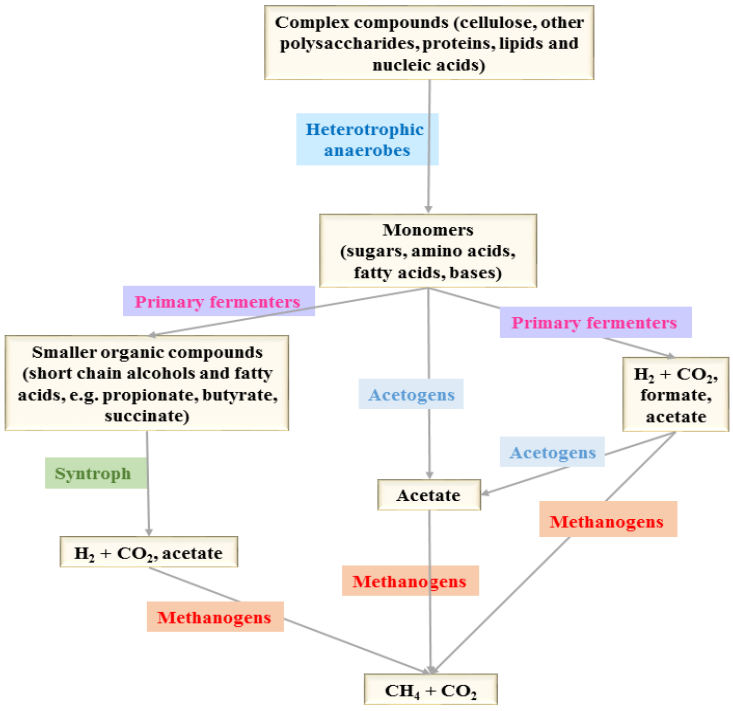

Figure 14. The process of anaerobic degradation of complex compounds.
Large polymers are first degraded to monomers by hydrolytic reactions. Monomers are further degraded to simple molecules, e.g. $H_2 + CO_2$, formate, and acetate, which are substrates for methanogenic archaea to produce methane; or to short chain alcohols and fatty acids, e.g. ethanol, propionate, and butyrate, which can be converted to $H_2 + CO_2$, formate, and acetate by syntrophic microorganisms and further consumed by methanogens.

This chapter was previously published as Zhao C., Liu Y. (2017) Direct Interspecies Electron Transfer Between Archaea and Bacteria. In: Witzany G. (eds) Biocommunication of Archaea. Springer, Cham. Reprinted by permission of Springer, Cham.

e.g. H_2, formate, acetate, and CO_2, which are substrates for methanogenic archaea to produce methane. These monomers can also be converted to short chain alcohols and fatty acids, e.g. ethanol, propionate, butyrate, and succinate, which can be further degraded to H_2, CO_2, and acetate by syntrophic microorganisms and then consumed by methanogens. Without methanogens, the degradation reactions by syntrophs under standard conditions are energetically unfavorable. Methanogens drive these reactions by consuming their products (acetate, $H_2 + CO_2$, and formate) quickly to very low concentrations. On the other hand, syntrophs provide the substrates for methanogens. This mutually beneficial process is syntrophy, which is interdependent lifestyle that the metabolism of a compound can undergo only when multiple organisms coexist (153-155).

As another example of syntrophy, anaerobic methane-oxidizing (or methanotrophic) archaea can form consortia with sulfate-reducing bacteria (SRB), oxidizing methane to CO_2 while reducing sulfate to H_2S (156). The anaerobic oxidization of methane (AOM) process usually occurs when methane is the only available electron donor and the concentrations of suitable electron acceptors are high, e.g. in marine sediments above methane hydrates with high sulfate concentrations or in organic-rich freshwater sediments with high nitrate concentrations (118).

Both methanogenesis and AOM play important roles in global climate because methane, as a potent greenhouse effect gas, has 25 times higher of the global warming potential than CO_2 (157). The concentration of methane in the atmosphere has increased over the past 100 years from 0.9 to 1.8 parts per million (ppm) (132). Currently, from the 2 Gt (1 Gt = 10^{15} g) of methane produced per year, ~ 1 Gt is formed globally from acetate, CO_2, formate by methanogenic archaea through methanogenesis in anoxic environments. Annually, ~ 1 Gt of methane is oxidized by anaerobic microbes through AOM, ~ 0.6 Gt is oxidized to CO_2 by aerobic microbes, and ~ 0.4 Gt escapes into the atmosphere (118).

2.2. Interspecies electron transfer

In syntrophic processes, energy is conserved and transferred between different species by electron movement through chemical bonds and across biological membranes. Two different extracellular interspecies electron transfer mechanisms are possible: (i) electrons are transferred indirectly with electron shuttles, e.g. H_2, formate, acetate, or sulfur compounds, from one microbe to another (Figure 15A); or (ii) electrons are transferred directly by electro-conductive cellular materials or minerals, known as direct interspecies electron transfer (DIET) (Figure 15B) (131).

Interspecies hydrogen transfer is a well-documented strategy of extracellular interspecies electron transfer, in which H_2 is continuously produced by syntrophic bacteria and consumed by methanogens. Interspecies hydrogen transfer was first recognized in a coculture of the "S organism", which converts ethanol to acetate and H_2, and *Methanobacterium ruminantium*, which consumes H_2 for methanogenesis (158). The generation of H_2 is energetically unfavorable

at H_2 partial pressures (pH_2) > 100 Pa (159). Methanogens can consume H_2 and maintain pH_2 <10 Pa, allowing H_2-producing microbes to bypass the energetic barrier (160). H_2 plays an important role in many syntrophic process because H_2 is small, highly diffusible, and can be metabolized by diverse groups of microbes, such as methanogens, SRB, and denitrifiers (153).

As H_2 is poorly soluble in water, formate is a preferred interspecies electron carrier in aqueous environments (153,160-164), especially in cocultures feeding on proteins (165) or fatty acids like propionate and butyrate (163,166). Formate has ~ three times higher diffusion coefficient than H_2 in solutions and allows lager mass transfer to methanogens, so many syntrophic communities favor formate over H_2 transfer (162). Additionally, some syntrophic interactions can use both H_2 and formate to transfer electrons (153,162,167,168). In a coculture with the dual H_2 and formate transfer mechanism, when the hydrogenase gene (*hybL*) of *Geobacter sulfurreducens* was deleted, the formate dehydrogenase gene (*fdnG*) was overexpressed (168).

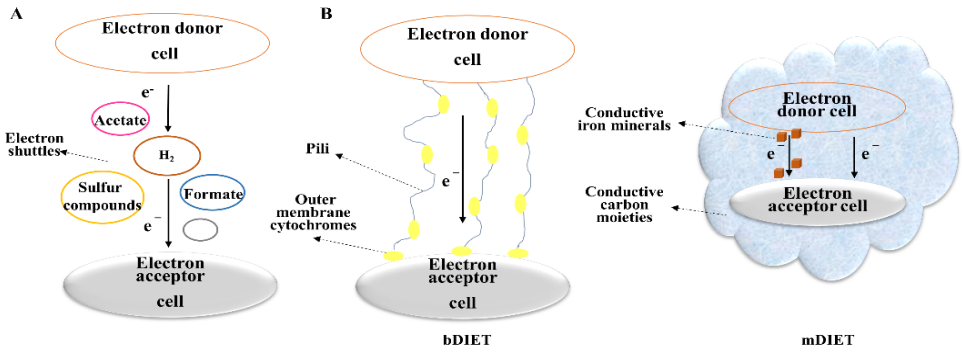

Figure 15. Schemes of extracellular interspecies electron transfer.
(A) Electron transfer via electron shuttles, e.g. H_2, formate, acetate, or sulfur compounds. (B) Direct interspecies electron transfer (DIET). Left: During biological DIET (bDIET), electrons are transferred by electro-conductive cellular materials, e.g. pili and/or extracellular cytochromes either localized on the cell surface or along pili. Right: During mineral DIET (mDIET), electrons are transferred via conductive iron minerals or conductive carbon moieties, e.g. magnetite, granulated activated carbon (GAC), biochar, graphite, or carbon cloth.

In addition to H_2 and formate, other molecules can also function as electron shuttles. Acetate, the substrate for acetoclastic methanogenesis, can carry electrons among syntrophic partners (169,170). Moreover, sulfur compounds (171-174), humics and humics equivalents (175-179), and flavins (180-182) can all work as interspecies electron carriers. For over 40 years, the indirect interspecies electron transfer with electron carriers had been considered as a main mechanism of extracellular interspecies electron transfer (154).

DIET is an alternative interspecies electron transfer strategy discovered about two decades ago. In syntrophic cocultures, cells often aggregate in close physical contact. This phenomenon promotes effective electron transfer and makes DIET feasible. DIET has been found in both methanogenesis (183-185) and AOM (186,187) processes.

2.3. Direct interspecies electron transfer (DIET)

DIET is achieved by electrical contacts between the electron donor and acceptor cells (Figure 15B**).** Conductive pili, iron minerals, and carbon moieties can all function as electrical contacts during DIET. Two types of DIET have been proposed: the biological DIET (bDIET) and mineral DIET (mDIET), which are conducted by biological materials (e.g. pili and extracellular cytochromes) and conductive minerals, respectively (188).

2.3.1. Biological DIET (bDIET)

Biological DIET was first documented in a coculture of two bacterial species, *Geobacter metallireducens* and *Geobacter sulfurreducens*, grown with ethanol as the electron donor and fumarate as the electron acceptor (185,189). *G. metallireducens* can oxidize ethanol to CO_2 but cannot use fumarate as an electron acceptor, whereas *G. sulfurreducens* can reduce fumarate to succinate but cannot metabolize ethanol. This *Geobacter* coculture formed large (1-2 mm in diameter), electrically conductive aggregates that promote interspecies electron exchange using conductive pili and cytochromes for electrical connections. Deletion of *pilA* (encoding the structural pilin protein) or *omcS* (encoding a multiheme *c*-type cytochrome mainly associated with pili) eliminated syntrophic metabolism (185). Furthermore, deletion of the hydrogenase gene (*hyb*) in *G. sulfurreducens* resulted in faster formation of the aggregates, suggesting that bDIET instead of interspecies hydrogen transfer is the primary interspecies electron transfer mechanism in this coculture (185).

Biological DIET has also been reported between bacteria and methanogenic archaea. The coculture of *G. metallireducens* and *Methanosaeta harundinacea* stoichiometrically converted ethanol to methane (184) (Figure 16). *M. harundinacea* is the first methanogen found to have the DIET ability, although it is still unclear how this archaeon accepts electrons during DIET. In the aggregates, *M. harundinacea* highly expressed methanogenic genes, and *G. metallireducens* highly expressed *pilA* and the genes for ethanol metabolism. Furthermore, a *pilA*-deficient *G. metallireducens* strain was not able to metabolize ethanol or produce methane in the coculture with *M. harundinacea*, indicating that pili were important for DIET between *M. harundinacea* and *G. metallireducens*. The amount of methane produced in this coculture was consistent with a complete conversion of the added ethanol to methane based on the following reactions:

$$2\ CH_3CH_2OH + 2\ H_2O \rightarrow 2\ CH_3COOH + 8\ H^+ + 8\ e^-$$ (*G. metallireducens*)

$$2\ CH_3COOH \rightarrow 2\ CH_4 + 2\ CO_2$$ (*M. harundinacea*)

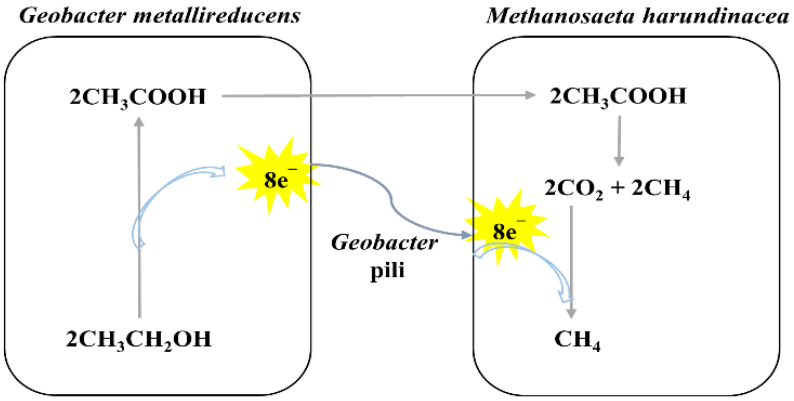

Figure 16. Mechanism of bDIET between *Geobacter metallireducens* and *Methanosaeta harundinacea*.
G. metallireducens oxidizes ethanol and transfers eight electrons to *M. harundinacea* via pili. *M. harundinacea* accepts electrons and produces methane from both acetate and CO_2.

$CO_2 + 8\ H^+ + 8\ e^- \rightarrow CH_4 + 2\ H_2O$ (*M. harundinacea*)
Sum reaction: $2\ CH_3CH_2OH \rightarrow 3\ CH_4 + CO_2$

As another methanogen found to have the bDIET ability, *Methanosarcina barkeri* formed aggregates (~ 0.1-0.2mm in diameter) with *G. metallireducens* and stoichiometrically converted ethanol to methane (183). A *pil*A-deficient *G. metallireducens* strain was not able to initiate the coculture, suggesting that conductive pili are important for DIET. Unlike *M. harundinacea*, *M. barkeri* can also utilize H_2 as an electron carrier in the coculture with *Desulfovibrio* (190) and *Pelobacter* (183). However, other known H_2-utilizing methanogens, e.g. *Methanospirillum hungatei* and *Methanobacterium formicicum*, do not have the DIET ability as discovered so far (184).

2.3.2. Mineral DIET (mDIET)

DIET has been shown to be possible without biological conductive materials (such as pili and cytochromes) in the presence of conductive minerals. Several examples of mDIET have been reported. (i) The addition of granulated activated carbon (GAC) can restore syntrophic metabolism in the coculture of *G. metallireducens* and *G. sulfurreducens* deficient in pili or cytochromes (175). GAC also accelerated methane production from ethanol in the coculture of *G. metallireducens* and *M. barkeri* (175). (ii) The addition of biochar or carbon cloth accelerated syntrophic metabolism in the coculture of *G. metallireducens* with *G. sulfurreducens* (191) or *M. barkeri* (192) with ethanol as the electron donor. Mutant strains lacking pili or pili-associated cytochromes restored DIET only in the presence of carbon cloth (192). (iii) Magnetite (Fe_3O_4) nanoparticles attached to pili was able to compensate for the absence of OmcS in a *Geobacter* coculture with ethanol and fumarate as the substrates (193). (iv) Magnetite

nanoparticles or carbon nanotubes stimulated methane production coupled to synthrophic butyrate oxidation in lake sediments (194). (v) A crystalline form of neutral red (2-amino-8-dimethylamino-3-methylphenazine) enhanced methane production in coal and food waste fed microbial communities and delivered electrons to *Methanosarcina mazei* (195).

2.4. Anaerobic oxidation of methane (AOM)

AOM often involves syntrophic associations between anaerobic methanotrophic archaea (ANME) and sulfate-, iron-, manganese-, or nitrate-reducing bacteria (196) (Figure 17). ANME are phylogenetically closely related to methanogenic archaea, and three distinct ANME groups have been identified: ANME-1, ANME-2, and ANME-3. The ANME-1 cluster is phylogenetically related to the *Methanomicrobiales* and *Methanosarcinales* orders but forms a

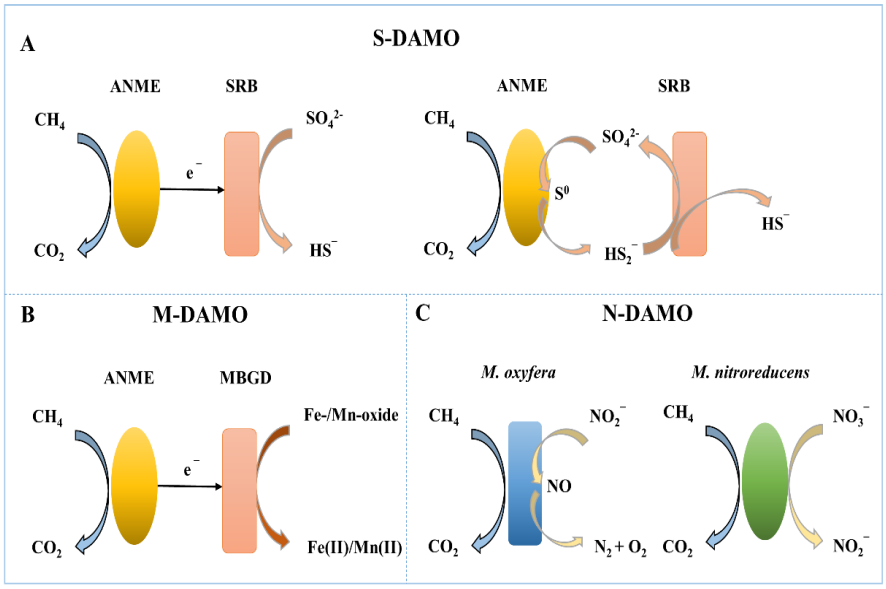

Figure 17. Three different models of anaerobic methane oxidation (AOM) with different electron acceptors.
(A) Sulfate-dependent anaerobic methane oxidation (S-DAOM). Anaerobic methanotrophic archaea (ANME) form aggregates with sulfate-reducing bacteria (SRB), coupling AOM with sulfate reduction. Alternative, ANME can autonomously perform AOM by reducing sulfate to zero-valent sulfur, which further reacts with environmental sulfide to form disulfide that is used by SRB. (B) Metal ion-dependent anaerobic methane oxidation (M-DAOM). ANME form aggregates with marine benthic group D (MBGD), coupling AOM with metal reduction. (C) Nitrite/nitrate-dependent anaerobic methane oxidation (N-DAOM). Both the bacterium *Candidatus* 'Methylomirabilis oxyfera' and the archaeon *Candidatus* 'Methanoperedens nitroreducens' can perform N-DAOM without partners.

separate cluster, ANME-2 is related to cultivated members of *Methanosarcinales* (197), and ANME-3 are more related to *Methanococcoides spp.* (198). ANME-1 and ANME-2 are mostly found in marine environments, while ANME-3 is mainly found in mud volcanoes and seep sediments (199-201).

AOM was first found to be coupled with sulfate reduction (Figure 17A), which is mediated by ANME (mostly belonging to the ANME-1 and ANME-2 clusters) and SRB (mostly belonging to the *Desulfosarcina*/*Desulfococcus* cluster of *Deltaproteobacteria*) (172,202,203). Sulfate-dependent anaerobic methane oxidation (S-DAOM) is mainly distributed in marine (196,204-208) and freshwater (209-214) environments. It plays an important role in the biogeochemical cycling of carbon and sulfur. Besides S-DAOM, metal-ion dependent anaerobic methane oxidation (M-DAOM) (Figure 17B) and nitrite/nitrate-dependent anaerobic methane oxidation (N-DAOM) (Figure 17C) have also been discovered (196).

2.4.1. Reaction mechanism of AOM

The AOM process has been proposed to follow a reverse methanogenesis pathway (Figure 18) according to the following studies. First, methyl-coenzyme M reductase (MCR), the terminal enzyme of methanogenesis, likely plays an important role in AOM. In microbial mats from anoxic methane seeps in the Black Sea, ANME cells were abundant (215), and the rate of S-DAOM was 10 times higher than that of methanogenesis (216). In this environment, MCR accounted for 7% of extracted proteins (217). Furthermore, the *mcrA* gene (encoding the α-subunit of MCR) was identified in ANME-1 and ANME-2 genomes (218). A crystal structure of ANME-1 MCR was highly similar to methanogenic MCR, suggesting that this enzyme is capable to catalyze the reverse methane-forming step (219). Second, most other methanogenic genes besides *mcr* are also present in ANME genomes. Enzymes for all methanogenic steps are encoded in an ANME-1 genome, except *mer* encoding a N^5, N^{10}-methylene-tetrahydromethanopterin (H_4MPT) reductase (220). Also, all genes required for methanogenesis from CO_2 are present and actively expressed in an ANME-2a organism except putative hydrogenase genes (221). Furthermore, the complete methanogenic pathway genes, including all *mcr* subunits and *mer*, were identified in the genome of an ANME-2d organism (*Candidatus* 'Methanoperedens nitroreducens') that is capable of independent N-DAOM (222).

2.4.2. Interspecies electron transfer in S-DAOM

In S-DAOM, electrons derived from methane oxidization by ANME presumably need to be transferred to SRB for sulfate reduction. However, the detailed mechanism of the electron transfer process is still not clear. Several hypotheses have been proposed (Figure 19):

(I) Electrons are transferred from ANME to SRB through the production and consumption of a diffusible metabolite, such as H_2, formate or methanethiol (220,223,224) (Figure 19A). This

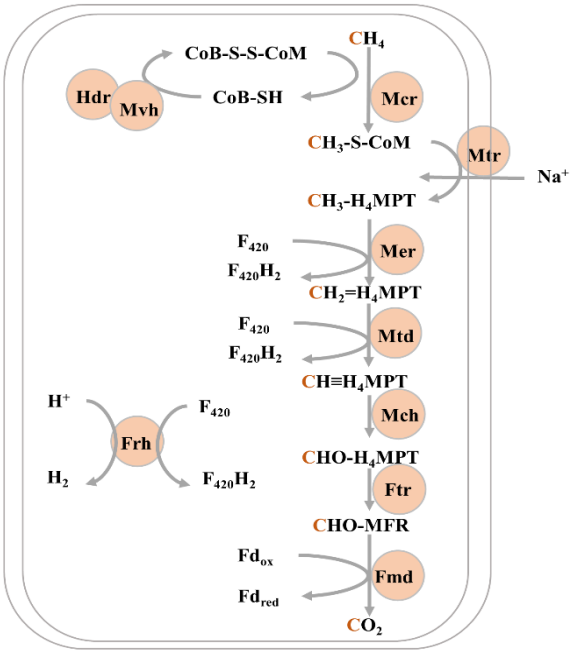

Figure 18. Proposed mechanism of AOM through the reverse methanogenesis pathway. Enzymes: Hdr, coenzyme B-coenzyme M heterodisulfide (CoB-S-S-CoM) reductase; Mvh, F_{420}-nonreducing hydrogenase; Mcr, methyl-coenzyme M (CH_3-S-CoM) reductase; Mtr, N^5-methyl-tetrahydromethanopterin (H_4MPT):coenzyme M (CoM) methyltransferase; Mer, N^5, N^{10}-methylene-H_4MPT reductase; Mtd, methylene-H_4MPT dehydrogenase; Mch, N^5, N^{10}-methenyl-H_4MPT cyclohydrolase; Ftr, formyl-methanofuran (MFR)-H_4MPT formyltransferase; Fmd, formyl-MFR dehydrogenase; Frh, F_{420}-reducing hydrogenase.

scenario is similar to the strategies for interspecies electron transfer during methanogenesis, but experimental evidence is lacking.

(II) An ANME-2 culture autonomously performed AOM by reducing sulfate to zero-valent sulfur (in the form of disulfide), which was disproportionated by SRB (174) **(**Figure 19B). However, this mechanism cannot be applied to ANME species without the ability of sulfate reduction.

(III) Biological DIET using cytochromes and pili has been proposed for electron transfer from ANME to SRB (Figure 19C). The genes encoding secreted multiheme *c*-type cytochromes were expressed in ANME-1 (220). Multiheme cytochromes are also present in ANME-2 genomes, and redox active transition metal ions (present in cytochromes) were detected in the space between cells in the ANME-SRB consortia (186). Furthermore, bDIET via nanowires (composed of pili and extracellular cytochromes) has been proposed to be a principal electron transfer mechanism in thermophilic AOM (TAOM) between ANME-1 and their SRB HotSeep-1 partner (225). The genome of HotSeep-1 (*Candidatus* 'Desulfofervidus auxilii') encodes genes

for pili and cytochromes productions. During consortial growth, HotSeep-1 highly expressed pili genes, and both ANME and HotSeep-1 overexpressed cytochrome genes (225).

(IV) For ANME species without cytochromes and pili, mDIET is possible (Figure 19D). For example, ANME-2a and ANME-2c can decouple AOM from SRB by using artificial electron acceptors, such as humic acids and soluble iron (226). This suggests that conductive materials can transfer electrons during AOM and that ANME-2 may couple AOM to metal-oxide reduction or other suitable electron acceptors. However, whether ANME-2/SRB can form aggregates without pili and whether the mechanism of DIET is fundamentally different between different ANME groups still need to be proved (227). Moreover, how widespread DIET is in various known ANME/SRB consortia and whether DIET enables AOM to be coupled with electron acceptors other than sulfate await further studies.

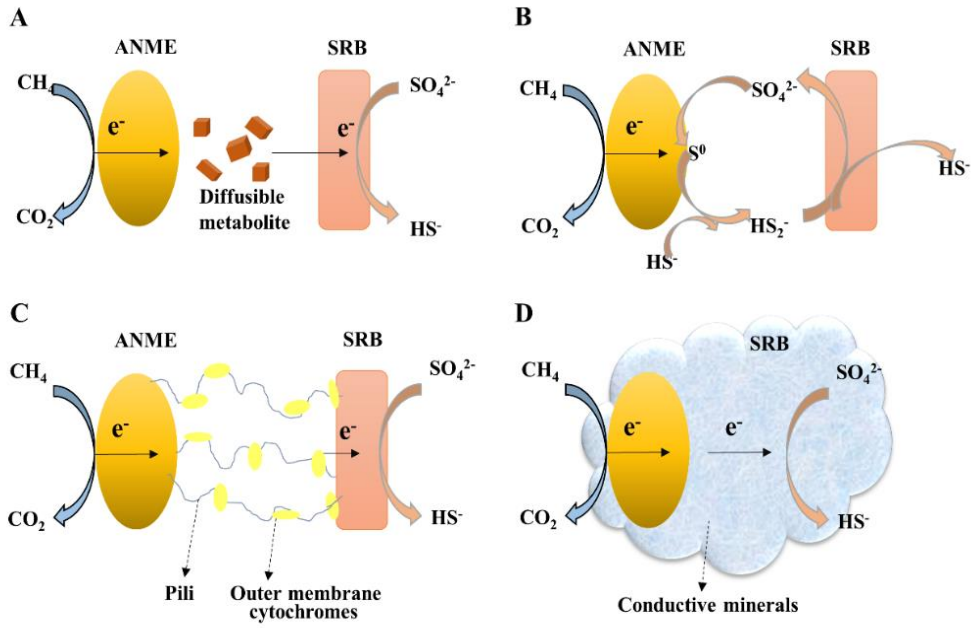

Figure 19. Proposed interspecies electron transfer mechanisms during S-DAOM.
(A) Electrons are transferred from ANME to SRB through diffusible metabolite, such as H_2, formate, or methanethiol. (B) ANME can autonomously perform AOM by reducing sulfate to zero-valent sulfur, which is disproportionated by SRB. (C) Electrons are transferred by bDIET with pili and extracellular cytochromes. (D) Electrons are transferred by mDIET with conductive mineral.

CHAPTER 3. IRON-SULFUR CLUSTER BIOSYNTHESIS IN METHANOGENIC ARCHAEA

3.1. Introduction

Iron-sulfur (Fe-S) clusters are the oldest and most versatile inorganic cofactors, present in all domains of life. Because iron and sulfide were presumably abundant on the anoxic Earth and high amounts of iron and sulfide can form Fe-S clusters spontaneously, Fe-S clusters are surmised to be one of most ancient cofactors in living organisms (21,228). With delocalized electron density over both the non-heme iron and inorganic sulfide, iron-sulfur clusters mediate biological electron transport in respiration and photosynthesis (229,230). Fe-S clusters also constitute the substrate binding sites of many redox and nonredox enzymes, such as the [4Fe-4S] cluster in aconitase (231). In DNA repair, Fe-S clusters play important structural and regulatory roles in the enzymes endonuclease III (15) and MutY (16). Fe-S clusters are also involved in gene regulation in most organisms, for example, [4Fe-4S] containing transcription factor FNR in Bacilli and Proteobacteria mediates an adaptive response under O_2 limiting condition (232). In addition, cells can use Fe-S clusters for iron/sulfur storage. For instance, [2Fe-2S] in biotin synthase donates sulfur for the conversion of desthiobiotin to biotin (19). These examples illustrate that Fe-S clusters are essential in various fundamental cellular processes.

Even though Fe-S clusters can be synthesized abiotically with reduced Fe and S, living organisms use complex machineries to make Fe-S cluster proteins. In general, the biosynthesis of Fe-S clusters requires two major steps: assembly and transfer (30,233). In the assembly step, a cysteine desulfurase (a pyridoxal-5'-phosphate-dependent enzyme) derives S from L-cysteine (234). The physiological Fe donor remains uncertain (235). A scaffold protein provides a molecular platform for Fe and S to meet and form a cluster *de novo* (236,237). In the transfer step, the pre-formed cluster is delivered to specific target apo-proteins either directly from the scaffold—with the help of energy dependent chaperones—or indirectly through Fe-S cluster carrier proteins (235). The protein machineries for Fe-S cluster biosynthesis are diverse in different organisms and vary depending on the growth conditions. Bacteria have three known machineries: the NIF, ISC, and SUF systems (235,238,239). Eukaryotes have the ISC system in the mitochondrion (37) and the SUF system in the plastid (38). Additionally, eukaryotes possess a CIA (cytosolic iron-sulfur assembly) machinery essential for maturation of Fe-S proteins in the cytosol and nucleus (39).

The SUF system is widely distributed in all three domains of life (61). The *suf* operon is diverse in different species (Figure 6), containing two to more than six different genes that encode protein functions such as cysteine desulfurase (*e.g.* SufS and SufE), scaffold (*e.g.* SufU and SufBCD), and carrier (*e.g.* SufA and HscA/B).

The SUF operon in *E. coli* includes six genes, *sufA*, *sufB*, *sufC*, *sufD*, *sufS*, and *sufE* (62). SufS-SufE complex work as a cysteine desulfurase to donate sulfur to the scaffold to assemble

Fe-S clusters. SufA was suggested to be a Fe-S cluster carrier protein (69,81). SufB was proposed to be an Fe-S scaffold protein (72) and a [4Fe-4S] cluster was observed in reconstituted SufB (73). It accept sulfur from SufE only when SufC is bound on SufB (73). SufD was proposed to escort iron entry into the scaffold complex (75). SufC is an ATPase of the ABC superfamily. It contains all three conserved motifs of typical ATP-hydrolyzing domains of ABC ATPases, Walker A and B motifs as well as an ATP binding cassette (ABC signature) (78). SufB and SufD are homologs, and both bind one SufC to form a $SufBC_2D$ complex (70). The crystal structure of SufC indicated that the unique Q-loop structure on its surface is probably the binding site for SufB or SufD (78). SufB, SufC, and SufD in *E. coli* form a $SufBC_2D$ complex, which was suggested to be a scaffold assembled a [4Fe-4S] cluster *de novo* (69,70) (70). This cluster was suggested to be located on $SufB^{C405}$, $SufB^{E434}$, and $SufD^{H360}$ (71,76).

As anaerobes, methanogens possess many more Fe-S cluster proteins because Fe-S clusters are often vulnerable to oxidants including O_2 itself (140). A genome sequence analysis predicted that *M. maripaludis* has at least 114 Fe-S cluster proteins representing 6.6% of its total proteins (133). This is more than double of that of *E. coli*, which is predicted to have ~3% of its total proteins with Fe-S clusters (133). A direct measurement of the intracellular acid-labile S and Fe contents estimated that the amount of Fe-S clusters in *M. maripaludis* is ~20 times higher than that in aerobically grown *E. coli* (141). Fe-S cluster proteins are directly involved in methanogenesis, the pathway from which methanogens obtain all or most of their energy. These proteins mostly have multiple clusters. For example, a crystal structure of the formyl-methanofuran dehydrogenase (Fmd) complex revealed that it had 46 [4Fe-4S] clusters (20), and the heterodisulfide reductase-[NiFe] hydrogenase (Hdr-Mvh) complex has 28 [4Fe-4S] clusters (142).

The Fe-S cluster biosynthesis pathway in methanogens is proposed to resemble the SUF system. Although methanogenic archaea produce numerous Fe-S cluster proteins, the major cluster biosynthetic machineries found in bacteria and eukaryotes are generally missing in archaea (145). Only three Fe-S cluster-related proteins are conserved in almost all archaea (146): SufB, SufC, and Nbp35/ApbC. Based upon a whole genome transposon mutagenesis study, *sufB* (locus tag: MMP1169) and *sufC* (locus tag: MMP1168) in *M. maripaludis* are likely to be essential while *nbp35/apbC* (locus tag: MMP0704) is suggested to be non-essential (152). Accordingly, we hypothesized that SufB and SufC form a $SufB_2C_2$ complex, which plays a crucial role in Fe-S cluster biosynthesis as a functional scaffold in methanogens.

3.2. Materials and methods

3.2.1. Strain and culture conditions

All strains used are described in Supplemental Table 1. *M. maripaludis* was grown in 28-ml aluminum seal tubes with 275 kPa of H_2:CO_2 (4:1, v/v) at 37°C in 5 ml of McC medium as

described previously (240). The 100 ml cultures were grown in 1-L bottles pressurized to 138 kPa with H_2:CO_2 (4:1, v/v). Puromycin (2.5 µg/ml) was added when needed. Before inoculation, 3 mM sodium sulfide was added as the sulfur source.

Escherichia coli strains were grown aerobically at 37°C in Luria–Bertani (LB) rich medium. When necessary, antibiotics were added at the following concentrations: 100 µg/ml ampicillin, 25 µg/ml kanamycin, 100 µg/ml spectinomycin, and 100 µg/ml chloramphenicol.

3.2.2. Production and Anoxic Purification of MMPSufCB in *M. maripaludis*

The *M. maripaludis* (MMP) *sufCB* operon was cloned into the pMEV4mTs (with an N-terminal strep-tag) vector. The resulting plasmid was transformed into the *M. maripaludis* strain S0001 by the PEG-mediated transformation method (138) for the expression of strep-tagged MMPSufBC. The following steps were carried out under anoxic conditions in an anaerobic chamber (Coy Laboratories) with an atmosphere of 95% (vol/vol) N_2 and 5% (vol/vol) H_2. All reagents and buffers were allowed to sit for enough time inside the chamber for complete deaeration. Cells (from 1-L culture) were collected by centrifugation at 4000 × g for 10 min at 4°C. Then the cell pellets were resuspended in the binding buffer containing 50 mM sodium *N*-(2-hydroxyethyl) piperazine-*N*′-(2-ethanesulfonic acid) (Hepes) at pH 7.5, 300 mM NaCl, and 5 mM $MgCl_2$. The cells were disrupted by two freeze/thaw cycles in the presence of one pellet of cOmplete ethylenediaminetetraacetic acid (EDTA)-free Protease Inhibitor Mixture (Roche) and 10 U of DNase I (Sigma). The cell lysate was then centrifuged at 14,000 rpm (23,000 × g) for 20 min at 4°C. The supernatant was loaded on a strep-tactin (IBA) column with 1 ml resin equilibrated with the binding buffer. The proteins bound to the strep-tactin resin were washed with the binding buffer. The strep-tagged protein was then eluted with the elution buffer containing 50 mM sodium Hepes (pH 7.5), 300 mM NaCl, 5 mM $MgCl_2$, and 2.5 mM desthiobiotin. The eluted fractions (~ 15 ml) were analyzed by sodium dodecyl sulfate polyacrylamide gel electrophoresis (SDS-PAGE) and concentrated to 0.25 ml with a 30-kDa molecular weight cutoff centrifugal filter (Millipore). The purified protein was then supplemented with glycerol to final glycerol concentration of 20% (vol/vol) and stored at -80°C until use.

3.2.3. Production and Anoxic Purification of M. thermolithotrophicus SufBC in E. coli

M. thermolithotrophicus sufC (locus tag: F555DRAFT_01626) and *M. thermolithotrophicus sufB* (locus tag: F555DRAFT_01627) genes were cloned into pET15b (with an N-terminal His_6-tag) and pDCH (with a C-terminal His_6-tag), respectively. The pET15b-His_6-SufC was co-transformed with pDCH-SufB without a tag for the expression of MTHSufBC complex. All mutations were constructed using the QuikChange mutagenesis kit (Agilent).

The resulting plasmids were individually transformed into the *E. coli* Rosetta 2(DE3) strain (Novagen) for expression of recombinant proteins. Cultures were grown in LB with 200 µM ammonium iron (III) citrate and 30 µM L-methionine at 37°C with 250 rpm shaking until they reached an absorbance at 600 nm of 0.6-0.8. Isopropyl β-D-1-thiogalactopyranoside (IPTG; 0.1 mM) was added to induce the overnight production of recombinant proteins at 25°C with 110 rpm rotation speed. The following steps were carried out under anoxic conditions in an anaerobic chamber (Coy Laboratories) with an atmosphere of 95% (vol/vol) N_2 and 5% (vol/vol) H_2. All reagents and buffers were allowed to sit for enough time inside the chamber for complete deaeration. Cells were collected by centrifugation at 4000 × g for 10 min at 4°C. Then the cell pellet was resuspended in the binding buffer 2 (50 mM sodium Hepes, 300 mM NaCl, 5 mM $MgCl_2$, 20 mM imidazole, pH 7.5). The supernatants were loaded on the Ni-NTA column (Qiagen) equilibrated with the binding buffer 1. The proteins bound on Ni-NTA column was washed with the washing buffer (50 mM sodium Hepes, 300 mM NaCl, 5 mM $MgCl_2$, 50 mM imidazole, pH 7.5). The His_6-tagged proteins were eluted with the elution buffer (50 mM sodium Hepes, 300 mM NaCl, 5 mM $MgCl_2$, 200 mM imidazole, pH 7.5). The purified protein was then supplemented with glycerol to final glycerol concentration of 20% (vol/vol) and stored at -80°C until use.

3.2.4. Analytical and Spectroscopic Measurements.

All analytical analyses were performed in triplicate. Protein concentrations were determined using the BCA Protein Assay Kit (Pierce). Iron was quantified by using the Quantichrom Iron Assay Kit (BioAssay Systems). UV-visible absorption spectra were recorded on a Nanodrop 2000c spectrometer with samples in cuvettes (optic path = 1 cm) closed with rubber stoppers under anoxic conditions.

X-band EPR spectra were recorded at 7–10 K on a Bruker EMX spectrometer equipped with a standard resonator and Oxford ESR-900 helium flow cryostat. Multiple microwave powers were tested so that resonances were measured under nonsaturating conditions. The *g* values were determined by simulating spectra using EasySpin 5.2.20 (241).

3.2.5. Gel filtration chromatography

The experiment was performed using a Superdex^{TM} 200 10/300 GL column (GE Healthcare) with 50 mM sodium Hepes, 200 mM NaCl, 5 mM $MgCl_2$, pH 7.5. The column was calibrated by the gel filtration markers kit for protein molecular weights 29,000-700,000 Da (Sigma-Aldrich). Protein samples were incubated with 10 mM EDTA and 10 mM DTH overnight and centrifuged at 14,000 × g for 10 mins to remove the precipitate before loading on the column. Fractions were collected and resolved on the SDS-PAGE.

3.2.6. Iron-sulfur cluster transfer reaction

All following experiments were performed anoxically in an anaerobic chamber with an atmosphere of 95% (vol/vol) N_2 and 5% (vol/vol) H_2. The His-tagged *E. coli* aconitase B (AcnB) was purified from the *E. coli* strain JW0114 from the ASKA collection (242) following the purification procedure as described (243). To prepare apo-AcnB, the purified protein was treated with 10 mM EDTA and 10 mM sodium dithionite (DTH) at 4°C overnight. To remove free Fe, the apo-AcnB was then buffer-exchanged using a PD MiniTrap G-25 column (GE Healthcare) pre-equilibrated with the buffer containing 50 mM sodium Hepes (pH 7.5), 300 mM NaCl, and 5 mM $MgCl_2$.

For cluster transfer, the apo-AcnB and strep-tagged MMPSufB_2C_2 were separately pretreated with 5 mM of 1, 4-dithiothreitol (DTT) for 30 min. Then the apo-AcnB (0.2 nmol) and tested proteins (1.0 nmol protein containing 0.4 nmol of [4Fe-4S]) were mixed together in a total reaction volume of 10 µL and incubated for 20 min at room temperature. For the aconitase activity assay, 5 µL of the cluster transfer reaction mixture (containing 0.1 nmol AcnB and 0.5 nmol MMPSufB_2C_2) was added to a freshly prepared mixture containing 50 mM sodium Hepes (pH 7.5), 300 mM NaCl, 5 mM $MgCl_2$, 0.25 mM $NADP^+$, 25 mM sodium citrate, 0.3 mM $MnCl_2$, and 1 µM of His-tagged *E. coli* isocitrate dehydrogenase (purified from the *E. coli* strain JW1122 from the ASKA collection (242)) in a total volume of 100 µL. The aconitase activity was assayed by monitoring the formation of NADPH through the increase in absorbance at 340 nm (244).

3.3. Results

3.3.1. SufB and SufC from methanogen form a SufB_2C_2 complex *in vivo*

We have studied the SufB and SufC proteins in two methanogenic species: *M. maripaludis*, a common methanogen model denoted MMP (245), and *M. thermolithotrophicus*, denoted MTH. Based on protein sequence alignments, SufC proteins in these two species have 74.19% identity, while SufB proteins have 74.44% identity, while MMPSufB/D homolog has a 25% identity with *E. coli* SufB and a 30% identity with *E. coli* SufD. To study complex formation, we first expressed MMPSufCB operon in *M. maripaludis*. We also expressed MTHSufB and MTHSufC in *E. coli*. The MMPSufB and MMPSufC proteins were not soluble in *E. coli*. However, MTHSufB and MTHSufC were successfully expressed as soluble proteins in *E. coli*.

Three evidence demonstrate methanogen SufB/C form a complex. (i) A pull-down experiment was done in its native host, *M. maripaludis*. MMPSufCB operon with an N-terminal strep-tag on SufC were cloned in a vector. After expression and anaerobical purification, these proteins were analyzed by SDS-PAGE gel. This pull-down experiment showed that MMPSufB interacted with MMPSufC *in vivo* (Figure 20A), with protein identities confirmed by mass

spectrometry. (ii) Similarly, the pull-down experiment was also investigated in *E. coli*. MTHSufC with an N-terminal His_6-tag and MTHSufB without a tag were cloned in different vector and expressed simultaneously. This pull-down experiment showed that MTHSufB interacted with MTHSufC *in vivo* as expected (Figure 20B). These protein identities were also confirmed by mass spectrometry.

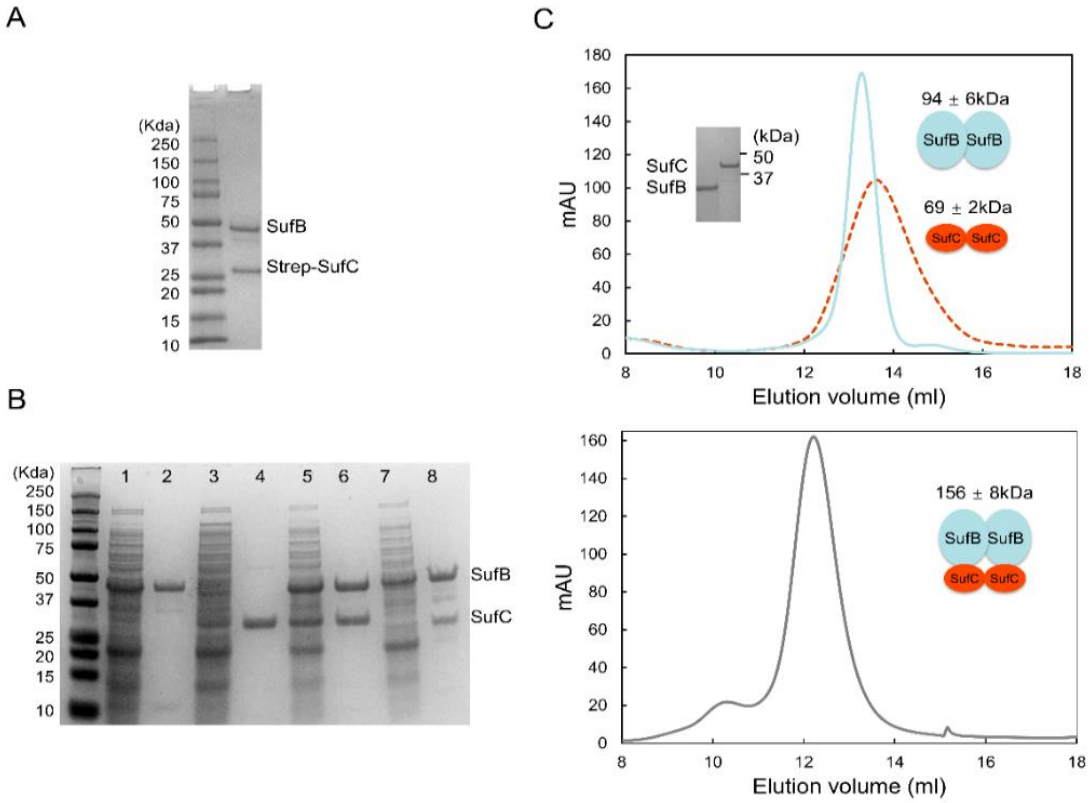

Figure 20. (A) A pull-down experiment showed that MMPSufB interacted with MMPSufC in *M. maripaludis. SufCB* operon was constructed with an N-terminal strep-tag on SufC. (B) A pull-down experiment showed that MTHSufB interacted with MTHSufC in *E. coli.* Lane 2 and lane 4 are elution (E) from the nickel chromatography purification. Lane 2: His_6-tagged SufC co-expressed with SufB without a tag; lane 4: His_6-tagged SufB co-expressed with SufC without a tag. Lane 1 and lane 3 are input of crude extracts (I) of lane 2 and lane 4, respectively. Both SDS-PAGE gel was stained by Coomassie blue. (C) Protein-protein interactions studied by gel filtration. The top panel: SufB (blue solid line) and SufC (red dashed line); embedded SDS-PAGE gel showed the band of SufC (left) and SufB (right). Embedded cartoons are SufB dimer (blue) and SufC dimer (red). The bottom panel: His_6-tagged SufC co-expressed with SufB (grey); embedded SDS-PAGE gel showed the bands of SufC (low) and SufB (upper). Embedded cartoon is $SufB_2C_2$ complex.

(iii) Size-exclusion chromatography of the MTHSufBC complex (Figure 20C) was done to study the stoichiometry of the complex. The results show: the purified MTHSufB eluted as a major peak with a molecular weight of about 94 ± 6 kDa corresponding to the size of a SufB dimer; the purified MTHSufC eluted as a major peak with a molecular weight of about 69 ± 2 kDa corresponding to the size of a SufC dimer; the purified MTHSufBC complex eluted as a major peak with a molecular weight of about 156 ± 8 kDa corresponding to the size of a $SufB_2C_2$ complex. These results suggest that methanogen SufB and SufC form a stable $SufB_2C_2$ complex *in vivo*.

3.3.2. The MMP$SufB_2C_2$ complex binds a [4Fe-4S] cluster in *M. maripaludis*

Scaffolds have the ability to assemble and transfer Fe-S clusters, as exemplified by NifU (246) and IscU (48). We therefore first investigated whether the MMP$SufB_2C_2$ complex can assemble an Fe-S cluster. Four lines of evidence demonstrate that the methanogen $SufB_2C_2$ complex bind a Fe-S cluster.

(i) The purified MMP$SufB_2C_2$ complex showed brownish color and displayed the characteristic UV-visible spectrum of a [4Fe-4S] cluster with only one broad absorption at around 420 nm (Figure 21A). Addition of 5 mM sodium dithionite (DTH) partially bleached the protein color and decreased the UV-Vis absorption (Figure 21A). Additionally, the Fe-S cluster on MMP$SufB_2C_2$ is rather labile, especially when it is exposed to air (Figure 21A).

(ii) Chemical analysis of Fe content indicated that the as-purified protein complex contained 1.57 ± 0.30 Fe per protomer.

(iii) The electron paramagnetic resonance (EPR) spectrum of the as-purified MMP$SufB_2C_2$ displayed a peak centered at g = 2.003 and represents an organic radical contaminant. The MMP$SufB_2C_2$ complex reduced by 5 mM sodium DTH displayed a signal with $g_{//} \sim 2.03$ and $g_{\perp} \sim 1.91$, characteristic of a $[4Fe\text{-}4S]^{1+}$ cluster (S_{tol} = ½) (Figure 21B). The same organic radical contaminant is overlaid with the [4Fe-4S] cluster signal.

(iv) MTH$SufB_2C_2$ complex has similar Fe content, UV-vis spectrum, and EPR spectrum of MMP$SufB_2C_2$ complex (Figure 21CD). The as-purified MTH$SufB_2C_2$ complex from *E. coli* has brownish color and contains 1.54 ± 0.32 Fe per protomer. It also displays an abroad absorption at ~420nm in the UV-vis spectrum (Figure 21C). DTH can also partially bleached the protein color and decreased the UV-Vis absorption (Figure 21C). The X-band EPR spectra of the as-purified MTH$SufB_2C_2$, displays a peak centered at $g \sim 2.01$, characteristic of a cubic $[3Fe\text{-}4S]^{1+}$ cluster (S_{tol} = ½), whereas the proteins reduced by 5 mM sodium DTH displayed a signal with $g_{//} \sim 2.00$ and $g_{\perp} \sim 1.91$, characteristic of a $[4Fe\text{-}4S]^{1+}$ cluster (S_{tol} = ½) (Figure 21D). Because the MMP$SufB_2C_2$ complex purified from its native host only contains a [4Fe-4S] cluster, this [3Fe-4S] cluster on the MTH$SufB_2C_2$ complex could possibly degrade from [4Fe-4S] cluster.

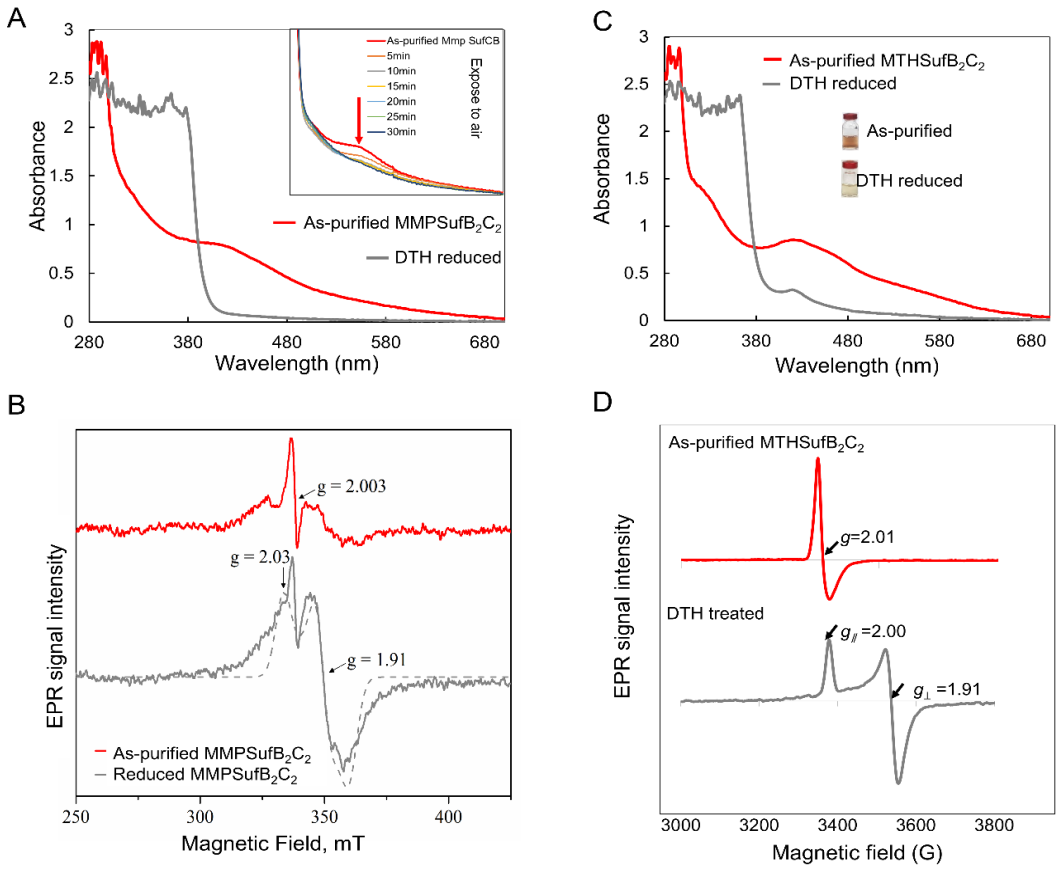

Figure 21. The $MMPSufB_2C_2$ complex binds a [4Fe-4S] cluster. (A) UV-Vis spectra of anoxically purified $MMPSufB_2C_2$ complex in the as-purified (red) and after DTH reduced (grey) states. (*Inset*) UV-Vis spectra of the protein exposed to air. The red arrow indicates the decrease of the absorbance at ~ 420 nm when the protein was exposed to air. (B) The X-band EPR spectra of anoxically purified $MMPSufB_2C_2$ complex in the as-purified (top) and DTH reduced (bottom) states. The DTH reduced spectrum was simulated as a nearly axial species with $g_{//}$ = 2.03 and $g_{\perp}$ = 1.91 (dashed trace). Both spectra of the as-purified and reduced samples contain an organic radical contaminant at approximately g = 2.003. Experimental conditions: microwave power, 1 mW; microwave frequency, 9.474 GHz; modulation amplitude, 10 G; temperature, 10 K. (C) UV-Vis spectra of anoxically purified $MTHSufB_2C_2$ complex. Proteins are in as-purified (red) and after DTH reduced (grey) states. (*Inset*) The as-purified and DTH reduced proteins. (D) The X-band EPR spectra of anoxically purified $MTHSufB_2C_2$ complex in the as-purified (red) and DTH reduced (grey) states. As-purified $MTHSufB_2C_2$ complex displays a peak centered at g ~ 2.01, characteristic of a cubic $[3Fe\text{-}4S]^{1+}$ cluster (S_{tol} = ½), whereas the proteins reduced by 5 mM sodium DTH displayed a signal with $g_{//}$ ~ 2.00 and $g_{\perp}$~ 1.91, characteristic of a $[4Fe\text{-}4S]^{1+}$ cluster (S_{tol} = ½). Experimental conditions: microwave power, 1 mW; microwave frequency, 9.473 GHz; modulation amplitude, 10 G; temperature, 10 K.

3.3.3. Three Cys residues, C218, C237, C240, are likely the [Fe-S] binding sites of the $SufB_2C_2$ complex

To determine the amino acid residues responsible for Fe-S cluster coordination, we performed mutational studies of MTHSufB and MTHSufC. In the *E. coli* $SufBC_2D$ complex, $SufB^{C405}$, $SufB^{E434}$, and $SufD^{H360}$ have been proposed to be the Fe-S cluster binding sites, and $SufB^{C254}$ is likely involved in S transfer (71,76). The C405, H360 and C254 residues on SufB are conserved in most archaea. The corresponding residues in MTHSufB are labeled in Figure 22. Additionally, MTHSufB has another cysteine residues (C145) conserved in almost all methanogens (Figure 22A). The bacterial SufC homologs do not have conserved Cys residues; however, MTHSufC has three C-terminal Cys residues (C218, C237, and C240) in a $CX_{18}CXXC$ motif in its C-terminus that is conserved in most methanogens (Figure 22B). These Cys and His

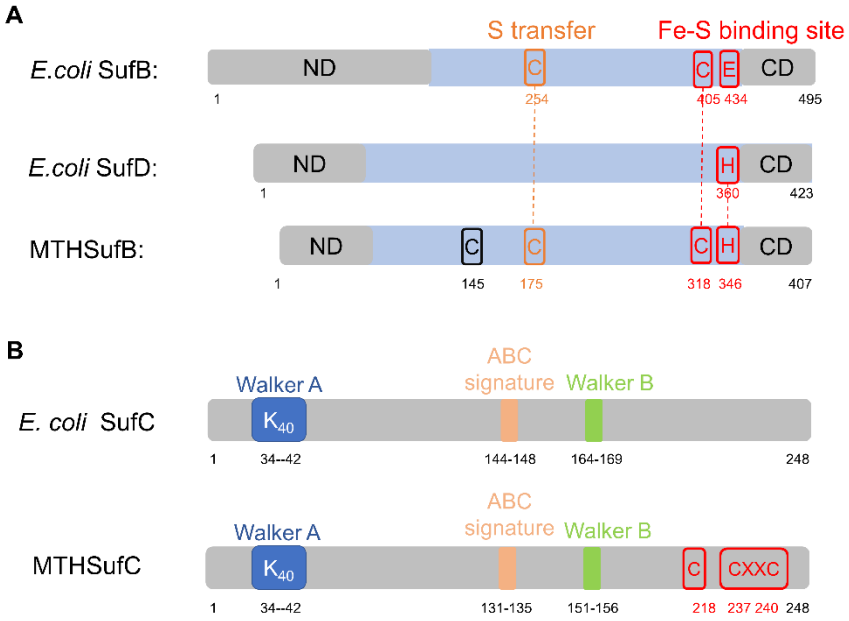

Figure 22. Sequence comparisons of *E. coli* and MTHSuf proteins. (A) An alignment of *E. coli* SufB (NCBI Reference Sequence: WP_042190429.1), SufD (NCBI Reference Sequence: WP_040083833.1) with SufB (locus tag: F555DRAFT_01627). The residues predicted to participate in cluster binding (red) and sulfur transfer (orange) are labeled. ND, N-terminal domain; CD, C-terminal domain. The numbers under each sequence indicate the corresponding amino acid positions. (B) An alignment of *E. coli* SufC (locus tag: Ga0063390_04487) with MTHSufC (locus tag: F555DRAFT_01626). The conserved Cys residues in archaea are labeled in red. Walker A (Blue), Walker B (green), and ABC (orange) motifs are labeled.

residues of MTHSufB/C were individually altered to Ser, and the mutant proteins were purified anoxically and characterized for their Fe-S cluster association by UV-visible and EPR spectrum.

Three evidences show that the Fe-S cluster binds to SufC. (i) SufC itself has cluster and sufB does not. As-purified MTHSufC showed brownish color, with 1.67 ± 0.14 iron per monomer. It also shows similar UV-visible spectrum and EPR spectrum of the MTHSufB$_2$C$_2$ complex (Figure 23AB). (ii) Mutations of sufC abolish Fe-S cluster on both sufC only and the SufB$_2$C$_2$ complex. The as-purified SufC mutations: MTHSufC(C218S), SufC(C237S), and SufC(C240S) proteins lost brownish color and UV-vis spectrum (Figure 23A). Iron on these three mutated SufC are not detectable. Similarly, the as-purified mutated MTHSufB$_2$C$_2$ complex, MTHSufB$_2$C$_2$ (C218/237/240S) complex, also lost the brownish color, UV-visible spectrum, and EPR spectrum (Figure 23CD). Iron is not detectable on this mutation, either. (iii) Mutations of SufB do not affect Fe-S cluster on the SufB$_2$C$_2$ complex. The as-purified MTHSufB$_2$(C145/175/318SH346S)C$_2$ complex shows similar UV-vis and EPR spectrum as the MTHSufB$_2$C$_2$ complex (Figure 23EF). Accordingly, these results suggest that the Fe-S cluster on the SufB$_2$C$_2$ complex was located on the three conserved cysteine residues of SufC and all three conserved Cys residues are required for Fe-S cluster binding on SufC.

3.3.4. The [4Fe-4S] cluster of MMPSufB$_2$C$_2$ can be transferred to apo-aconitase

We then investigated the ability of MMPSufB$_2$C$_2$ to transfer its [4Fe-4S] cluster to an apo-protein, the [4Fe-4S] cluster-dependent *E. coli* aconitase B (AcnB), *in vitro*. Fe-S cluster transfer from MMPSufB$_2$C$_2$ to apo-AcnB was monitored by the activation of the catalytic function of AcnB. The as-purified MMPSufB$_2$C$_2$ or apo-AcnB individually had no detectable activity as expected. However, the incubation of these two proteins together restored ~ 67% of the activity of the as-purified AcnB (Figure 24), demonstrating MMPSufB$_2$C$_2$ can transfer a [4Fe-4S] cluster to apo-proteins. Therefore, SufB$_2$C$_2$ is potentially a functional scaffold in methanogens.

3.4. Discussion

3.4.1. Insight into the Fe-S cluster biosynthesis in methanogens

In vitro biochemical experiments and *in vivo* functional analysis in this study provide the first insights into the mechanism of Fe-S cluster biosynthesis in methanogens. We found methanogen use SufB$_2$C$_2$ complex as a functional scaffold. This scaffold can assemble a [4Fe-4S] cluster on three conserved residues, C218, C237, and C240, on SufC. This Fe-S cluster on the scaffold can be transferred to an apo-protein. An earlier study suggested that methanogens use sulfide instead of free cysteine as the sulfur source for Fe-S cluster biosynthesis (247). Based on these findings, we propose the model of SUF system in methanogens (Figure 25). An iron donor and sulfide donor donate iron and sulfur, respectively. The iron and sulfur are then

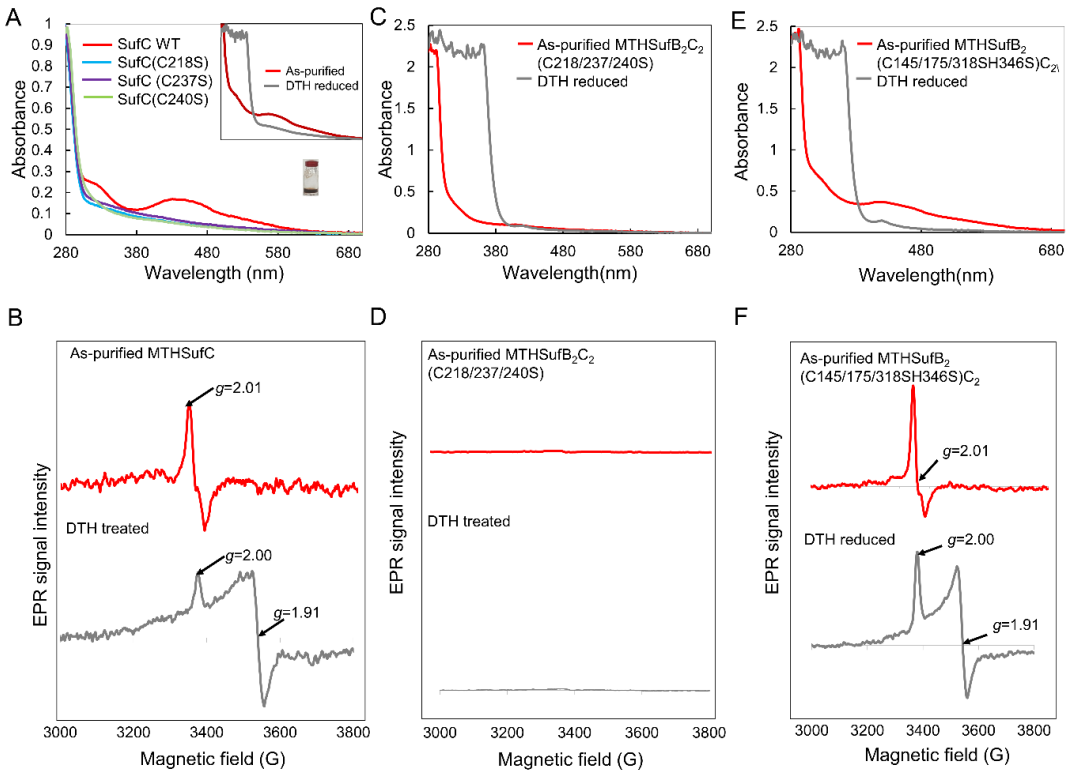

Figure 23. (A) UV-Vis spectra of anoxically purified MTHSufC and its three mutations: MTHSufC(C218S), MTHSufC(C237S), and MTHSufC(C240S). The concentrations of all proteins were 40 µM. (*Inset*) UV-Vis spectra of anoxically purified MTHSufC in as-purified (red) and after DTH reduced (grey) states. (B) The X-band EPR spectra of anoxically purified MTHSufC in the as-purified (red) and DTH reduced (grey) states. The as-purified MTHSufC displayed a peak centered at $g \sim 2.01$, characteristic of a cubic $[3Fe\text{-}4S]^{1+}$ cluster ($S_{tol} = ½$), whereas the proteins reduced by 5 mM sodium DTH displayed a signal with $g_{//} \sim 2.00$ and $g_{\perp} \sim 1.91$, characteristic of a $[4Fe\text{-}4S]^{1+}$ cluster ($S_{tol} = ½$). Experimental conditions: microwave power, 5 mW; microwave frequency, 9.476 GHz; modulation amplitude, 10 G; temperature, 10 K. UV-Vis spectra of anoxically purified protein: $MTHSufB_2C_2$ (C218/237/240S) complex (C) and $MTHSufB_2$(C145/175/318SH346S)C_2 complex (E). The X-band EPR spectra of anoxically purified proteins: $MTHSufB_2C_2$ (C218/237/240S) complex (D) and $MTHSufB_2$(C145/175/318SH346S)C_2 complex (F). As-purified $MTHSufB_2$(C145/175/318SH346S)C_2 complex, displayed a peak centered at $g \sim 2.01$, characteristic of a cubic $[3Fe\text{-}4S]^{1+}$ cluster ($S_{tol} = ½$), whereas the proteins reduced by 5 mM sodium DTH displayed a signal with $g_{//} \sim 2.00$ and $g_{\perp} \sim 1.91$, characteristic of a $[4Fe\text{-}4S]^{1+}$ cluster ($S_{tol} = ½$). No EPR spectrum is detected in $MTHSufB_2C_2$ (C218/237/240S) complex. Experimental conditions: microwave power, 1 mW; microwave frequency, 9.473 GHz; modulation amplitude, 10 G; temperature, 10 K.

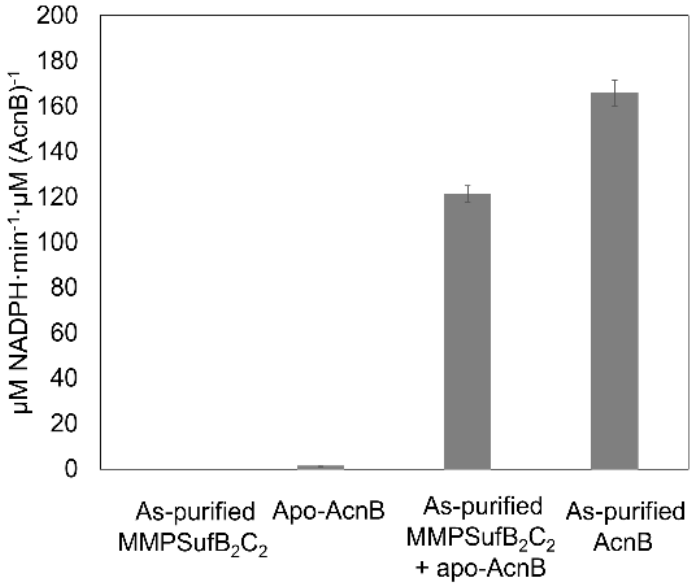

Figure 24. Activation of apo-AcnB by [4Fe-4S]-containing $MMPSufB_2C_2$ complex. Apo-AcnB was incubated with as-purified $MMPSufB_2C_2$ complex, and the aconitase activity was followed by the formation of NADPH as described in the materials and methods section. As controls, the as-purified $MMPSufB_2C_2$ complex, apo-AcnB, and as-purified AcnB were assayed individually. Data are mean ± standard deviation from three replicates.

assembled on the $SufB_2C_2$ scaffold and form a [4Fe-4S] cluster on SufC. The clusters will be then transferred to the target iron-sulfur proteins by carriers.

The Suf system, possibly present in early anaerobic forms of life, was suggested to be the most ancient Fe-S cluster biogenesis pathway (72). Phylogenetic analysis suggests that the *suf* genes first emerged among archaea and then horizontally transferred to bacteria and eukaryotes (72,248,249). The ancestral *suf* operon possibly has only two genes (*sufB* and *sufC*), and additional genes (*sufD*, *sufS*, *sufE*, *sufU*, and *sufA*) were recruited gradually during evolution possibly as an adaption to aerobic lifestyle (72). With the increasing oxygen level on earth, large amounts of the preferred iron donor, ferrous iron, turned to ferric iron and become less available for the Suf system. SufD evolved and functions for iron acquisition (72). Additionally, most of the sulfur donor, sulfide, turned to sulfate when exposed to increasing amount of oxygen. SufS and SufE evolved in response to the altered sulfur metabolism (72). Methanogens, as the obligate anaerobes, only have SufB and SufC proteins involved in Fe-S maturation. This study supports the view that $SufB_2C_2$ complex is the most ancient scaffold.

3.4.2. Comparisons of bacterial, eukaryotic, and archaeal SUF system

The detailed SUF system difference between methanogens and the well-studied bacterial and eukaryotic SUF system are discussed in the following several points.

First, the SUF system is probably the only system for Fe-S cluster maturation in methanogens. Only the core components of the SUF system are highly conserved throughout methanogens (146), suggesting that methanogens, and archaea in general, use the SUF system as the housekeeping system to synthesize Fe-S clusters. This is consistent with most gram-positive bacteria (250). However, SUF system can be a housekeeping Fe-S biosynthesis system or work redundantly with other systems in bacteria and eukaryotes. The Gram-negative bacterium *E. coli* uses the ISC system as the housekeeping system while the SUF system can be induced under oxidative stress or iron starvation situations (91). Most Gram-positive bacteria, like *Enterococcus faecalis*, only have one Fe-S cluster biosynthesis system, SUF (251). Fe-S clusters in eukaryotes are synthesized by the mitochondrial ISC system, the cytosolic Fe/S assembly (CIA) system, and the plastid SUF system originated from endosymbiotic cyanobacteria in photosynthetic organisms (30).

Second, only the *sufB* and *C* homologs are expressed from the SUF operon in most archaea (252), other SUF components are mostly missing in archaea. An operon that only contains *sufB* and *sufC* is much more prevalent in archaea than in bacterial genomes. In bacteria, the *sufBC* operon usually exists in bacteria characterized as obligate anaerobes or facultative anaerobes (72). Only a few eukaryotic genomes contain a *sufBC* operon, including the fused version of *sufB*

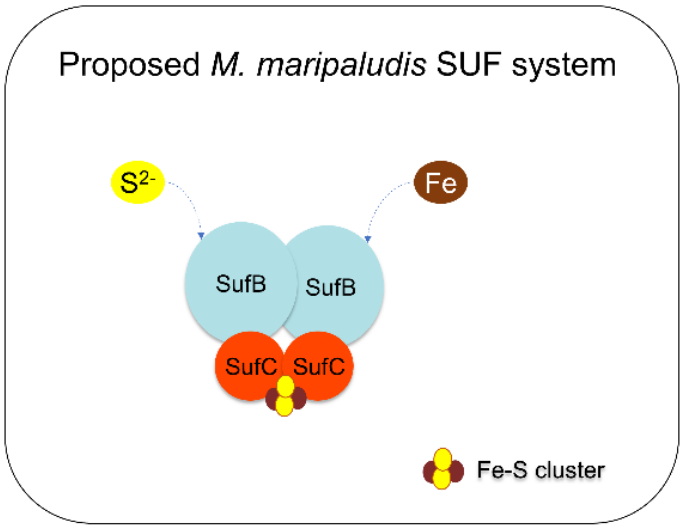

Figure 25. Proposed models of the SUF machinery in methanogens. Iron donor and sulfide donate iron and sulfur, respectively. The iron and sulfur meet each other and then assembled on the $SufB_2C_2$ scaffold, forming a [4Fe-4S] cluster on SufC.

and *sufC* operon, the simplest SUF operon, such as the unicellular, anaerobic, eukaryotic protist *Blastocystis* (248). Most bacterial and eukaryotic *suf* operons are diverse, containing two to more than six different genes (Figure 6).

Third, we found that the iron-sulfur cluster on the MTH$SufB_2C_2$ scaffold is bound to SufC rather than to SufB *in vivo*. However, the iron-sulfur cluster was suggested to be located on three conserved residues: $SufB^{C405}$, $SufB^{E434}$, and $SufD^{H360}$ inside the $SufBC_2D$ scaffold in the *E. coli* SUF system (74), which is the interface of the SufB and SufD heterodimer. Moreover, SufB in *E. coli* was an Fe-S cluster protein based on the observation that the reconstituted SufB has a [4Fe-4S] cluster (73), and it was also proposed to be an Fe-S scaffold protein (72).

CHAPTER 4. THE NBP35 HOMOLOG ACTS AS A NONESSENTIAL [4FE-4S] TRANSFER PROTEIN IN METHANOGENIC ARCHAEA

4.1. Introduction

Iron-sulfur (Fe-S) clusters are perhaps the oldest and most versatile inorganic cofactors in biochemistry and are essential in various fundamental cellular processes in all domains of life (6,7,228). The most common types of biological Fe-S clusters are the [2Fe-2S], [3Fe-4S], and [4Fe-4S] clusters. Although Fe-S clusters can be synthesized abiotically with reduced Fe and S, living organisms use complex protein machineries to make Fe-S clusters. In general, the machineries at least include a S donor, an Fe donor, and an Fe-S cluster scaffold (29,30). The S donor in most organisms is a cysteine desulfurase (a pyridoxal-5'-phosphate-dependent enzyme) that derives S from L-cysteine (253). The physiological Fe donor remains uncertain (32). An Fe-S cluster scaffold protein provides a molecular platform for Fe and S to meet and form an intact cluster *de novo* (254,255). Then the pre-formed cluster is delivered to specific target apo-proteins either directly from the scaffold or indirectly through Fe-S cluster carrier proteins (32).

The protein machineries for Fe-S cluster biosynthesis are diverse in different organisms and also vary depending on the growth conditions. Bacteria have three known machineries: the NIF (nitrogen fixation), ISC (iron-sulfur cluster), and SUF (sulfur formation) systems (32,35,256). The NIF system is responsible for the maturation of nitrogenase in N_2-fixing bacteria and is also present in some other anaerobic and microaerobic bacteria. The ISC system serves as the constitutive machinery in various bacteria (*e.g. E. coli*). The SUF system in *E. coli* is induced under Fe limitation and oxidative stress, whereas it is the sole system in a number of other bacteria (*e.g.* mycobacteria and bacilli). Eukaryotes have the ISC system in the mitochondrion (257) and the SUF system in the plastid (258). These two systems were likely derived from their prokaryotic ancestors by endosymbiosis. Additionally, eukaryotes possess a CIA (cytosolic iron-sulfur assembly) machinery essential for the maturation of Fe-S proteins in cytosol and nucleus (39).

The eukaryotic Nbp35 (nucleotide binding protein 35) and Cfd1 (cytosolic Fe-S cluster deficient 1) proteins form a heterocomplex that functions as an essential Fe-S cluster scaffold in the CIA machinery (39). Nbp35 and Cfd1 are homologous to each other, and their sequences have two common features (Figure 26): a deviant Walker A box or P-loop motif (characterized by two lysine residues) (259) and a CXXC motif at the C-terminal region. Nbp35 has an additional N-terminal ferredoxin-like domain (Figure 26). The Nbp35-Cfd1 complex binds two types of [4Fe-4S] clusters: one is stably coordinated by the N-terminal cysteine residues of Nbp35, and the other one binds to the C-terminal CXXC motif of both Cfd1 and Nbp35, bridging the protein-protein interaction interface (50,260,261). The bridging [4Fe-4S] cluster is transiently assembled and can be transferred to apo-proteins (50,150,262). The deviant Walker A motif is required for ATP binding and hydrolysis, and the ATPase activity is essential for *in vivo* Fe-S cluster assembly and transfer (260,263,264).

The bacterial Nbp35/Cfd1 homolog is named as ApbC (alternative pyrimidine biosynthetic protein C) in *Salmonella enterica*. The ApbC protein can assemble an Fe-S cluster and transfer the cluster to apo-proteins *in vitro* (149,265). Mutations of *apbC* in *S. enterica* prevented the growth on tricarballylate because ApbC is required for the maturation of TcuB (tricarballylate utilization protein B), a [4Fe-4S]-containing enzyme required for tricarballylate metabolism (265). The Walker A and C-terminal CXXC motifs are required for the *in vivo* function of ApbC

(149). These results suggest that the bacterial ApbC acts as an Fe-S cluster carrier protein that transfers an intact cluster to a specific target apo-protein (*i.e.*, TcuB).

The Nbp35/ApbC homologs are present in most sequenced archaea (266), although their physiological function remains unclear. A previous study showed that several archaeal homologs can complement the tricarballylate growth deficiency of the *S. enterica* Δ*apbC* mutant (148). Furthermore, the Nbp35/ApbC homolog from *M. maripaludis* (locus tag: MMP0704)—when heterologously expressed and purified from *E. coli*—can be reconstituted *in vitro* with an Fe-S cluster, although the cluster type was unclear (148). Here we show that MMP0704 purified from its native host has a [4Fe-4S] cluster that can be transferred to the apo-aconitase. Moreover, MMP0704 is nonessential for the viability of *M. maripaludis* under our tested growth conditions. These results suggest that MMP0704 is an Fe-S cluster transfer protein only required for the maturation of specific target proteins.

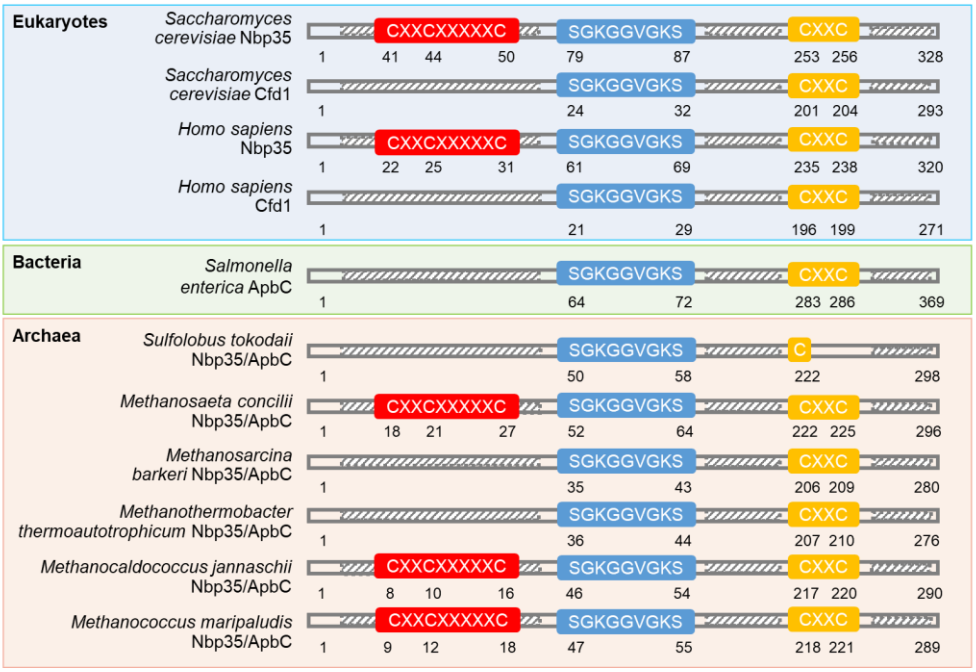

Figure 26. Comparison of conserved motifs of Nbp35, Cfd1, and ApbC homologs based on multiple sequence alignment. The CX_2CX_5C motif of the N-terminal ferredoxin-like domain responsible for Fe-S cluster binding is labeled in red; the deviant Walker A motif is labeled in blue; and the C-terminal CXXC motif responsible for Fe-S cluster binding is labeled in orange. The numbers under each sequence indicate the corresponding amino acid positions. The selected proteins for comparisons include *Saccharomyces cerevisiae* Nbp35 (locus tag: YGL091C), *Saccharomyces cerevisiae* Cfd1 (locus tag: H811_YJM1400I00176), *Homo sapiens* Nbp35 (locus tag: NUBP1), *Homo sapiens* Cfd1 (locus tag: NUBP2), *Salmonella enterica* ApbC (locus tag: STM2154), *Sulfolobus tokodaii* Nbp35/ApbC (locus tag: ST0174), *Methanosaeta concilii* Nbp35/ApbC (locus tag: MCON_0751), *Methanosarcina barkeri* Nbp35/ApbC (locus tag: Mbar_A2615), *Methanothermobacter thermoautotrophicum* Nbp35/ApbC (locus tag: MTH1176), *Methanocaldococcus jannaschii* Nbp35/ApbC (locus tag: MJ0283), and *Methanococcus maripaludis* Nbp35/ApbC (locus tag: MMP0704).

4.2. Materials and methods

4.2.1. Strain, media, and culture conditions

M. maripaludis strains were grown in 28-ml glass tubes with aluminum seals under 275 kPa of H_2:CO_2 (4:1, vol/vol) at 37°C in 5 ml of McN (minimal medium), McNA (McN + 10 mM sodium acetate), or McC (McNA + 0.2% [wt/vol] casamino acids + 0.2% [wt/vol] yeast extract) as described previously (267). The standard McN medium contains 25 μM ferrous ammonium sulfate, and the Fe-limiting McN media contain 0.5, 1.5, 5, or 10 μM ferrous ammonium sulfate. The 100 ml cultures were grown in 1-L bottles pressurized with 138 kPa of H_2:CO_2 (4:1, vol/vol). Puromycin (2.5 μg/ml) was added when needed. Before inoculation, 3 mM sodium sulfide was added as the sulfur source. When comparing the growth of the parent strain and the mutant, puromycin was omitted. The inocula were 0.1 ml of cultures (~10^7 cells) grown in the same medium per 5 ml culture. The growth was determined by measuring the increase in absorbance at 600 nm.

4.2.2. Construction of the Δ*mmp0704* mutant

The replacement of the *M. maripaludis mmp0704* gene with a *hpt* (8-azahypoxanthine transferase)-*pac* (puromycin N-acetyltransferase) cassette was generated in the *M. maripaludis* strain S0001 (245) by double homologous recombination (138,268). To make the plasmid p5L-R-*mmp0704* (Figure 27), the upstream and downstream regions of the *mmp0704* gene were amplified from the *M. maripaludis* S0001 genomic DNA. Then the plasmid p5L-R-*mmp0704* was transformed into *M. maripaludis* S0001 cells by the polyethylene glycol (PEG)-mediated transformation method (138). Upon transformation, genomic integration of the *hpt-pac* cassette through homologous recombination was positively selected with puromycin (2.5 μg/ml). Colonies of the selected transformants were subjected to PCR amplification to confirm complete integration (Figure 27).

4.2.3. Expression and anoxic purification of strep-tagged MMP0704 in *M. Maripaludis*

The *mmp0704* gene was cloned into the pAW42 vector (245) with an N-terminal strep-tag. The resulting plasmid was transformed into the *M. maripaludis* strain S0001 by the PEG-mediated transformation method (138) to generate the strain S798 for the expression of strep-tagged MMP0704. The following steps were carried out under anoxic conditions in an anaerobic chamber (Coy Laboratories) with an atmosphere of 95% (vol/vol) N_2 and 5% (vol/vol) H_2. All reagents and buffers were allowed to sit for enough time inside the chamber for complete deaeration. Strain S798 cells (from 1-L culture) were collected by centrifugation at 4000 × g for 10 min at 4°C. Then the cell pellets were resuspended in the binding buffer containing 50 mM sodium N-(2-hydroxyethyl) piperazine-N′-(2-ethanesulfonic acid) (Hepes) at pH 7.5, 300 mM NaCl, and 5 mM $MgCl_2$. The cells were disrupted by two freeze/thaw cycles in the presence of one pellet of cOmplete ethylenediaminetetraacetic acid (EDTA)-free Protease Inhibitor Mixture (Roche) and 10 U of DNase I (Sigma). The cell lysate was then centrifuged at 14,000 rpm (23,000 × g) for 20 min at 4°C. The supernatant was loaded on a strep-tactin (IBA) column with 1 ml resin equilibrated with the binding buffer. The proteins bound to the strep-tactin resin were washed with the binding buffer. The strep-tagged protein was then eluted with the elution buffer containing 50 mM sodium Hepes (pH 7.5), 300 mM NaCl, 5 mM $MgCl_2$, and 2.5 mM

desthiobiotin. The eluted fractions (~ 15 ml) were analyzed by sodium dodecyl sulfate polyacrylamide gel electrophoresis (SDS-PAGE) and concentrated to 0.25 ml with a 30-kDa molecular weight cutoff centrifugal filter (Millipore). The purified protein was then supplemented with glycerol to final glycerol concentration of 20% (vol/vol) and stored at -80°C until use.

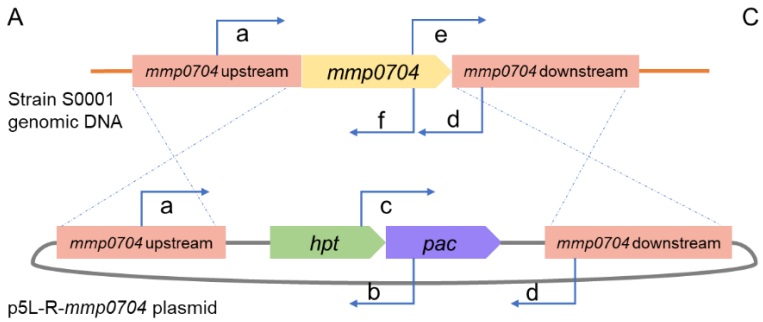

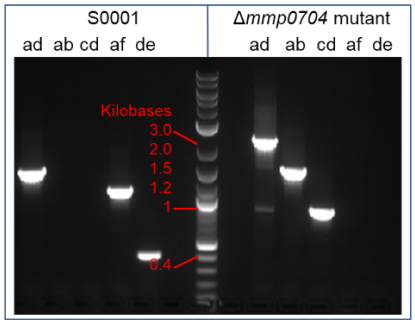

B

Primers	Sequences
a	5'-CTCTCCACAGGGCCGAAAATACGG-3'
b	5'-CTGTCATGGAAGGTCGTCTCCTC-3'
c	5'-CCGGATACAAAGTAAAAACTATTGTAAAAATTGAAGTTG-3'
d	5'-CGAGCGCCTTTTTATTTGGAAGC-3'
e	5'-GACGGAGTGGTAATCGTCACAACCCC-3'
f	5'-GGGGTTGTGACGATTACCACTCCGTC-3'

D

Primer pairs	Expected PCR product length (bp) of strain S0001	Expected PCR product length (bp) of Δ*mmp0704* mutant
ad	1518	2407
ab	0	1583
cd	0	919
af	1134	0
de	410	0

Figure 27. Deletion of *mmp0704* in *M. maripaludis*. (A) Construction of a *mmp0704* deletion. The p5L-R-*mmp0704* plasmid was constructed with the 1000 bp upstream and downstream fragments of *mmp0704* (870 bp) flanking the *hpt-pac* cassette. Upon transformation of p5L-R-*mmp0704* into the parent strain S0001, puromycin resistance can be acquired by double homologous recombination leading to the replacement of *mmp0704* with the *hpt-pac* cassette (1759 bp). Upper: *M. maripaludis* S0001 genomic DNA; lower: p5L-R-*mmp0704* plasmid. Blue arrows: six primers (a, b, c, d, e, f) were used for PCR to confirm of the replacement of *mmp0704*. (B) Primer sequences. (C) PCR results. The amplifications were performed using primers listed in (B). The primer pairs are labeled on top of each lane of the agarose gel. (D) The expected PCR product lengths using genomic DNA from S0001 and the Δ*mmp0704* mutant strains as templates.

4.2.4. Analytical and spectroscopic measurements

All analytical analyses were performed in triplicate. Protein concentrations were determined using the BCA Protein Assay Kit (Pierce). Iron was quantified by using the Quantichrom Iron Assay Kit (BioAssay Systems). UV-visible absorption spectra were recorded on a Nanodrop 2000c spectrometer with samples in cuvettes (optic path = 1 cm) sealed with rubber stoppers under anoxic conditions.

The X-band electron paramagnetic resonance (EPR) spectra were recorded at 7–10 K with a Bruker EMX spectrometer equipped with a standard resonator and an Oxford ESR-900 helium flow cryostat. Multiple microwave powers were tested so that resonances were measured under nonsaturating conditions. The *g* values were determined by simulating spectra using EasySpin 5.2.20 (241).

4.2.5. Iron-sulfur cluster transfer and aconitase activity assays

All following experiments were performed anoxically in an anaerobic chamber with an atmosphere of 95% (vol/vol) N_2 and 5% (vol/vol) H_2. The His-tagged *E. coli* aconitase B (AcnB) was purified from the *E. coli* strain JW0114 from the ASKA collection (242) following the purification procedure as described (243). To prepare apo-AcnB, the purified protein was treated with 10 mM EDTA and 10 mM sodium dithionite (DTH) at 4°C overnight. To remove free Fe, the apo-AcnB was then buffer-exchanged using a PD MiniTrap G-25 column (GE Healthcare) pre-equilibrated with the buffer containing 50 mM sodium Hepes (pH 7.5), 300 mM NaCl, and 5 mM $MgCl_2$.

For cluster transfer, the apo-AcnB and strep-tagged MMP0704 were separately pretreated with 5 mM of 1, 4-dithiothreitol (DTT) for 30 min. Then the apo-AcnB (0.2 nmol) and MMMP0704 (2.2 nmol protein containing 0.4 nmol of [4Fe-4S]) were mixed together in a total reaction volume of 10 µL and incubated for 20 min at room temperature. For the aconitase activity assay, 5 µL of the cluster transfer reaction mixture (containing 0.1 nmol AcnB and 1.1 nmol MMP0704) was added to a freshly prepared mixture containing 50 mM sodium Hepes (pH 7.5), 300 mM NaCl, 5 mM $MgCl_2$, 0.25 mM $NADP^+$, 25 mM sodium citrate, 0.3 mM $MnCl_2$, and 1 µM of His-tagged *E. coli* isocitrate dehydrogenase (purified from the *E. coli* strain JW1122 from the ASKA collection (242)) in a total volume of 100 µL. The aconitase activity was assayed by monitoring the formation of NADPH through the increase in absorbance at 340 nm (269).

4.2.6. Phylogenetic analysis

Protein homologs were identified using BLASTp searches (https://img.jgi.doe.gov/cgi-bin/w/main.cgi) against selected genomes. The sequence-based phylogenetic tree was constructed with MEGA X (1) using the Maximum Likelihood algorithm (270) with bootstrap (271) calculated from 100 repeats.

4.3. Results and discussion

4.3.1. Nbp35/ApbC homologs are highly conserved in archaea

The Nbp35/Cfd1/ApbC homologs are present in all of the 173 finished archaeal genomes in the Integrated Microbial Genomes database (https://img.jgi.doe.gov/cgi-bin/w/main.cgi). The sequence-based phylogenetic tree (Figure 28) shows that the bacterial, archaeal, and eukaryotic homologs form distinct clades, consistent with the phylogenetic pattern of ribosomal RNA genes. This suggests that the ancestral gene of Nbp35/Cfd1/ApbC was evolved before the divergence of the three domains, and Nbp35 and Cfd1 are paralogs possibly evolved by gene duplication in the eukaryotic common ancestor.

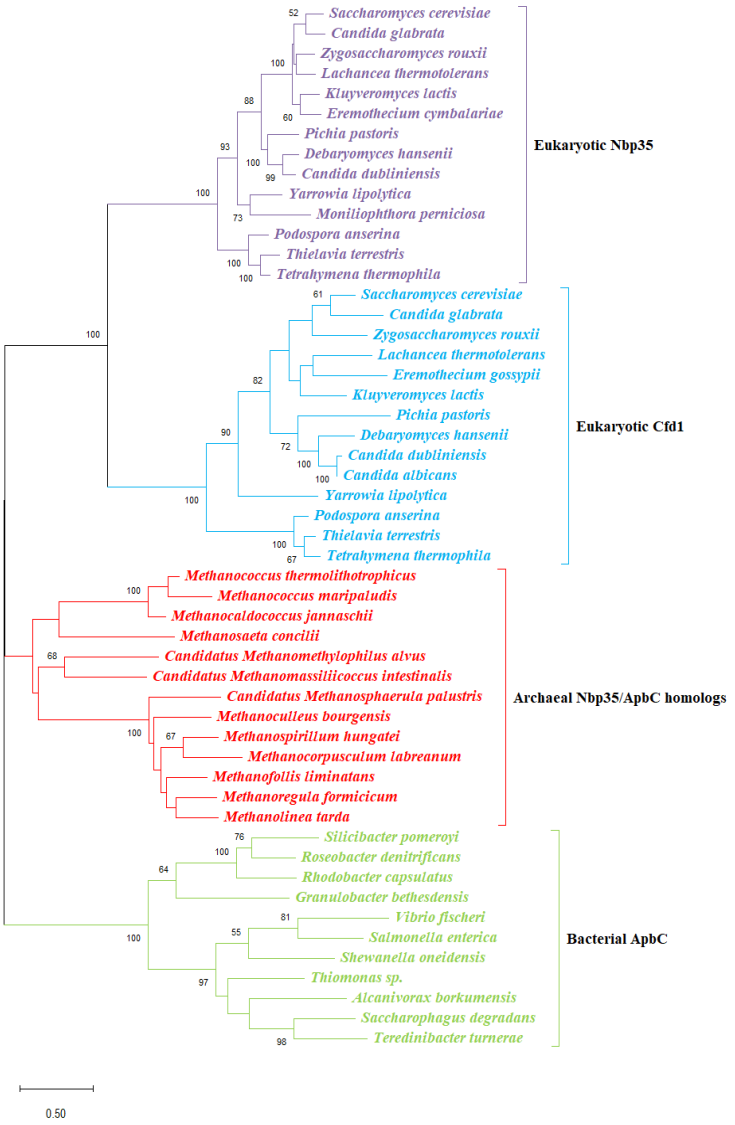

Figure 28. Phylogenetic tree of Nbp35, Cfd1, and ApbC homologs.
The evolutionary history was inferred by using the Maximum Likelihood method in MEGA X (1). The tree with the highest log likelihood (-20463.59) is shown. Initial tree(s) for the heuristic search were obtained automatically by applying Neighbor-Join and BioNJ algorithms to a matrix of pairwise distances estimated using a JTT model, and then selecting the topology with superior log likelihood value. A discrete Gamma distribution was used to model evolutionary rate differences among sites (5 categories (+*G*, parameter = 1.2858)). The rate variation model allowed for some sites to be evolutionarily invariable ([+*I*], 4.28% sites). The tree is drawn to scale, with branch lengths measured in the number of substitutions per site. This analysis involved 52 amino acid sequences. There was a total of 456 positions in the final dataset. The bootstrap values were calculated with 100 replicates, and values >50% are labeled on the nodes. The scale bar represents 0.5 amino acid substitution per site. The corresponding species of the eukaryotic Nbp35 proteins (purple), the eukaryotic Cfd1 proteins (blue), the bacterial ApbC proteins (green), and the archaeal Nbp35/ApbC homologs (red) are labeled for each branch.

The Walker A motif is conserved in almost all archaeal homologs, except that in *Sulfolobales sp.* HSU1 and *Hadesarchaea archaeon* DG-33. The N-terminal CX_2CX_5C motif, which binds a stable [4Fe-4S] cluster in eukaryotic Nbp35, is only present in some methanogens (*e.g. M. maripaludis*, *Methanocaldococcus jannaschii*, *Methanosaeta concilii*, and *Methanosaeta harundinacea*) (Figure 26). Non-methanogens generally lack the N-terminal cysteines. The C-terminal CXXC motif, which is the binding site of a transient [4Fe-4S] cluster in the eukaryotic Nbp35-Cfd1 heterocomplex, is conserved in most methanogens except *Methanothermobacter marburgensis* and *Methanomassiliicoccus luminyensis*. Interestingly, many TACK archaea (including Thaumarchaeota, Aigarchaeota, Crenarchaeota, and Korarchaeota) only have one C-terminal cysteine corresponding to Cys253 of the *S. cerevisiae* Nbp35 (Figure 26). Some non-methanogenic euryarchaea (*e.g. Aciduliprofundum boonei*) do not have C-terminal cysteines.

4.3.2. The Nbp35/ApbC homolog (MMP0704) from *M. maripaludis* binds a [4Fe-4S] cluster

A previous study showed that MMP0704 recombinantly expressed and purified from *E. coli* can be reconstituted *in vitro* with an Fe-S cluster, however the cluster type was unclear (148). In this study, the strep-tagged MMMP0704 was recombinantly expressed from its native host *M. maripaludis* and purified under anoxic conditions. Three evidences demonstrate that this protein binds an Fe-S cluster. (i) The as-purified (following affinity purification steps inside an anaerobic chamber without addition of a reducing agent) MMP0704 was brownish in color and displayed the characteristic UV-visible spectrum of a [4Fe-4S] cluster with a broad absorption at around 420 nm (Figure 29A). Addition of 5 mM sodium dithionite (DTH) partially bleached the protein color and decreased the UV-visible absorption (Figure 29A). The Fe-S cluster of MMP0704 is oxygen-labile, as indicated by the decrease of UV-visible absorption when the protein was exposed to air (Figure 29B). (ii) Chemical analysis of the Fe content showed that the as-purified MMP0704 contained 0.73 ± 0.08 Fe per monomer. The low Fe content suggests that the Fe-S cluster is loosely bound to the protein and may be lost during the purification process. (iii) The EPR spectrum of MMP0704 reduced by 5 mM sodium DTH has a nearly axial spectrum with $g_{//} = 2.05$ and $g_{\perp} = 1.90$, characteristic of a $[4Fe\text{-}4S]^{1+}$ cluster ($S_{tol} = ½$) (272) (Figure 29C). In the as-purified state, only a signal of an organic radical contaminant was observed (Figure 29C) (273). Therefore, MMP0704 is a [4Fe-4S] protein in *M. maripaludis*.

4.3.3. The [4Fe-4S] cluster of MMP0704 can be transferred to apo-aconitase

We then investigated the ability of MMP0704 to transfer its cluster to an apo-protein *in vitro*. The [4Fe-4S] cluster-dependent *E. coli* aconitase B (AcnB) was tested as a recipient. Fe-S cluster transfer from the as-purified MMP0704 to apo-AcnB was monitored by the activation of AcnB. Although the as-purified MMP0704 or apo-AcnB individually had no detectable activity, the incubation of these two proteins together restored ~ 70% of the activity of the as-purified AcnB (Figure 29D). This result demonstrates that MMP0704 can transfer a [4Fe-4S] cluster to apo-proteins and acts as a cluster transfer protein in methanogens.

4.3.4. The *mmp0704* gene is not essential for the viability of *M. maripaludis*

To study the physiological function of Nbp35/ApbC homologs in methanogens, the *mmp0704* gene was replaced by a *hpt-pac* cassette as described in the materials and methods. The mutation was confirmed by PCR (Figure 27C). The growth phenotypes of the *M.*

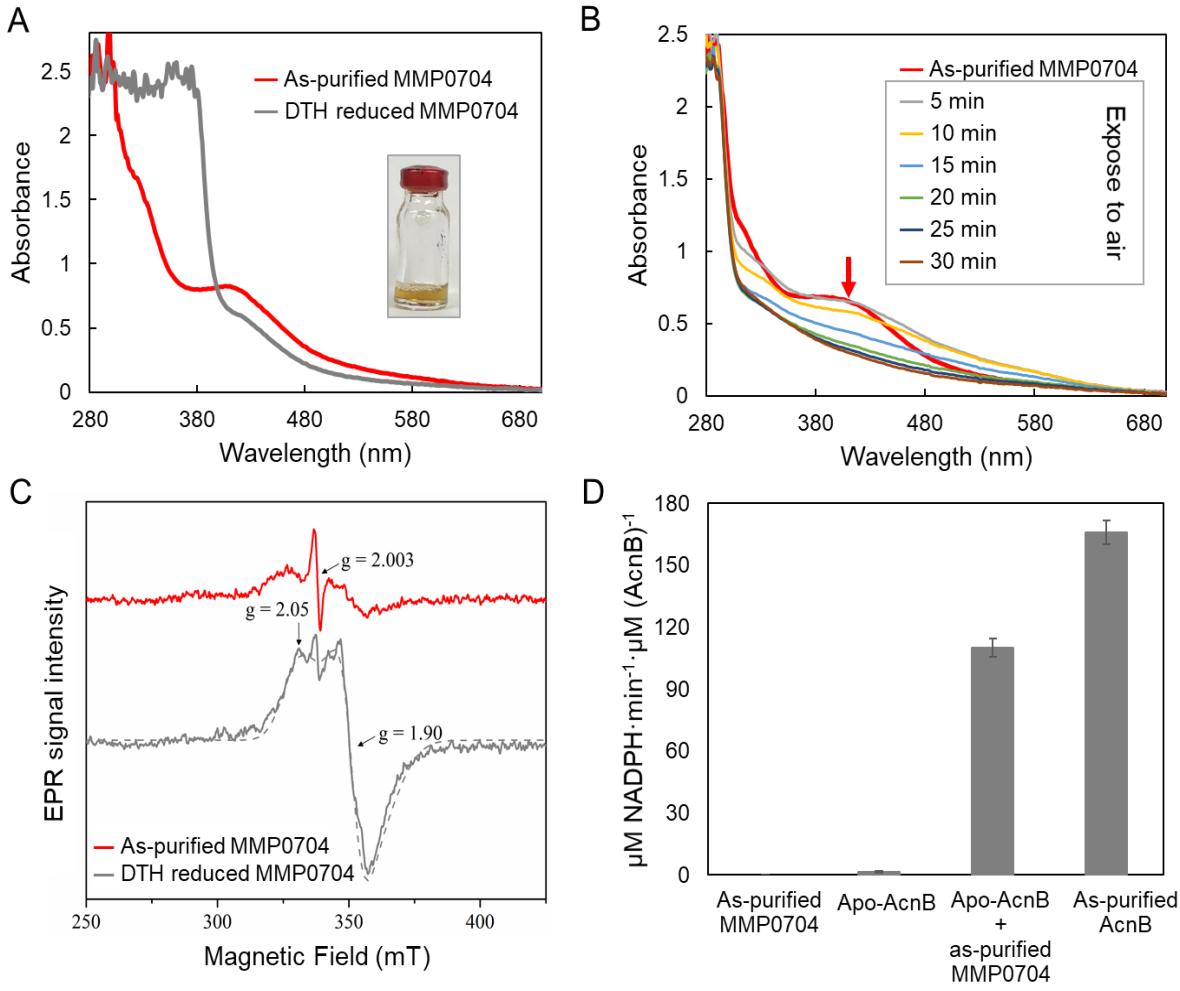

Figure 29. The MMP0704 protein purified from *M. maripaludis* contains a [4Fe-4S] cluster that can be transferred to apo-AcnB. (A) UV-Vis spectra of anoxically purified MMP0704 (20 μM) in the as-purified (red) and after DTH reduced (grey) states. (*Inset*) The as-purified protein was brownish in color. (B) Oxygen sensitivity of anoxically purified MMP0704. The red arrow indicates the decrease of the absorbance at ~ 420 nm when the protein was exposed to air. (C) The X-band EPR spectra of anoxically purified MMP0704 (1.2 mM) in the as-purified (top red trace) and DTH reduced (bottom grey trace) states. The DTH reduced spectrum was simulated as a nearly axial species with $g_{//} = 2.05$ and $g_{\perp} = 1.90$ (dashed trace). Both spectra of the as-purified and reduced samples contain an organic radical contaminant at approximately $g = 2.003$. Experimental conditions: microwave power, 1 mW; microwave frequency, 9.476 GHz; modulation amplitude, 10 G; temperature, 7.4 K. (D) Activation of apo-AcnB by [4Fe-4S]-containing MMP0704. Apo-AcnB was incubated with as-purified MMP0704, and the aconitase activity was followed by the formation of NADPH as described in the materials and methods section. As controls, the as-purified MMP0704, apo-AcnB, and as-purified AcnB were assayed individually. Data are mean ± standard deviation from three replicates.

maripaludis Δ*mmp0704* mutant strain and the parent strain S0001 were compared under various conditions. No significant growth deficiency was observed in rich (supplemented with acetate, casamino acids, and yeast extracts) or minimal medium (with CO_2 as the sole carbon source) (Figure 30A). Furthermore, the Δ*mmp0704* mutant and the parent strains grew similarly under Fe-limiting conditions (with 0.5 µM, 1 µM, 5 µM, and 10 µM Fe in the minimal medium) (Figure 30B). These results suggest that MMP0704 is nonessential in *M. maripaludis* and may only be involved in the maturation of a specific target protein(s) under certain growth conditions.

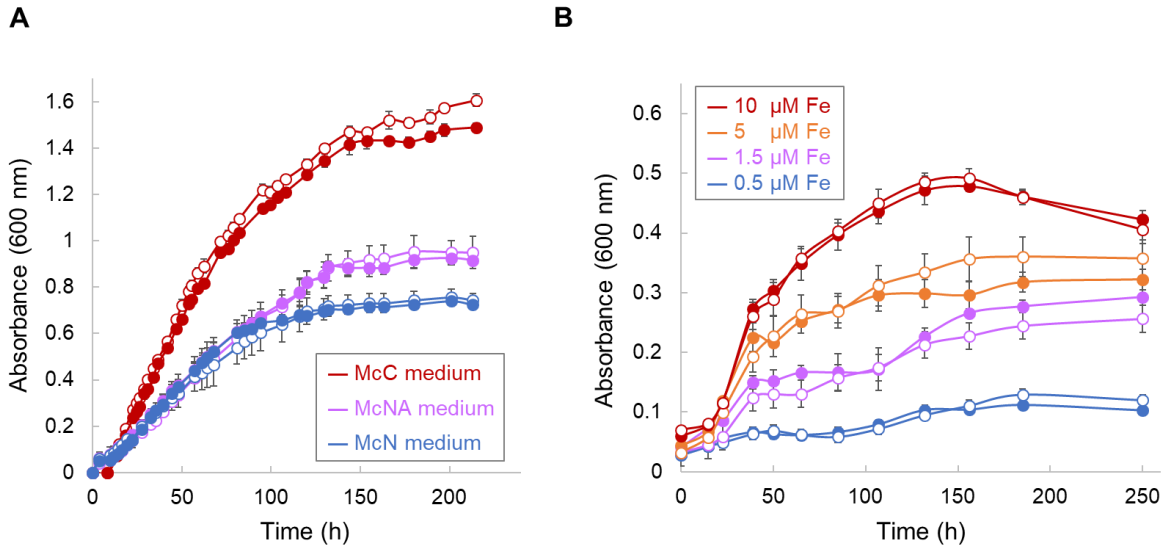

Figure 30. Growth of the *M. maripaludis* parent strain S0001 (closed circle) and the Δ*mmp0704* mutant strain (open circle). (A) Growth in the McC medium (red), McNA medium (purple), and minimal McN medium (blue). The standard McN medium contains 25 µM ferrous ammonium sulfate. (B) Growth in the Fe-limiting McN medium with 0.5 (blue), 1.5 (purple), 5 (orange), or 10 (red) µM ferrous ammonium sulfate. Data are mean ± standard deviation from three replicate cultures.

CHAPTER 5. CONCLUSIONS

Methanogens and bacteria living in syntrophic consortia take advantage of the metabolic abilities of their syntrophic partners to overcome energetic barriers and break down compounds that they cannot digest by themselves. Methanogenesis and anaerobic oxidization of methane (AOM) are the main processes involved in these syntrophic consortia. Interspecies electron transfer, which is a major type of microbial communication in syntrophic processes, has a significant impact on the global carbon cycle. Direct interspecies electron transfer (DIET) is achieved by electrical contacts between the electron donor and acceptor cells. DIET is potentially an important mechanism for electron transfer in syntrophic anaerobic consortia, especially in methanogenesis and AOM processes. DIET has so far been reported in the cocultures of *G. metallireducens* and *G. sulfurreducens*, *G. metallireducens* and *M. harundinacea*, *G. metallireducens* and *M. barkeri*, ANME-2 and sulfate-reducing *Deltaproteobacteria*, and ANME-1 and sulfate reducing HotSeep-1. However, there is still much work needed to understand the mechanism of DIET and its contribution to the global cycling of carbon and other nutrients.

Many essential enzymes involved in methanogenesis are iron-sulfur proteins. Fe-S clusters are synthesized by different systems depending on the organism and organelles. In bacteria, the ISC system is the housekeeping system, while the SUF system is activated under iron-limiting and oxidative stress conditions. Some bacteria only have SUF system. Eukaryotes use the ISC system in the mitochondria, the SUF system in the plastid, and the CIA system in the cytosol and nucleus. However, the mechanism which methanogens use for Fe-S cluster biosynthesis is still unclear. In this work, we studied three Fe-S cluster related proteins conserved in almost all archaea: SufB, SufC, and the Nbp35/ApbC homolog (MMP0704), to investigate Fe-S cluster biosynthesis in methanogens.

We found that methanogens use the SUF system to synthesize Fe-S clusters. In this SUF system, a $SufB_2C_2$ complex is a scaffold protein. It contains a labile [4Fe-4S] cluster and can transfer the cluster to and activate apo-AcnB. The labile [4Fe-4S] cluster on the $SufB_2C_2$ complex is located on the C-terminus of SufC protein. Three conserved cysteine residues on the MMPSufC proteins, C218, C237, C240, are essential for the Fe-S cluster assembly and transfer abilities of the MMP$SufB_2C_2$ complex. Moreover, SufC is an Fe-S protein. Its [4Fe-4S] cluster can also be transferred to and activate apo-AcnB. But its transfer ability is 2-fold lower than the $SufB_2C_2$ complex, suggesting that the SufB combination on SufC can enhance the Fe-S cluster transfer reaction. Additionally, we found that SufC is an ATPase in *M. maripaludis*, and that its activity can also be highly enhanced when it binds to SufB. However, whether the ATPase activity is required for the Fe-S cluster assembly and transfer abilities of $SufB_2C_2$ complex is still not clear. The lysine residue (K40) in the Walker A motif of SufC is required for ATP hydrolysis as reported in *E. coli*. Therefore, the lysine residue can be mutated to investigate the importance of the ATPase activity in the future.

We also found that MMP0704 is a specific scaffold/carrier protein for Fe-S cluster maturation in methanogens. Although conserved in archaea, MMP0704 is not an essential scaffold/carrier protein for Fe-S maturation in *M. maripaludis* as shown by our knockout mutagenesis study and is not essential for cell growth, which is consistent with a previous whole genome transposon mutagenesis in *M. maripaludis* (152). Previous work also showed that MMP0704 can be reconstituted with a Fe-S cluster *in vitro* and can correct the tricarballylate growth defect of an *S. enterica apbC* mutant (148). Our work here showed the as-purified

MMP0704 from *M. maripaludis* is an [4Fe-4S] protein and this [4Fe-4S] can be transferred to activate AcnB, suggesting that MMP0704 is an Fe-S cluster scaffold/carrier protein for Fe-S maturation. Moreover, the growth phenotype study on the MMP0704 mutant showed no growth defect under Fe-limiting conditions. This result supports the notion that MMP0704 is not a general scaffold/carrier used to assemble or transfer Fe-S clusters to most proteins and it could be a specific scaffold/carrier for one or several non-essential Fe-S proteins. The physiological target(s) of Mmp0704 awaits further studies. Additionally, whether MMP0704 is a scaffold or carrier protein still needs further investigation.

In conclusion, we found methanogens use this SUF system to synthesize Fe-S cluster and the $SufB_2C_2$ complex as scaffold protein. Methanogens were suggested to use cysteine as sulfur donor before. However, the iron donor for the Fe-S cluster, the electron donor, and the general carrier proteins for Fe-S cluster biosynthesis in methanogens still need further investigation.

APPENDIX. COPYRIGHT INFORMATION

Thank you for your order with RightsLink / Springer Nature

no-reply@copyright.com
Wed 6/12/2019 1:08 PM
To: Cuiping Zhao <czhao14@lsu.edu>

SPRINGER NATURE

Thank you for your order!

Dear Cuiping Zhao,

Thank you for placing your order through Copyright Clearance Center's RightsLink® service.

Order Summary

Licensee:	Cuiping Zhao
Order Date:	Jun 12, 2019
Order Number:	4606620354785
Publication:	Springer eBook
Title:	Direct Interspecies Electron Transfer Between Archaea and Bacteria
Type of Use:	Thesis/Dissertation
Order Total:	0.00 USD

View or print complete details of your order and the publisher's terms and conditions.

Sincerely,

Copyright Clearance Center

Tel: +1-855-239-3415 / +1-978-646-2777
customercare@copyright.com
https://myaccount.copyright.com

Copyright Clearance Center RightsLink®

SPRINGER NATURE LICENSE TERMS AND CONDITIONS
Jun 18, 2019

This Agreement between Cuiping Zhao ("You") and Springer Nature ("Springer Nature") consists of your license details and the terms and conditions provided by Springer Nature and Copyright Clearance Center.

License Number 4606620354785
License date Jun 12, 2019
Licensed Content Publisher Springer Nature
Licensed Content Publication Springer eBook

Licensed Content Title	Direct Interspecies Electron Transfer Between Archaea and Bacteria
Licensed Content Author	Cuiping Zhao, Yuchen Liu
Licensed Content Date	Jan 1, 2017
Type of Use	Thesis/Dissertation
Requestor type	academic/university or research institute
Format	print and electronic
Portion	full article/chapter
Will you be translating?	no
Circulation/distribution	<501
Author of this Springer Nature content	yes
Title	IRON-SULFUR CLUSTER BIOSYNTHESIS IN METHANOGENS
Institution name	Louisiana State University
Expected presentation date	Aug 2019
Total	0.00 USD

Terms and Conditions

Springer Nature Terms and Conditions for RightsLink Permissions Springer Nature Customer Service Centre GmbH (the Licensor) hereby grants you a non-exclusive, world-wide licence to reproduce the material and for the purpose and requirements specified in the attached copy of your order form, and for no other use, subject to the conditions below:

The Licensor warrants that it has, to the best of its knowledge, the rights to license reuse of this material. However, you should ensure that the material you are requesting is original to the Licensor and does not carry the copyright of another entity (as credited in the published version).

If the credit line on any part of the material you have requested indicates that it was reprinted or adapted with permission from another source, then you should also seek permission from that source to reuse the material.

Where print only permission has been granted for a fee, separate permission must be obtained for any additional electronic re-use.

Permission granted free of charge for material in print is also usually granted for any electronic version of that work, provided that the material is incidental to your work as a whole and that the electronic version is essentially equivalent to, or substitutes for, the print version.

A licence for 'post on a website' is valid for 12 months from the licence date. This licence does not cover use of full text articles on websites.

Where 'reuse in a dissertation/thesis' has been selected the following terms apply: Print rights of the final author's accepted manuscript (for clarity, NOT the published version) for up to 100 copies, electronic rights for use only on a personal website or institutional repository as defined by the Sherpa guideline (www.sherpa.ac.uk/romeo/).

Permission granted for books and journals is granted for the lifetime of the first edition and does not apply to second and subsequent editions (except where the first edition permission was granted free of charge or for signatories to the STM Permissions Guidelines http://www.stm-assoc.org/copyright-legal-affairs/permissions/permissions-guidelines/), and does not apply for editions in other languages unless additional translation rights have been granted separately in the licence.

Rights for additional components such as custom editions and derivatives require additional permission and may be subject to an additional fee. Please apply to Journalpermissions@springernature.com/bookpermissions@springernature.com for these rights.

The Licensor's permission must be acknowledged next to the licensed material in print. In electronic form, this acknowledgement must be visible at the same time as the figures/tables/illustrations or abstract, and must be hyperlinked to the journal/book's homepage. Our required acknowledgement format is in the Appendix below.

Use of the material for incidental promotional use, minor editing privileges (this does not include cropping, adapting, omitting material or any other changes that affect the meaning, intention or moral rights of the author) and copies for the disabled are permitted under this licence.

Minor adaptations of single figures (changes of format, colour and style) do not require the Licensor's approval. However, the adaptation should be credited as shown in Appendix below.

Appendix — Acknowledgements:

For Journal Content:

Reprinted by permission from [the Licensor]: [Journal Publisher (e.g. Nature/Springer/Palgrave)] [JOURNAL NAME] [REFERENCE CITATION (Article name, Author(s) Name), [COPYRIGHT] (year of publication)

For Advance Online Publication papers:

Reprinted by permission from [the Licensor]: [Journal Publisher (e.g. Nature/Springer/Palgrave)] [JOURNAL NAME] [REFERENCE CITATION (Article name, Author(s) Name), [COPYRIGHT] (year of publication), advance online publication, day month year (doi: 10.1038/sj.[JOURNAL ACRONYM].)

For Adaptations/Translations:

Adapted/Translated by permission from [the Licensor]: [Journal Publisher (e.g.

Nature/Springer/Palgrave)] [JOURNAL NAME] [REFERENCE CITATION (Article name, Author(s) Name), [COPYRIGHT] (year of publication)
Note: For any republication from the British Journal of Cancer, the following credit line style applies:
Reprinted/adapted/translated by permission from [the Licensor]: on behalf of Cancer Research UK: : [Journal Publisher (e.g. Nature/Springer/Palgrave)] [JOURNAL NAME] [REFERENCE CITATION (Article name, Author(s) Name), [COPYRIGHT] (year of publication)

For Advance Online Publication papers:
Reprinted by permission from The [the Licensor]: on behalf of Cancer Research UK: [Journal Publisher (e.g. Nature/Springer/Palgrave)] [JOURNAL NAME] [REFERENCE CITATION (Article name, Author(s) Name), [COPYRIGHT] (year of publication), advance online publication, day month year (doi: 10.1038/sj. [JOURNAL ACRONYM])

For Book content:
Reprinted/adapted by permission from [the Licensor]: [Book Publisher (e.g. Palgrave Macmillan, Springer etc) [Book Title] by [Book author(s)] [COPYRIGHT] (year of publication)

Other Conditions:

Version 1.1
Questions? customercare@copyright.com or +1-855-239-3415 (toll free in the US) or +1-978-646-2777.

REFERENCES

1. Kumar, S., Stecher, G., Li, M., Knyaz, C., and Tamura, K. (2018) MEGA X: Molecular Evolutionary Genetics Analysis across Computing Platforms. *Mol Biol Evol* **35**, 1547-1549

2. Fuss, J. O., Tsai, C. L., Ishida, J. P., and Tainer, J. A. (2015) Emerging critical roles of Fe-S clusters in DNA replication and repair. *Biochim Biophys Acta* **1853**, 1253-1271

3. Stehling, O., Sheftel, A. D., and Lill, R. (2009) Chapter 12 Controlled expression of iron-sulfur cluster assembly components for respiratory chain complexes in mammalian cells. *Methods in enzymology* **456**, 209-231

4. Kessler, D., and Papenbrock, J. (2005) Iron-sulfur cluster biosynthesis in photosynthetic organisms. *Photosynth Res* **86**, 391-407

5. Rocha, A. G., and Dancis, A. (2016) Life without Fe-S clusters. *Molecular Microbiology* **99**, 821-826

6. Johnson, D. C., Dean, D. R., Smith, A. D., and Johnson, M. K. (2005) Structure, function, and formation of biological iron-sulfur clusters. *Annu Rev Biochem* **74**, 247-281

7. Pain, D., and Dancis, A. (2016) Roles of Fe-S proteins: from cofactor synthesis to iron homeostasis to protein synthesis. *Curr Opin Genet Dev* **38**, 45-51

8. Noodleman, L., and Case, D. A. (1992) Density-functional theory of spin polarization and spin coupling in iron—sulfur clusters. in *Adv Inorg Chem* (Cammack, R. ed.), Academic Press. pp 423-470

9. Glaser, T., Hedman, B., Hodgson, K. O., and Solomon, E. I. (2000) Ligand K-edge X-ray absorption spectroscopy: a direct probe of ligand-metal covalency. *Acc Chem Res* **33**, 859-868

10. Beinert, H., Holm, R. H., and Munck, E. (1997) Iron-sulfur clusters: nature's modular, multipurpose structures. *Science* **277**, 653-659

11. Liu, J., Chakraborty, S., Hosseinzadeh, P., Yu, Y., Tian, S. L., Petrik, I., Bhagi, A., and Lu, Y. (2014) Metalloproteins Containing Cytochrome, Iron-Sulfur, or Copper Redox Centers. *Chemical Reviews* **114**, 4366-4469

12. Beinert, H., Kennedy, M. C., and Stout, C. D. (1996) Aconitase as Ironminus signSulfur Protein, Enzyme, and Iron-Regulatory Protein. *Chem Rev* **96**, 2335-2374

13. Dobbek, H., Svetlitchnyi, V., Gremer, L., Huber, R., and Meyer, O. (2001) Crystal structure of a carbon monoxide dehydrogenase reveals a [Ni-4Fe-5S] cluster. *Science* **293**, 1281-1285

14. Crane, B. R., Siegel, L. M., and Getzoff, E. D. (1995) Sulfite reductase structure at 1.6 A: evolution and catalysis for reduction of inorganic anions. *Science* **270**, 59-67

15. Cunningham, R. P., Asahara, H., Bank, J. F., Scholes, C. P., Salerno, J. C., Surerus, K., Munck, E., McCracken, J., Peisach, J., and Emptage, M. H. (1989) Endonuclease III is an iron-sulfur protein. *Biochemistry* **28**, 4450-4455

16. Porello, S. L., Cannon, M. J., and David, S. S. (1998) A substrate recognition role for the $[4Fe\text{-}4S]^{2+}$ cluster of the DNA repair glycosylase MutY. *Biochemistry* **37**, 6465-6475

17. Alen, C., and Sonenshein, A. L. (1999) Bacillus subtilis aconitase is an RNA-binding protein. *Proceedings of the National Academy of Sciences of the United States of America* **96**, 10412-10417

18. Tang, Y., and Guest, J. R. (1999) Direct evidence for mRNA binding and post-transcriptional regulation by Escherichia coli aconitases. *Microbiology* **145 (Pt 11)**, 3069-3079

19. Ugulava, N. B., Sacanell, C. J., and Jarrett, J. T. (2001) Spectroscopic changes during a single turnover of biotin synthase: destruction of a [2Fe-2S] cluster accompanies sulfur insertion. *Biochemistry* **40**, 8352-8358

20. Wagner, T., Ermler, U., and Shima, S. (2016) The methanogenic CO_2 reducing-and-fixing enzyme is bifunctional and contains 46 [4Fe-4S] clusters. *Science* **354**, 114-117

21. Eck, R. V., and Dayhoff, M. O. (1966) Evolution of the structure of ferredoxin based on living relics of primitive amino acid sequences. *Science* **152**, 363-366

22. Meyer, J. (2008) Iron-sulfur protein folds, iron-sulfur chemistry, and evolution. *Journal of biological inorganic chemistry : JBIC : a publication of the Society of Biological Inorganic Chemistry* **13**, 157-170

23. Tan, G., Liu, D., Pan, F., Zhao, J., Li, T., Ma, Y., Shen, B., and Lyu, J. (2016) His-87 ligand in mitoNEET is crucial for the transfer of iron sulfur clusters from mitochondria to cytosolic aconitase. *Biochem Biophys Res Commun* **470**, 226-232

24. Huang, J., and Cowan, J. A. (2009) Iron-sulfur cluster biosynthesis: role of a semi-conserved histidine. *Chemical communications*, 3071-3073

25. Bak, D. W., and Elliott, S. J. (2014) Alternative FeS cluster ligands: tuning redox potentials and chemistry. *Curr Opin Chem Biol* **19**, 50-58

26. Robbins, A. H., and Stout, C. D. (1989) Structure of activated aconitase: formation of the [4Fe-4S] cluster in the crystal. *Proceedings of the National Academy of Sciences of the United States of America* **86**, 3639-3643

27. Harmer, J. E., Hiscox, M. J., Dinis, P. C., Fox, S. J., Iliopoulos, A., Hussey, J. E., Sandy, J., Van Beek, F. T., Essex, J. W., and Roach, P. L. (2014) Structures of lipoyl synthase

reveal a compact active site for controlling sequential sulfur insertion reactions. *Biochem J* **464**, 123-133

28. Malkin, R., and Rabinowitz, J. C. (1966) The reconstitution of clostridial ferredoxin. *Biochem Biophys Res Commun* **23**, 822-827

29. Py, B., and Barras, F. (2010) Building Fe-S proteins: bacterial strategies. *Nature reviews. Microbiology* **8**, 436-446

30. Lill, R. (2009) Function and biogenesis of iron-sulphur proteins. *Nature* **460**, 831-838

31. Zheng, L., White, R. H., Cash, V. L., Jack, R. F., and Dean, D. R. (1993) Cysteine desulfurase activity indicates a role for NIFS in metallocluster biosynthesis. *Proceedings of the National Academy of Sciences of the United States of America* **90**, 2754-2758

32. Blanc, B., Gerez, C., and Ollagnier de Choudens, S. (2015) Assembly of Fe/S proteins in bacterial systems: Biochemistry of the bacterial ISC system. *Biochim Biophys Acta* **1853**, 1436-1447

33. Raulfs, E. C., O'Carroll, I. P., Dos Santos, P. C., Unciuleac, M. C., and Dean, D. R. (2008) In vivo iron-sulfur cluster formation. *Proceedings of the National Academy of Sciences of the United States of America* **105**, 8591-8596

34. Yuvaniyama, P., Agar, J. N., Cash, V. L., Johnson, M. K., and Dean, D. R. (2000) NifS-directed assembly of a transient [2Fe-2S] cluster within the NifU protein. *Proceedings of the National Academy of Sciences* **97**, 599-604

35. Roche, B., Aussel, L., Ezraty, B., Mandin, P., Py, B., and Barras, F. (2013) Iron/sulfur proteins biogenesis in prokaryotes: formation, regulation and diversity. *Biochim Biophys Acta* **1827**, 455-469

36. Wayne Outten, F. (2015) Recent advances in the Suf Fe–S cluster biogenesis pathway: Beyond the Proteobacteria. *Biochimica et Biophysica Acta (BBA) - Molecular Cell Research* **1853**, 1464-1469

37. Braymer, J. J., and Lill, R. (2017) Iron–sulfur cluster biogenesis and trafficking in mitochondria. *Journal of Biological Chemistry* **292**, 12754-12763

38. Lu, Y. (2018) Assembly and Transfer of Iron–Sulfur Clusters in the Plastid. *Frontiers in plant science* **9**

39. Netz, D. J., Mascarenhas, J., Stehling, O., Pierik, A. J., and Lill, R. (2014) Maturation of cytosolic and nuclear iron-sulfur proteins. *Trends Cell Biol* **24**, 303-312

40. Jacobson, M. R., Cash, V. L., Weiss, M. C., Laird, N. F., Newton, W. E., and Dean, D. R. (1989) Biochemical and genetic analysis of the nifUSVWZM cluster from Azotobacter vinelandii. *Mol Gen Genet* **219**, 49-57

41. Frazzon, J., and Dean, D. R. (2003) Formation of iron-sulfur clusters in bacteria: an emerging field in bioinorganic chemistry. *Curr Opin Chem Biol* **7**, 166-173

42. Joerger, R. D., and Bishop, P. E. (1988) Bacterial alternative nitrogen fixation systems. *Crit Rev Microbiol* **16**, 1-14

43. Bulen, W. A., and LeComte, J. R. (1966) The nitrogenase system from Azotobacter: two-enzyme requirement for N2 reduction, ATP-dependent H2 evolution, and ATP hydrolysis. *Proceedings of the National Academy of Sciences of the United States of America* **56**, 979-986

44. Kim, J., and Rees, D. C. (1992) Crystallographic structure and functional implications of the nitrogenase molybdenum-iron protein from azotobacter vinelandii. *Nature* **360**, 553-560

45. Chan, M. K., Kim, J., and Rees, D. C. (1993) The nitrogenase FeMo-cofactor and P-cluster pair: 2.2 A resolution structures. *Science* **260**, 792-794

46. Georgiadis, M. M., Komiya, H., Chakrabarti, P., Woo, D., Kornuc, J. J., and Rees, D. C. (1992) Crystallographic structure of the nitrogenase iron protein from Azotobacter vinelandii. *Science* **257**, 1653-1659

47. Agar, J. N., Zheng, L., Cash, V. L., Dean, D. R., and Johnson, M. K. (2000) Role of the IscU Protein in Iron−Sulfur Cluster Biosynthesis: IscS-mediated Assembly of a [Fe2S2] Cluster in IscU. *Journal of the American Chemical Society* **122**, 2136-2137

48. Agar, J. N., Krebs, C., Frazzon, J., Huynh, B. H., Dean, D. R., and Johnson, M. K. (2000) IscU as a scaffold for iron-sulfur cluster biosynthesis: sequential assembly of [2Fe-2S] and [4Fe-4S] clusters in IscU. *Biochemistry* **39**, 7856-7862

49. Zheng, L., Cash, V. L., Flint, D. H., and Dean, D. R. (1998) Assembly of iron-sulfur clusters. Identification of an iscSUA-hscBA-fdx gene cluster from Azotobacter vinelandii. *J Biol Chem* **273**, 13264-13272

50. Netz, D. J., Pierik, A. J., Stumpfig, M., Muhlenhoff, U., and Lill, R. (2007) The Cfd1-Nbp35 complex acts as a scaffold for iron-sulfur protein assembly in the yeast cytosol. *Nat Chem Biol* **3**, 278-286

51. Lill, R., Dutkiewicz, R., Freibert, S. A., Heidenreich, T., Mascarenhas, J., Netz, D. J., Paul, V. D., Pierik, A. J., Richter, N., and Stümpfig, M. (2015) The role of mitochondria and the CIA machinery in the maturation of cytosolic and nuclear iron–sulfur proteins. *European journal of cell biology* **94**, 280-291

52. Netz, D. J., Stumpfig, M., Dore, C., Muhlenhoff, U., Pierik, A. J., and Lill, R. (2010) Tah18 transfers electrons to Dre2 in cytosolic iron-sulfur protein biogenesis. *Nat Chem Biol* **6**, 758-765

53. Zhang, Y., Lyver, E. R., Nakamaru-Ogiso, E., Yoon, H., Amutha, B., Lee, D. W., Bi, E., Ohnishi, T., Daldal, F., Pain, D., and Dancis, A. (2008) Dre2, a conserved eukaryotic Fe/S cluster protein, functions in cytosolic Fe/S protein biogenesis. *Mol Cell Biol* **28**, 5569-5582

54. Hausmann, A., Aguilar Netz, D. J., Balk, J., Pierik, A. J., Muhlenhoff, U., and Lill, R. (2005) The eukaryotic P loop NTPase Nbp35: an essential component of the cytosolic and nuclear iron-sulfur protein assembly machinery. *Proceedings of the National Academy of Sciences of the United States of America* **102**, 3266-3271

55. Roy, A., Solodovnikova, N., Nicholson, T., Antholine, W., and Walden, W. E. (2003) A novel eukaryotic factor for cytosolic Fe-S cluster assembly. *EMBO J* **22**, 4826-4835

56. Urzica, E., Pierik, A. J., Muhlenhoff, U., and Lill, R. (2009) Crucial role of conserved cysteine residues in the assembly of two iron-sulfur clusters on the CIA protein Nar1. *Biochemistry* **48**, 4946-4958

57. Balk, J., Pierik, A. J., Netz, D. J. A., Mühlenhoff, U., and Lill, R. (2004) The hydrogenase- like Nar1p is essential for maturation of cytosolic and nuclear iron–sulphur proteins. *The EMBO journal* **23**, 2105-2115

58. Stehling, O., Vashisht, A. A., Mascarenhas, J., Jonsson, Z. O., Sharma, T., Netz, D. J., Pierik, A. J., Wohlschlegel, J. A., and Lill, R. (2012) MMS19 assembles iron-sulfur proteins required for DNA metabolism and genomic integrity. *Science* **337**, 195-199

59. Weerapana, E., Wang, C., Simon, G. M., Richter, F., Khare, S., Dillon, M. B. D., Bachovchin, D. A., Mowen, K., Baker, D., and Cravatt, B. F. (2010) Quantitative reactivity profiling predicts functional cysteines in proteomes. *Nature* **468**, 790

60. Srinivasan, V., Netz, D. J., Webert, H., Mascarenhas, J., Pierik, A. J., Michel, H., and Lill, R. (2007) Structure of the yeast WD40 domain protein Cia1, a component acting late in iron-sulfur protein biogenesis. *Structure* **15**, 1246-1257

61. Takahashi, Y., and Tokumoto, U. (2002) A third bacterial system for the assembly of iron-sulfur clusters with homologs in archaea and plastids. *J Biol Chem* **277**, 28380-28383

62. Patzer, S. I., and Hantke, K. (1999) SufS is a NifS-like protein, and SufD is necessary for stability of the [2Fe-2S] FhuF protein in Escherichia coli. *J Bacteriol* **181**, 3307-3309

63. Mihara, H., Maeda, M., Fujii, T., Kurihara, T., Hata, Y., and Esaki, N. (1999) A nifS-like gene, csdB, encodes an Escherichia coli counterpart of mammalian selenocysteine lyase. Gene cloning, purification, characterization and preliminary x-ray crystallographic studies. *J Biol Chem* **274**, 14768-14772

64. Mihara, H., Kurihara, T., Yoshimura, T., and Esaki, N. (2000) Kinetic and mutational studies of three NifS homologs from Escherichia coli: mechanistic difference between L-cysteine desulfurase and L-selenocysteine lyase reactions. *J Biochem* **127**, 559-567

65. Lima, C. D. J. J. o. m. b. (2002) Analysis of the E. coli NifS CsdB protein at 2.0 Å reveals the structural basis for perselenide and persulfide intermediate formation. **315**, 1199-1208

66. Loiseau, L., Ollagnier-de-Choudens, S., Nachin, L., Fontecave, M., and Barras, F. (2003) Biogenesis of Fe-S cluster by the bacterial Suf system: SufS and SufE form a new type of cysteine desulfurase. *J Biol Chem* **278**, 38352-38359

67. Ollagnier-de-Choudens, S., Lascoux, D., Loiseau, L., Barras, F., Forest, E., and Fontecave, M. (2003) Mechanistic studies of the SufS-SufE cysteine desulfurase: evidence for sulfur transfer from SufS to SufE. *FEBS Lett* **555**, 263-267

68. Outten, F. W., Wood, M. J., Munoz, F. M., and Storz, G. (2003) The SufE protein and the SufBCD complex enhance SufS cysteine desulfurase activity as part of a sulfur transfer pathway for Fe-S cluster assembly in Escherichia coli. *J Biol Chem* **278**, 45713-45719

69. Chahal, H. K., Dai, Y., Saini, A., Ayala-Castro, C., and Outten, F. W. (2009) The SufBCD Fe-S scaffold complex interacts with SufA for Fe-S cluster transfer. *Biochemistry* **48**, 10644-10653

70. Wollers, S., Layer, G., Garcia-Serres, R., Signor, L., Clemancey, M., Latour, J. M., Fontecave, M., and Ollagnier de Choudens, S. (2010) Iron-sulfur (Fe-S) cluster assembly: the SufBCD complex is a new type of Fe-S scaffold with a flavin redox cofactor. *J Biol Chem* **285**, 23331-23341

71. Hirabayashi, K., Yuda, E., Tanaka, N., Katayama, S., Iwasaki, K., Matsumoto, T., Kurisu, G., Outten, F. W., Fukuyama, K., Takahashi, Y., and Wada, K. (2015) Functional Dynamics Revealed by the Structure of the SufBCD Complex, a Novel ATP-binding Cassette (ABC) Protein That Serves as a Scaffold for Iron-Sulfur Cluster Biogenesis. *J Biol Chem* **290**, 29717-29731

72. Boyd, E. S., Thomas, K. M., Dai, Y., Boyd, J. M., and Outten, F. W. (2014) Interplay between oxygen and Fe-S cluster biogenesis: insights from the Suf pathway. *Biochemistry* **53**, 5834-5847

73. Layer, G., Gaddam, S. A., Ayala-Castro, C. N., Ollagnier-de Choudens, S., Lascoux, D., Fontecave, M., and Outten, F. W. (2007) SufE transfers sulfur from SufS to SufB for iron-sulfur cluster assembly. *J Biol Chem* **282**, 13342-13350

74. Yuda, E., Tanaka, N., Fujishiro, T., Yokoyama, N., Hirabayashi, K., Fukuyama, K., Wada, K., and Takahashi, Y. (2017) Mapping the key residues of SufB and SufD essential for biosynthesis of iron-sulfur clusters. *Scientific reports* **7**, 9387

75. Saini, A., Mapolelo, D. T., Chahal, H. K., Johnson, M. K., and Outten, F. W. (2010) SufD and SufC ATPase activity are required for iron acquisition during in vivo Fe-S cluster formation on SufB. *Biochemistry* **49**, 9402-9412

76. Yuda, E., Tanaka, N., Fujishiro, T., Yokoyama, N., Hirabayashi, K., Fukuyama, K., Wada, K., and Takahashi, Y. (2017) Mapping the key residues of SufB and SufD essential for biosynthesis of iron-sulfur clusters. *Scientific reports* **7**, 9387

77. Nachin, L., Loiseau, L., Expert, D., and Barras, F. (2003) SufC: an unorthodox cytoplasmic ABC/ATPase required for [Fe-S] biogenesis under oxidative stress. *EMBO J* **22**, 427-437

78. Kitaoka, S., Wada, K., Hasegawa, Y., Minami, Y., Fukuyama, K., and Takahashi, Y. (2006) Crystal structure of Escherichia coli SufC, an ABC-type ATPase component of the SUF iron-sulfur cluster assembly machinery. *FEBS Lett* **580**, 137-143

79. Eccleston, J. F., Petrovic, A., Davis, C. T., Rangachari, K., and Wilson, R. J. (2006) The kinetic mechanism of the SufC ATPase: the cleavage step is accelerated by SufB. *J Biol Chem* **281**, 8371-8378

80. Petrovic, A., Davis, C. T., Rangachari, K., Clough, B., Wilson, R. J., and Eccleston, J. F. (2008) Hydrodynamic characterization of the SufBC and SufCD complexes and their interaction with fluorescent adenosine nucleotides. *Protein Sci* **17**, 1264-1274

81. Gupta, V., Sendra, M., Naik, S. G., Chahal, H. K., Huynh, B. H., Outten, F. W., Fontecave, M., and Ollagnier de Choudens, S. (2009) Native Escherichia coli SufA, coexpressed with SufBCDSE, purifies as a [2Fe-2S] protein and acts as an Fe-S transporter to Fe-S target enzymes. *Journal of the American Chemical Society* **131**, 6149-6153

82. Tan, G., Lu, J., Bitoun, Jacob P., Huang, H., and Ding, H. (2009) IscA/SufA paralogues are required for the [4Fe-4S] cluster assembly in enzymes of multiple physiological pathways in *Escherichia coli* under aerobic growth conditions. *Biochemical Journal* **420**, 463-472

83. Lu, J., Yang, J., Tan, G., and Ding, H. (2008) Complementary roles of SufA and IscA in the biogenesis of iron–sulfur clusters in Escherichia coli. *Biochemical Journal* **409**, 535-543

84. Ollagnier-de-Choudens, S., Sanakis, Y., and Fontecave, M. (2004) SufA/IscA: reactivity studies of a class of scaffold proteins involved in [Fe-S] cluster assembly. *J Biol Inorg Chem* **9**, 828-838

85. Giel, J. L., Rodionov, D., Liu, M., Blattner, F. R., and Kiley, P. J. (2006) IscR-dependent gene expression links iron- sulphur cluster assembly to the control of O2-regulated genes in Escherichia coli. *Molecular microbiology* **60**, 1058-1075

86. Fleischhacker, A. S., Stubna, A., Hsueh, K.-L., Guo, Y., Teter, S. J., Rose, J. C., Brunold, T. C., Markley, J. L., Münck, E., and Kiley, P. J. (2012) Characterization of the [2Fe-2S] cluster of Escherichia coli transcription factor IscR. *Biochemistry* **51**, 4453-4462

87. Giel, J. L., Nesbit, A. D., Mettert, E. L., Fleischhacker, A. S., Wanta, B. T., and Kiley, P. J. (2013) Regulation of iron–sulphur cluster homeostasis through transcriptional control of the Isc pathway by [2 Fe–2 S]–IscR in E scherichia coli. *Molecular microbiology* **87**, 478-492

88. Desnoyers, G., Morissette, A., Prévost, K., and Massé, E. (2009) Small RNA-induced differential degradation of the polycistronic mRNA iscRSUA. *The EMBO journal* **28**, 1551-1561

89. Lee, J.-H., Yeo, W.-S., and Roe, J.-H. (2003) Regulation of the sufABCDSE operon by Fur. *The Journal of Microbiology* **41**, 109-114

90. Yeo, W. S., Lee, J. H., Lee, K. C., and Roe, J. H. (2006) IscR acts as an activator in response to oxidative stress for the suf operon encoding Fe- S assembly proteins. *Molecular microbiology* **61**, 206-218

91. Outten, F. W., Djaman, O., and Storz, G. (2004) A suf operon requirement for Fe-S cluster assembly during iron starvation in Escherichia coli. *Mol Microbiol* **52**, 861-872

92. Lee, J. H., Yeo, W. S., and Roe, J. H. (2004) Induction of the sufA operon encoding Fe-S assembly proteins by superoxide generators and hydrogen peroxide: involvement of OxyR, IHF and an unidentified oxidant-responsive factor. *Mol Microbiol* **51**, 1745-1755

93. Lyu, Z., Shao, N., Akinyemi, T., and Whitman, W. B. (2018) Methanogenesis. *Current biology : CB* **28**, R727-R732

94. Thauer, R. K. (1994) Methanogenesis: Ecology, physiology, biochemistry and genetics: edited by James G. Ferry, Chapman & Hall, 1993. $75.00 (x + 536 pages) ISBN 0 412 03531 6. *Trends in Biochemical Sciences* **19**, 266

95. Whitman, W. B., Bowen, T. L., and Boone, D. R. (2006) The methanogenic bacteria. *The Prokaryotes: Volume 3: Archaea. Bacteria: Firmicutes, Actinomycetes*, 165-207

96. Garrity, G. M., Holt, J. G., Whitman, W. B., Keswani, J., Boone, D. R., Koga, Y., Miller, T. L., Stetter, K. O., Zellner, G., and Chong, S. C. (2001) Phylum All. Euryarchaeota phy. nov. in *Bergey's Manual® of Systematic Bacteriology*, Springer. pp 211-355

97. Sakai, S., Imachi, H., Hanada, S., Ohashi, A., Harada, H., and Kamagata, Y. (2008) Methanocella paludicola gen. nov., sp. nov., a methane-producing archaeon, the first isolate of the lineage 'Rice Cluster I', and proposal of the new archaeal order Methanocellales ord. nov. *Int J Syst Evol Microbiol* **58**, 929-936

98. Sorokin, D. Y., Merkel, A. Y., Abbas, B., Makarova, K. S., Rijpstra, W. I. C., Koenen, M., Sinninghe Damste, J. S., Galinski, E. A., Koonin, E. V., and van Loosdrecht, M. C. M. (2018) Methanonatronarchaeum thermophilum gen. nov., sp. nov. and 'Candidatus Methanohalarchaeum thermophilum', extremely halo(natrono)philic methyl-reducing methanogens from hypersaline lakes comprising a new euryarchaeal class Methanonatronarchaeia classis nov. *Int J Syst Evol Microbiol* **68**, 2199-2208

99. Borrel, G., Parisot, N., Harris, H. M., Peyretaillade, E., Gaci, N., Tottey, W., Bardot, O., Raymann, K., Gribaldo, S., Peyret, P., O'Toole, P. W., and Brugere, J. F. (2014) Comparative genomics highlights the unique biology of Methanomassiliicoccales, a Thermoplasmatales-related seventh order of methanogenic archaea that encodes pyrrolysine. *BMC Genomics* **15**, 679

100. Paul, K., Nonoh, J. O., Mikulski, L., and Brune, A. (2012) "Methanoplasmatales," Thermoplasmatales-related archaea in termite guts and other environments, are the seventh order of methanogens. *Appl Environ Microbiol* **78**, 8245-8253

101. Evans, P. N., Parks, D. H., Chadwick, G. L., Robbins, S. J., Orphan, V. J., Golding, S. D., and Tyson, G. W. (2015) Methane metabolism in the archaeal phylum Bathyarchaeota revealed by genome-centric metagenomics. *Science* **350**, 434-438

102. Vanwonterghem, I., Evans, P. N., Parks, D. H., Jensen, P. D., Woodcroft, B. J., Hugenholtz, P., and Tyson, G. W. (2016) Methylotrophic methanogenesis discovered in the archaeal phylum Verstraetearchaeota. *Nat Microbiol* **1**, 16170

103. Ueno, Y., Yamada, K., Yoshida, N., Maruyama, S., and Isozaki, Y. (2006) Evidence from fluid inclusions for microbial methanogenesis in the early Archaean era. *Nature* **440**, 516-519

104. Liu, Y., and Whitman, W. B. (2008) Metabolic, phylogenetic, and ecological diversity of the methanogenic archaea. *Ann N Y Acad Sci* **1125**, 171-189

105. Sakai, S., Imachi, H., Sekiguchi, Y., Ohashi, A., Harada, H., and Kamagata, Y. (2007) Isolation of key methanogens for global methane emission from rice paddy fields: a novel isolate affiliated with the clone cluster rice cluster I. *Appl Environ Microbiol* **73**, 4326-4331

106. Sollinger, A., Schwab, C., Weinmaier, T., Loy, A., Tveit, A. T., Schleper, C., and Urich, T. (2016) Phylogenetic and genomic analysis of Methanomassiliicoccales in wetlands and animal intestinal tracts reveals clade-specific habitat preferences. *FEMS Microbiol Ecol* **92**

107. Petitjean, C., Deschamps, P., Lopez-Garcia, P., Moreira, D., and Brochier-Armanet, C. (2015) Extending the conserved phylogenetic core of archaea disentangles the evolution of the third domain of life. *Mol Biol Evol* **32**, 1242-1254

108. Kiener, A., and Leisinger, T. (1983) Oxygen Sensitivity of Methanogenic Bacteria. *Systematic and Applied Microbiology* **4**, 305-312

109. Fetzer, S., Bak, F., and Conrad, R. (1993) Sensitivity of Methanogenic Bacteria from Paddy Soil to Oxygen and Desiccation. *Fems Microbiology Ecology* **12**, 107-115

110. Ma, K., and Lu, Y. (2011) Regulation of microbial methane production and oxidation by intermittent drainage in rice field soil. *FEMS Microbiol Ecol* **75**, 446-456

111. Lyu, Z., and Lu, Y. (2018) Metabolic shift at the class level sheds light on adaptation of methanogens to oxidative environments. *The ISME journal* **12**, 411-423

112. Yuan, Y., Conrad, R., and Lu, Y. (2011) Transcriptional response of methanogen mcrA genes to oxygen exposure of rice field soil. *Environmental microbiology reports* **3**, 320-328

113. Thauer, R. K., Kaster, A. K., Goenrich, M., Schick, M., Hiromoto, T., and Shima, S. (2010) Hydrogenases from methanogenic archaea, nickel, a novel cofactor, and H2 storage. *Annual review of biochemistry* **79**, 507-536

114. Liu, Y., Sieprawska-Lupa, M., Whitman, W. B., and White, R. H. (2010) Cysteine is not the sulfur source for iron-sulfur cluster and methionine biosynthesis in the methanogenic archaeon Methanococcus maripaludis. *The Journal of biological chemistry* **285**, 31923-31929

115. Zehnder, A. J. B., Stams, A. J. M., and Jetten, M. S. M. (1992) Methanogenesis from acetate: a comparison of the acetate metabolism in Methanothrix soehngenii and Methanosarcina spp. *FEMS Microbiology Reviews* **8**, 181-197

116. Berghuis, B. A., Yu, F. B., Schulz, F., Blainey, P. C., Woyke, T., and Quake, S. R. (2019) Hydrogenotrophic methanogenesis in archaeal phylum Verstraetearchaeota reveals the shared ancestry of all methanogens. *Proceedings of the National Academy of Sciences* **116**, 5037-5044

117. Daniels, L., Fuchs, G., Thauer, R. K., and Zeikus, J. G. (1977) Carbon monoxide oxidation by methanogenic bacteria. *J Bacteriol* **132**, 118-126

118. Thauer, R. K., Kaster, A. K., Seedorf, H., Buckel, W., and Hedderich, R. (2008) Methanogenic archaea: ecologically relevant differences in energy conservation. *Nat Rev Microbiol* **6**, 579-591

119. Bapteste, E., Brochier, C., and Boucher, Y. (2005) Higher-level classification of the Archaea: evolution of methanogenesis and methanogens. *Archaea* **1**, 353-363

120. Oremland, R., and King, G. (1989) Microbial mats: physiological ecology of benthic microbial communities.

121. McGenity, T., McGenity, T., van der Meer, J., de Lorenzo, V., and Timmis, K. (2010) Handbook of hydrocarbon and lipid microbiology.

122. Borrel, G., Adam, P. S., and Gribaldo, S. (2016) Methanogenesis and the Wood-Ljungdahl Pathway: An Ancient, Versatile, and Fragile Association. *Genome Biol Evol* **8**, 1706-1711

123. Williams, T. A., Szollosi, G. J., Spang, A., Foster, P. G., Heaps, S. E., Boussau, B., Ettema, T. J. G., and Embley, T. M. (2017) Integrative modeling of gene and genome

evolution roots the archaeal tree of life. *Proceedings of the National Academy of Sciences of the United States of America* **114**, E4602-E4611

124. Kendall, M. M., and Boone, D. R. (2006) The Order Methanosarcinales. in *The Prokaryotes: Volume 3: Archaea. Bacteria: Firmicutes, Actinomycetes* (Dworkin, M., Falkow, S., Rosenberg, E., Schleifer, K.-H., and Stackebrandt, E. eds.), Springer New York, New York, NY. pp 244-256

125. Gottschalk, G., and Thauer, R. K. (2001) The Na(+)-translocating methyltransferase complex from methanogenic archaea. *Biochim Biophys Acta* **1505**, 28-36

126. Setzke, E., Hedderich, R., Heiden, S., and Thauer, R. K. (1994) H2: heterodisulfide oxidoreductase complex from Methanobacterium thermoautotrophicum. Composition and properties. *Eur J Biochem* **220**, 139-148

127. Herrmann, G., Jayamani, E., Mai, G., and Buckel, W. (2008) Energy conservation via electron-transferring flavoprotein in anaerobic bacteria. *J Bacteriol* **190**, 784-791

128. Deppenmeier, U. (2004) The membrane-bound electron transport system of Methanosarcina species. *J Bioenerg Biomembr* **36**, 55-64

129. Vinothkumar, K. R., Smits, S. H., and Kuhlbrandt, W. (2005) pH-induced structural change in a sodium/proton antiporter from Methanococcus jannaschii. *EMBO J* **24**, 2720-2729

130. Zhao, C., and Liu, Y. (2017) Direct Interspecies Electron Transfer Between Archaea and Bacteria. in *Biocommunication of Archaea*, Springer. pp 27-40

131. Morris, B. E., Henneberger, R., Huber, H., and Moissl-Eichinger, C. (2013) Microbial syntrophy: interaction for the common good. *FEMS Microbiol Rev* **37**, 384-406

132. Lelieveld, J. O. S., Crutzen, P. J., and Dentener, F. J. (1998) Changing concentration, lifetime and climate forcing of atmospheric methane. *Tellus B* **50**, 128-150

133. Andreini, C., Rosato, A., and Banci, L. (2017) The Relationship between Environmental Dioxygen and Iron-Sulfur Proteins Explored at the Genome Level. *PLoS One* **12**, e0171279

134. Richards, M. A., Lie, T. J., Zhang, J., Ragsdale, S. W., Leigh, J. A., and Price, N. D. (2016) Exploring Hydrogenotrophic Methanogenesis: a Genome Scale Metabolic Reconstruction of Methanococcus maripaludis. *J Bacteriol* **198**, 3379-3390

135. Jones, W. J., Paynter, M. J. B., and Gupta, R. (1983) Characterization of Methanococcus maripaludis sp. nov., a new methanogen isolated from salt marsh sediment. *Archives of Microbiology* **135**, 91-97

136. Hendrickson, E. L., Kaul, R., Zhou, Y., Bovee, D., Chapman, P., Chung, J., Conway de Macario, E., Dodsworth, J. A., Gillett, W., Graham, D. E., Hackett, M., Haydock, A. K.,

Kang, A., Land, M. L., Levy, R., Lie, T. J., Major, T. A., Moore, B. C., Porat, I., Palmeiri, A., Rouse, G., Saenphimmachak, C., Soll, D., Van Dien, S., Wang, T., Whitman, W. B., Xia, Q., Zhang, Y., Larimer, F. W., Olson, M. V., and Leigh, J. A. (2004) Complete genome sequence of the genetically tractable hydrogenotrophic methanogen Methanococcus maripaludis. *J Bacteriol* **186**, 6956-6969

137. Long, F., Wang, L., Lupa, B., and Whitman, W. B. (2017) A Flexible System for Cultivation of Methanococcus and Other Formate-Utilizing Methanogens. *Archaea* **2017**, 7046026

138. Sarmiento, F., Leigh, J. A., and Whitman, W. B. (2011) Genetic systems for hydrogenotrophic methanogens. *Methods in enzymology* **494**, 43-73

139. Sarmiento, F., Mrázek, J., and Whitman, W. B. (2013) Genome-scale analysis of gene function in the hydrogenotrophic methanogenic archaeon Methanococcus maripaludis. *Proceedings of the National Academy of Sciences* **110**, 4726-4731

140. Imlay, J. A. (2006) Iron-sulphur clusters and the problem with oxygen. *Mol Microbiol* **59**, 1073-1082

141. Liu, Y., Sieprawska-Lupa, M., Whitman, W. B., and White, R. H. (2010) Cysteine is not the sulfur source for iron-sulfur cluster and methionine biosynthesis in the methanogenic archaeon Methanococcus maripaludis. *J Biol Chem* **285**, 31923-31929

142. Wagner, T., Koch, J., Ermler, U., and Shima, S. (2017) Methanogenic heterodisulfide reductase (HdrABC-MvhAGD) uses two noncubane [4Fe-4S] clusters for reduction. *Science* **357**, 699-703

143. Meuer, J., Bartoschek, S., Koch, J., Kunkel, A., and Hedderich, R. (1999) Purification and catalytic properties of Ech hydrogenase from Methanosarcina barkeri. *Eur J Biochem* **265**, 325-335

144. Michel, R., Massanz, C., Kostka, S., Richter, M., and Fiebig, K. (1995) Biochemical Characterization of the 8-hydroxy-5-deazaflavin-reactive Hydrogenase from Methanosarcina barkeri Fusaro. *European Journal of Biochemistry* **233**, 727-735

145. Liu, Y., Beer, L. L., and Whitman, W. B. (2012) Methanogens: a window into ancient sulfur metabolism. *Trends in microbiology* **20**, 251-258

146. Yoon, S. H., Reiss, D. J., Bare, J. C., Tenenbaum, D., Pan, M., Slagel, J., Moritz, R. L., Lim, S., Hackett, M., Menon, A. L., Adams, M. W., Barnebey, A., Yannone, S. M., Leigh, J. A., and Baliga, N. S. (2011) Parallel evolution of transcriptome architecture during genome reorganization. *Genome Res* **21**, 1892-1904

147. Tsaousis, A. D., Gentekaki, E., Eme, L., Gaston, D., and Roger, A. J. (2014) Evolution of the cytosolic iron-sulfur cluster assembly machinery in Blastocystis species and other microbial eukaryotes. *Eukaryotic cell* **13**, 143-153

148. Boyd, J. M., Drevland, R. M., Downs, D. M., and Graham, D. E. (2009) Archaeal ApbC/Nbp35 homologs function as iron-sulfur cluster carrier proteins. *J Bacteriol* **191**, 1490-1497

149. Boyd, J. M., Sondelski, J. L., and Downs, D. M. (2009) Bacterial ApbC protein has two biochemical activities that are required for in vivo function. *J Biol Chem* **284**, 110-118

150. Netz, D. J., Pierik, A. J., Stumpfig, M., Bill, E., Sharma, A. K., Pallesen, L. J., Walden, W. E., and Lill, R. (2012) A bridging [4Fe-4S] cluster and nucleotide binding are essential for function of the Cfd1-Nbp35 complex as a scaffold in iron-sulfur protein maturation. *J Biol Chem* **287**, 12365-12378

151. Schneider, E., Wilken, S., and Schmid, R. (1994) Nucleotide-induced conformational changes of MalK, a bacterial ATP binding cassette transporter protein. *J Biol Chem* **269**, 20456-20461

152. Sarmiento, F., Mrazek, J., and Whitman, W. B. (2013) Genome-scale analysis of gene function in the hydrogenotrophic methanogenic archaeon Methanococcus maripaludis. *Proc Natl Acad Sci U S A* **110**, 4726-4731

153. Stams, A. J., de Bok, F. A., Plugge, C. M., van Eekert, M. H., Dolfing, J., and Schraa, G. (2006) Exocellular electron transfer in anaerobic microbial communities. *Environmental microbiology* **8**, 371-382

154. McInerney, M. J., Sieber, J. R., and Gunsalus, R. P. (2009) Syntrophy in anaerobic global carbon cycles. *Curr Opin Biotechnol* **20**, 623-632

155. Purwantini, E., Torto-Alalibo, T., Lomax, J., Setubal, J. C., Tyler, B. M., and Mukhopadhyay, B. (2014) Genetic resources for methane production from biomass described with the Gene Ontology. *Front Microbiol* **5**, 634

156. Joye, S. B. (2012) Microbiology: A piece of the methane puzzle. *Nature* **491**, 538-539

157. Forster, P., Ramaswamy, V., Artaxo, P., Berntsen, T., Betts, R., Fahey, D. W., Haywood, J., Lean, J., Lowe, D. C., Myhre, G., Nganga, J., Prinn, R., Raga, G., Schultz, M., and Van Dorland, R. (2007) Changes in atmospheric constituents and in radiative forcing. (Solomon, S., Qin, D., Manning, M., Chen, Z., Marquis, M., Averyt, K. B., Tignor, M., and Miller, H. L. eds.), Cambridge University Press, Cambridge, United Kingdom

158. Bryant, M. P., Wolin, E. A., Wolin, M. J., and Wolfe, R. S. (1967) *Methanobacillus omelianskii,* a symbiotic association of two species of bacteria. *Archiv fur Mikrobiologie* **59**, 20-31

159. Schink, B., and Stams, A. J. M. (2013) Syntrophism among prokaryotes. in *The prokaryotes: prokaryotic communities and ecophysiology* (Rosenberg, E., DeLong, E. F., Lory, S., Stackebrandt, E., and Thompson, F. eds.), Springer Berlin Heidelberg, Berlin, Heidelberg. pp 471-493

160. Stams, A. J., and Plugge, C. M. (2009) Electron transfer in syntrophic communities of anaerobic bacteria and archaea. *Nat Rev Microbiol* **7**, 568-577

161. Thiele, J. H., and Zeikus, J. G. (1988) Control of interspecies electron flow during anaerobic digestion: significance of formate transfer versus hydrogen transfer during syntrophic methanogenesis in flocs. *Applied and environmental microbiology* **54**, 20-29

162. Boone, D. R., Johnson, R. L., and Liu, Y. (1989) Diffusion of the interspecies electron carriers H_2 and formate in methanogenic ecosystems and its implications in the measurement of K_m for H_2 or formate uptake. *Applied and environmental microbiology* **55**, 1735-1741

163. de Bok, F. A., Plugge, C. M., and Stams, A. J. (2004) Interspecies electron transfer in methanogenic propionate degrading consortia. *Water Res* **38**, 1368-1375

164. Hattori, S., Luo, H., Shoun, H., and Kamagata, Y. (2001) Involvement of formate as an interspecies electron carrier in a syntrophic acetate-oxidizing anaerobic microorganism in coculture with methanogens. *Journal of bioscience and bioengineering* **91**, 294-298

165. Zindel, U., Freudenberg, W., Rieth, M., Andreesen, J. R., Schnell, J., and Widdel, F. (1988) Eubacterium acidaminophilum sp. nov., a versatile amino acid-degrading anaerobe producing or utilizing H_2 or formate. *Archiv fur Mikrobiologie* **150**, 254-266

166. Sousa, D. Z., Smidt, H., Alves, M. M., and Stams, A. J. (2007) Syntrophomonas zehnderi sp. nov., an anaerobe that degrades long-chain fatty acids in co-culture with Methanobacterium formicicum. *Int J Syst Evol Microbiol* **57**, 609-615

167. Dong, X., and Stams, A. J. (1995) Evidence for H_2 and formate formation during syntrophic butyrate and propionate degradation. *Anaerobe* **1**, 35-39

168. Rotaru, A. E., Shrestha, P. M., Liu, F., Ueki, T., Nevin, K., Summers, Z. M., and Lovley, D. R. (2012) Interspecies electron transfer via hydrogen and formate rather than direct electrical connections in cocultures of *Pelobacter carbinolicus* and *Geobacter sulfurreducens*. *Applied and environmental microbiology* **78**, 7645-7651

169. Platen, H., and Schink, B. (1987) Methanogenic degradation of acetone by an enrichment culture. *Archiv fur Mikrobiologie* **149**, 136-141

170. Platen, H., Janssen, P. H., and Schink, B. (1994) Fermentative degradation of acetone by an enrichment culture in membrane-separated culture devices and in cell suspensions. *FEMS microbiology letters* **122**, 27-32

171. Biebl, H., and Pfennig, N. (1978) Growth yields of green sulfur bacteria in mixed cultures with sulfur and sulfate reducing bacteria. *Archiv fur Mikrobiologie* **117**, 9-16

172. Boetius, A., Ravenschlag, K., Schubert, C. J., Rickert, D., Widdel, F., Gieseke, A., Amann, R., Jorgensen, B. B., Witte, U., and Pfannkuche, O. (2000) A marine microbial consortium apparently mediating anaerobic oxidation of methane. *Nature* **407**, 623-626

173. Kaden, J., S Galushko, A., and Schink, B. (2002) Cysteine-mediated electron transfer in syntrophic acetate oxidation by cocultures of *Geobacter sulfurreducens* and *Wolinella succinogenes*. *Archiv fur Mikrobiologie* **178**, 53-58

174. Milucka, J., Ferdelman, T. G., Polerecky, L., Franzke, D., Wegener, G., Schmid, M., Lieberwirth, I., Wagner, M., Widdel, F., and Kuypers, M. M. (2012) Zero-valent sulphur is a key intermediate in marine methane oxidation. *Nature* **491**, 541-546

175. Liu, F. H., Rotaru, A. E., Shrestha, P. M., Malvankar, N. S., Nevin, K. P., and Lovley, D. R. (2012) Promoting direct interspecies electron transfer with activated carbon. *Energ Environ Sci* **5**, 8982-8989

176. Newman, D. K., and Kolter, R. (2000) A role for excreted quinones in extracellular electron transfer. *Nature* **405**, 94-97

177. Lovley, D. R., Fraga, J. L., Coates, J. D., and Blunt-Harris, E. L. (1999) Humics as an electron donor for anaerobic respiration. *Environmental microbiology* **1**, 89-98

178. Lovley, D. R., Fraga, J. L., Blunt-Harris, E. L., Hayes, L. A., Phillips, E. J. P., and Coates, J. D. (1998) Humic substances as a mediator for microbially catalyzed metal reduction. *Acta Hydroch Hydrob* **26**, 152-157

179. Lovley, D. R., Coates, J. D., Blunt-Harris, E. L., Phillips, E. J. P., and Woodward, J. C. (1996) Humic substances as electron acceptors for microbial respiration. *Nature* **382**, 445-448

180. Brutinel, E. D., and Gralnick, J. A. (2012) Shuttling happens: soluble flavin mediators of extracellular electron transfer in *Shewanella*. *Applied microbiology and biotechnology* **93**, 41-48

181. Marsili, E., Baron, D. B., Shikhare, I. D., Coursolle, D., Gralnick, J. A., and Bond, D. R. (2008) *Shewanella* secretes flavins that mediate extracellular electron transfer. *Proceedings of the National Academy of Sciences of the United States of America* **105**, 3968-3973

182. von Canstein, H., Ogawa, J., Shimizu, S., and Lloyd, J. R. (2008) Secretion of flavins by *Shewanella* species and their role in extracellular electron transfer. *Applied and environmental microbiology* **74**, 615-623

183. Rotaru, A. E., Shrestha, P. M., Liu, F., Markovaite, B., Chen, S., Nevin, K. P., and Lovley, D. R. (2014) Direct interspecies electron transfer between *Geobacter metallireducens* and *Methanosarcina barkeri*. *Applied and environmental microbiology* **80**, 4599-4605

184. Rotaru, A.-E., Shrestha, P. M., Liu, F., Shrestha, M., Shrestha, D., Embree, M., Zengler, K., Wardman, C., Nevin, K. P., and Lovley, D. R. (2014) A new model for electron flow during anaerobic digestion: direct interspecies electron transfer to *Methanosaeta* for the reduction of carbon dioxide to methane. *Energ Environ Sci* **7**, 408-415

185. Summers, Z. M., Fogarty, H. E., Leang, C., Franks, A. E., Malvankar, N. S., and Lovley, D. R. (2010) Direct exchange of electrons within aggregates of an evolved syntrophic coculture of anaerobic bacteria. *Science* **330**, 1413-1415

186. McGlynn, S. E., Chadwick, G. L., Kempes, C. P., and Orphan, V. J. (2015) Single cell activity reveals direct electron transfer in methanotrophic consortia. *Nature* **526**, 531-535

187. Wegener, G., Krukenberg, V., Riedel, D., Tegetmeyer, H. E., and Boetius, A. (2015) Intercellular wiring enables electron transfer between methanotrophic archaea and bacteria. *Nature* **526**, 587-590

188. Shrestha, P. M., and Rotaru, A. E. (2014) Plugging in or going wireless: strategies for interspecies electron transfer. *Front Microbiol* **5**, 237

189. Shrestha, P. M., Rotaru, A. E., Aklujkar, M., Liu, F., Shrestha, M., Summers, Z. M., Malvankar, N., Flores, D. C., and Lovley, D. R. (2013) Syntrophic growth with direct interspecies electron transfer as the primary mechanism for energy exchange. *Environ Microbiol Rep* **5**, 904-910

190. McInerney, M. J., and Bryant, M. P. (1981) Anaerobic degradation of lactate by syntrophic associations of *Methanosarcina barkeri* and *Desulfovibrio* Species and Effect of H_2 on Acetate Degradation. *Applied and environmental microbiology* **41**, 346-354

191. Chen, S., Rotaru, A. E., Shrestha, P. M., Malvankar, N. S., Liu, F., Fan, W., Nevin, K. P., and Lovley, D. R. (2014) Promoting interspecies electron transfer with biochar. *Sci Rep* **4**, 5019

192. Chen, S., Rotaru, A. E., Liu, F., Philips, J., Woodard, T. L., Nevin, K. P., and Lovley, D. R. (2014) Carbon cloth stimulates direct interspecies electron transfer in syntrophic co-cultures. *Bioresour Technol* **173**, 82-86

193. Liu, F., Rotaru, A. E., Shrestha, P. M., Malvankar, N. S., Nevin, K. P., and Lovley, D. R. (2015) Magnetite compensates for the lack of a pilin-associated *c*-type cytochrome in extracellular electron exchange. *Environmental microbiology* **17**, 648-655

194. Zhang, J., and Lu, Y. (2016) Conductive Fe_3O_4 nanoparticles accelerate syntrophic methane production from butyrate oxidation in two different lake sediments. *Front Microbiol* **7**, 1316

195. Beckmann, S., Welte, C., Li, X., Oo, Y. M., Kroeninger, L., Heo, Y., Zhang, M., Ribeiro, D., Lee, M., Bhadbhade, M., Marjo, C. E., Seidel, J., Deppenmeier, U., and Manefield, M. (2016) Novel phenazine crystals enable direct electron transfer to methanogens in anaerobic digestion by redox potential modulation. *Energ Environ Sci* **9**, 644-655

196. Cui, M., Ma, A., Qi, H., Zhuang, X., and Zhuang, G. (2015) Anaerobic oxidation of methane: an "active" microbial process. *Microbiologyopen* **4**, 1-11

197. Hinrichs, K.-U., and Boetius, A. (2003) The anaerobic oxidation of methane: new insights in microbial ecology and biogeochemistry. in *Ocean Margin Systems* (Wefer, G., Billett, D., Hebbeln, D., Jørgensen, B. B., Schlüter, M., and van Weering, T. C. E. eds.), Springer Berlin Heidelberg, Berlin, Heidelberg. pp 457-477

198. Knittel, K., Losekann, T., Boetius, A., Kort, R., and Amann, R. (2005) Diversity and distribution of methanotrophic archaea at cold seeps. *Applied and environmental microbiology* **71**, 467-479

199. Knittel, K., and Boetius, A. (2009) Anaerobic oxidation of methane: progress with an unknown process. *Annu Rev Microbiol* **63**, 311-334

200. Niemann, H., Lösekann, T., De Beer, D., Elvert, M., Nadalig, T., Knittel, K., Amann, R., Sauter, E. J., Schlüter, M., and Klages, M. (2006) Novel microbial communities of the Haakon Mosby mud volcano and their role as a methane sink. *Nature* **443**, 854-858

201. Lösekann, T., Knittel, K., Nadalig, T., Fuchs, B., Niemann, H., Boetius, A., and Amann, R. (2007) Diversity and abundance of aerobic and anaerobic methane oxidizers at the Haakon Mosby Mud Volcano, Barents Sea. *Applied and environmental microbiology* **73**, 3348-3362

202. Kai-Uwe Hinrichs, John M. Hayes, Sean P. Sylva, Peter G. Brewer, and DeLong, E. F. (1999) Methane-consuming archaebacteria in marine sediments. *Nature* **398**, 802-805

203. Bian, L., Hinrichs, K.-U., Xie, T., Brassell, S. C., Iversen, N., Fossing, H., Jørgensen, B. B., and Hayes, J. M. (2001) Algal and archaeal polyisoprenoids in a recent marine sediment: Molecular isotopic evidence for anaerobic oxidation of methane. *Geochem Geophy Geosy* **2**, 2000GC000112

204. Reeburgh, W. S. (1976) Methane consumption in Cariaco Trench waters and sediments. *Earth Planet Sci Lett* **28**, 337-344

205. Rusanov, I., Levi, A., Pimenov, N. V., Iusupov, S. K., and Ivanov, M. V. (2002) The biogeochemical cycle of methane in the northwestern shelf of the Black Sea. *Microbiology* **71**, 558-566

206. Durisch-Kaiser, E., Klauser, L., Wehrli, B., and Schubert, C. (2005) Evidence of intense archaeal and bacterial methanotrophic activity in the Black Sea water column. *Applied and environmental microbiology* **71**, 8099-8106

207. Orphan, V. J., Ussler Iii, W., Naehr, T. H., House, C. H., Hinrichs, K. U., and Paull, C. K. (2004) Geological, geochemical, and microbiological heterogeneity of the seafloor around methane vents in the Eel River Basin, offshore California. *Chem Geol* **205**, 265-289

208. Treude, T., Orphan, V., Knittel, K., Gieseke, A., House, C. H., and Boetius, A. (2007) Consumption of methane and CO_2 by methanotrophic microbial mats from gas seeps of the anoxic black sea. *Applied and environmental microbiology* **73**, 2271-2283

209. Murase, J., and Kimura, M. (1996) Methane production and its fate in paddy fields. *Soil Sci Plant Nutr* **42**, 187-190

210. Grossman, E. L., Cifuentes, L. A., and Cozzarelli, I. M. (2002) Anaerobic methane oxidation in a landfill-leachate plume. *Environ Sci Technol* **36**, 2436-2442

211. Eller, G., Känel, L., and Krüger, M. (2005) Cooccurrence of aerobic and anaerobic methane oxidation in the water column of Lake Plusssee. *Applied and environmental microbiology* **71**, 8925-8928

212. Alain, K., Holler, T., Musat, F., Elvert, M., Treude, T., and Kruger, M. (2006) Microbiological investigation of methane- and hydrocarbon-discharging mud volcanoes in the Carpathian Mountains, Romania. *Environmental microbiology* **8**, 574-590

213. Miyashita, A., Mochimaru, H., Kazama, H., Ohashi, A., Yamaguchi, T., Nunoura, T., Horikoshi, K., Takai, K., and Imachi, H. (2009) Development of 16S rRNA gene-targeted primers for detection of archaeal anaerobic methanotrophs (ANMEs). *FEMS microbiology letters* **297**, 31-37

214. Smemo, K. A., and Yavitt, J. B. (2007) Evidence for anaerobic CH_4 oxidation in freshwater peatlands. *Geomicrobiol* **24**, 583-597

215. Michaelis, W., Seifert, R., Nauhaus, K., Treude, T., Thiel, V., Blumenberg, M., Knittel, K., Gieseke, A., Peterknecht, K., Pape, T., Boetius, A., Amann, R., Jorgensen, B. B., Widdel, F., Peckmann, J., Pimenov, N. V., and Gulin, M. B. (2002) Microbial reefs in the Black Sea fueled by anaerobic oxidation of methane. *Science* **297**, 1013-1015

216. Ye, K., Malinina, L., and Patel, D. J. (2003) Recognition of small interfering RNA by a viral suppressor of RNA silencing. *Nature* **426**, 874-878

217. Krüger, M., Meyerdierks, A., Glöckner, F. O., Amann, R., Widdel, F., Kube, M., Reinhardt, R., Kahnt, J., Böcher, R., Thauer, R. K., and Shima, S. (2003) A conspicuous nickel protein in microbial mats that oxidize methane anaerobically. *Nature* **426**, 878-881

218. Hallam, S. J., Girguis, P. R., Preston, C. M., Richardson, P. M., and DeLong, E. F. (2003) Identification of methyl coenzyme M reductase A (mcrA) genes associated with methane-oxidizing archaea. *Applied and environmental microbiology* **69**, 5483-5491

219. Shima, S., Krueger, M., Weinert, T., Demmer, U., Kahnt, J., Thauer, R. K., and Ermler, U. (2012) Structure of a methyl-coenzyme M reductase from Black Sea mats that oxidize methane anaerobically. *Nature* **481**, 98-101

220. Meyerdierks, A., Kube, M., Kostadinov, I., Teeling, H., Glockner, F. O., Reinhardt, R., and Amann, R. (2010) Metagenome and mRNA expression analyses of anaerobic methanotrophic archaea of the ANME-1 group. *Environmental microbiology* **12**, 422-439

221. Wang, F. P., Zhang, Y., Chen, Y., He, Y., Qi, J., Hinrichs, K. U., Zhang, X. X., Xiao, X., and Boon, N. (2014) Methanotrophic archaea possessing diverging methane-oxidizing and electron-transporting pathways. *ISME J* **8**, 1069-1078

222. Haroon, M. F., Hu, S., Shi, Y., Imelfort, M., Keller, J., Hugenholtz, P., Yuan, Z., and Tyson, G. W. (2013) Anaerobic oxidation of methane coupled to nitrate reduction in a novel archaeal lineage. *Nature* **500**, 567-570

223. Hoehler, T. M., Alperin, M. J., Albert, D. B., and Martens, C. S. (1994) Field and laboratory studies of methane oxidation in an anoxic marine sediment' Evidence for a methanogen-sulfate reducer consortium. *Global Biogeochem Cycles* **8**, 451-463

224. Moran, J. J., Beal, E. J., Vrentas, J. M., Orphan, V. J., Freeman, K. H., and House, C. H. (2008) Methyl sulfides as intermediates in the anaerobic oxidation of methane. *Environmental microbiology* **10**, 162-173

225. Krukenberg, V., Harding, K., Richter, M., Glockner, F. O., Gruber-Vodicka, H. R., Adam, B., Berg, J. S., Knittel, K., Tegetmeyer, H. E., Boetius, A., and Wegener, G. (2016) *Candidatus* Desulfofervidus auxilii, a hydrogenotrophic sulfate-reducing bacterium involved in the thermophilic anaerobic oxidation of methane. *Environmental microbiology* **18**, 3073-3091

226. Scheller, S., Yu, H., Chadwick, G. L., McGlynn, S. E., and Orphan, V. J. (2016) Artificial electron acceptors decouple archaeal methane oxidation from sulfate reduction. *Science* **351**, 703-707

227. Timmers, P. H. A., Welte, C. U., Koehorst, J. J., Plugge, C. M., Jetten, M. S. M., and Stams, A. J. M. (2017) Reverse methanogenesis and respiration in methanotrophic archaea. *Archaea* **2017**, 1-22

228. Meyer, J. (2008) Iron-sulfur protein folds, iron-sulfur chemistry, and evolution. *J. Biol. Inorg. Chem.* **13**, 157-170

229. Johnson, D. C., Dean, D. R., Smith, A. D., and Johnson, M. K. (2005) Structure, function, and formation of biological iron-sulfur clusters. *Annu. Rev. Biochem.* **74**, 247-281

230. Pain, D., and Dancis, A. (2016) Roles of Fe-S proteins: from cofactor synthesis to iron homeostasis to protein synthesis. *Curr. Opin. Genet. Dev.* **38**, 45-51

231. Beinert, H., Kennedy, M. C., and Stout, C. D. (1996) Aconitase as iron-sulfur protein, enzyme, and iron-regulatory protein. *Chem. Rev.* **96**, 2335-2374

232. Mettert, E. L., and Kiley, P. J. (2015) Fe-S proteins that regulate gene expression. *Biochim. Biophys. Acta* **1853**, 1284-1293

233. Py, B., and Barras, F. (2010) Building Fe-S proteins: bacterial strategies. *Nat. Rev. Microbiol.* **8**, 436-446

234. Zheng, L., White, R. H., Cash, V. L., Jack, R. F., and Dean, D. R. (1993) Cysteine desulfurase activity indicates a role for NIFS in metallocluster biosynthesis. *Proc. Natl. Acad. Sci. U.S.A.* **90**, 2754-2758

235. Blanc, B., Gerez, C., and Ollagnier de Choudens, S. (2015) Assembly of Fe/S proteins in bacterial systems: Biochemistry of the bacterial ISC system. *Biochim. Biophys. Acta* **1853**, 1436-1447

236. Yuvaniyama, P., Agar, J. N., Cash, V. L., Johnson, M. K., and Dean, D. R. (2000) NifS-directed assembly of a transient [2Fe-2S] cluster within the NifU protein. *Proc. Natl. Acad. Sci. U.S.A.* **97**, 599-604

237. Raulfs, E. C., O'Carroll, I. P., Dos Santos, P. C., Unciuleac, M. C., and Dean, D. R. (2008) *In vivo* iron-sulfur cluster formation. *Proc. Natl. Acad. Sci. U.S.A.* **105**, 8591-8596

238. Roche, B., Aussel, L., Ezraty, B., Mandin, P., Py, B., and Barras, F. (2013) Iron/sulfur proteins biogenesis in prokaryotes: formation, regulation and diversity. *Biochim. Biophys. Acta* **1827**, 455-469

239. Wayne Outten, F. (2015) Recent advances in the Suf Fe–S cluster biogenesis pathway: Beyond the Proteobacteria. *Biochim. Biophys. Acta, Mol. Cell. Res.* **1853**, 1464-1469

240. Whitman, W. B., Shieh, J., Sohn, S., Caras, D. S., and Premachandran, U. (1986) Isolation and characterization of 22 mesophilic methanococci. *Systematic and Applied Microbiology* **7**, 235-240

241. Stoll, S., and Schweiger, A. (2006) EasySpin, a comprehensive software package for spectral simulation and analysis in EPR. *J Magn Reson* **178**, 42-55

242. Kitagawa, M., Ara, T., Arifuzzaman, M., Ioka-Nakamichi, T., Inamoto, E., Toyonaga, H., and Mori, H. (2005) Complete set of ORF clones of Escherichia coli ASKA library (a complete set of E. coli K-12 ORF archive): unique resources for biological research. *DNA Res* **12**, 291-299

243. Liu, Y., Vinyard, D. J., Reesbeck, M. E., Suzuki, T., Manakongtreecheep, K., Holland, P. L., Brudvig, G. W., and Söll, D. (2016) A [3Fe-4S] cluster is required for tRNA thiolation in archaea and eukaryotes. *Proc Natl Acad Sci U S A* **113**, 12703-12708

244. Gardner, P. R., and Fridovich, I. (1992) Inactivation-reactivation of aconitase in Escherichia coli. A sensitive measure of superoxide radical. *J Biol Chem* **267**, 8757-8763

245. Walters, A. D., Smith, S. E., and Chong, J. P. (2011) Shuttle vector system for Methanococcus maripaludis with improved transformation efficiency. *Appl Environ Microbiol* **77**, 2549-2551

246. Dos Santos, P. C., Smith, A. D., Frazzon, J., Cash, V. L., Johnson, M. K., and Dean, D. R. (2004) Iron-sulfur cluster assembly: NifU-directed activation of the nitrogenase Fe protein. *J Biol Chem* **279**, 19705-19711

247. Liu, Y., Zhu, X., Nakamura, A., Orlando, R., Soll, D., and Whitman, W. B. (2012) Biosynthesis of 4-thiouridine in tRNA in the methanogenic archaeon Methanococcus maripaludis. *J Biol Chem* **287**, 36683-36692

248. Tsaousis, A. D., Ollagnier de Choudens, S., Gentekaki, E., Long, S., Gaston, D., Stechmann, A., Vinella, D., Py, B., Fontecave, M., Barras, F., Lukes, J., and Roger, A. J. (2012) Evolution of Fe/S cluster biogenesis in the anaerobic parasite Blastocystis. *Proceedings of the National Academy of Sciences of the United States of America* **109**, 10426-10431

249. Stairs, Courtney W., Eme, L., Brown, Matthew W., Mutsaers, C., Susko, E., Dellaire, G., Soanes, Darren M., van der Giezen, M., and Roger, Andrew J. (2014) A SUF Fe-S Cluster Biogenesis System in the Mitochondrion-Related Organelles of the Anaerobic Protist Pygsuia. *Current Biology* **24**, 1176-1186

250. Riboldi, G. P., de Oliveira, J. S., and Frazzon, J. (2011) Enterococcus faecalis SufU scaffold protein enhances SufS desulfurase activity by acquiring sulfur from its cysteine-153. *Biochim Biophys Acta* **1814**, 1910-1918

251. Riboldi, G. P., Larson, T. J., and Frazzon, J. (2011) Enterococcus faecalis sufCDSUB complements Escherichia coli sufABCDSE. *FEMS Microbiol Lett* **320**, 15-24

252. Yoon, S. H., Reiss, D. J., Bare, J. C., Tenenbaum, D., Pan, M., Slagel, J., Moritz, R. L., Lim, S., Hackett, M., Menon, A. L., Adams, M. W. W., Barnebey, A., Yannone, S. M., Leigh, J. A., and Baliga, N. S. (2011) Parallel evolution of transcriptome architecture during genome reorganization. *Genome research* **21**, 1892-1904

253. Zheng, L., White, R. H., Cash, V. L., Jack, R. F., and Dean, D. R. (1993) Cysteine desulfurase activity indicates a role for NifS in metallocluster biosynthesis. *Proc Natl Acad Sci USA* **90**, 2754-2758

254. Raulfs, E. C., O'Carroll, I. P., Dos Santos, P. C., Unciuleac, M. C., and Dean, D. R. (2008) *In vivo* iron-sulfur cluster formation. *Proc Natl Acad Sci USA* **105**, 8591-8596

255. Yuvaniyama, P., Agar, J. N., Cash, V. L., Johnson, M. K., and Dean, D. R. (2000) NifS-directed assembly of a transient [2Fe-2S] cluster within the NifU protein. *Proc Natl Acad Sci USA* **97**, 599-604

256. Outten, F. W. (2015) Recent advances in the Suf Fe-S cluster biogenesis pathway: Beyond the Proteobacteria. *Biochim Biophys Acta* **1853**, 1464-1469

257. Braymer, J. J., and Lill, R. (2017) Iron–sulfur cluster biogenesis and trafficking in mitochondria. *J Biol Chem* **292**, 12754-12763

258. Lu, Y. (2018) Assembly and transfer of iron–sulfur clusters in the plastid. *Front Plant Sci* **9**, 336

259. Grossman, J. D., Camire, E. J., and Perlstein, D. L. (2018) Approaches to interrogate the role of nucleotide hydrolysis by metal trafficking NTPases: The Nbp35–Cfd1 iron–sulfur cluster scaffold as a case study. *Methods Enzymol* **599**, 293-325

260. Hausmann, A., Aguilar Netz, D. J., Balk, J., Pierik, A. J., Muhlenhoff, U., and Lill, R. (2005) The eukaryotic P loop NTPase Nbp35: an essential component of the cytosolic and nuclear iron-sulfur protein assembly machinery. *Proc Natl Acad Sci USA* **102**, 3266-3271

261. Stehling, O., Netz, D. J., Niggemeyer, B., Rosser, R., Eisenstein, R. S., Puccio, H., Pierik, A. J., and Lill, R. (2008) Human Nbp35 is essential for both cytosolic iron-sulfur protein assembly and iron homeostasis. *Mol Cell Biol* **28**, 5517-5528

262. Pallesen, L. J., Solodovnikova, N., Sharma, A. K., and Walden, W. E. (2013) Interaction with Cfd1 increases the kinetic lability of FeS on the Nbp35 scaffold. *J Biol Chem* **288**, 23358-23367

263. Camire, E. J., Grossman, J. D., Thole, G. J., Fleischman, N. M., and Perlstein, D. L. (2015) The Yeast Nbp35-Cfd1 Cytosolic Iron-Sulfur Cluster Scaffold Is an ATPase. *J Biol Chem* **290**, 23793-23802

264. Grossman, J. D., Gay, K. A., Camire, E. J., Walden, W. E., and Perlstein, D. L. (2019) Coupling nucleotide binding and hydrolysis to iron-sulfur cluster acquisition and transfer revealed through genetic dissection of the Nbp35 ATPase site. *Biochemistry* **58 (15)**, 2017-2027

265. Boyd, J. M., Pierik, A. J., Netz, D. J., Lill, R., and Downs, D. M. (2008) Bacterial ApbC can bind and effectively transfer iron-sulfur clusters. *Biochemistry* **47**, 8195-8202

266. Liu, Y. (2010) Methanococcales. 573-581

267. Whitman, W. B., Shieh, J., Sohn, S., Caras, D. S., and Premachandran, U. (1986) Isolation and characterization of 22 mesophilic methanococci. *Syst Appl Microbiol* **7**, 235-240

268. Lyu, Z., Chou, C.-w., Shi, H., Patel, R., Duin, E. C., and Whitman, W. B. (2017) Mmp10 is required for post-translational methylation of arginine at the active site of methyl-coenzyme M reductase. *bioRxiv*, 211441

269. Gardner, P., and Fridovich, I. (1992) Inactivation-reactivation of aconitase in *Escherichia coli*: A sensitive measure of superoxide radical. *J Biol Chem* **267**, 8757-8763

270. Le, S. Q., and Gascuel, O. (2008) An improved general amino acid replacement matrix. *Mol Biol Evol* **25**, 1307-1320

271. Felsenstein, J. (1985) CONFIDENCE LIMITS ON PHYLOGENIES: AN APPROACH USING THE BOOTSTRAP. *Evolution; international journal of organic evolution* **39**, 783-791

272. Liu, J., Chakraborty, S., Hosseinzadeh, P., Yu, Y., Tian, S., Petrik, I., Bhagi, A., and Lu, Y. (2014) Metalloproteins containing cytochrome, iron-sulfur, or copper redox centers. *Chem Rev* **114**, 4366-4469

273. Weil, J. A., and Bolton, J. R. (2007) *Electron paramagnetic resonance: elementary theory and practical applications*, John Wiley & Sons

VITA

Cuiping Zhao was born in Anhui Province, China, in 1992. As a child, she dreamed of being a scientist. After many years hard study, she will receive her doctoral degree in August 2019. As the oldest child in her family, her parents educated her to have a high sense of responsibility and to be diligent. She received a Bachelor of Science degree from Anhui University in July 2013. In January 2016, she received the opportunity to pursue her doctoral degree with Dr. Yuchen Liu and Dr. David J. Vinyard in the Department of Biological Science at Louisiana State University.